TR - O -0055

- - - 40

光ファイバを用いたミリ波サブキャリア伝送技術の研究

小川博世

1993. 2. 16.

ATR光電波通信研究所

復　帰　報　告　書

1992年2月5日

1. 氏名　　小川博世

2. 所属　　無線通信第２研究室

3. 研究テーマ　光ファイバを用いたミリ波サブキャリア伝送技術の研究

4. 滞在期間　　平成２年１月～平成５年２月

5. 復帰先　　NTT無線システム研究所衛星通信研究部

6. 主な成果の概要（詳細は６ページから）
   6.1 光ファイバを用いたミリ波分配ネットワークの提案
   6.2 光／マイクロ波集積回路の提案
   6.3 ミリ波サブキャリア伝送実験による光ファイバリンクの評価
   6.4 光デバイスの非線型特性の光ファイバリンクへの応用
   6.5 高機能型光ファイバリンクの提案

7. 特記事項

研究の当初は数GHz程度の伝送しかできなかったが、最近では光ファイバリンクで直接50GHz帯FM伝送までできるようになったことは特記すべきである。

8. まとめ

３年間を通して光とマイクロ・ミリ波の両領域にまたがる分野に関する研究を行うことができた。今後ますますこの分野は無線／光通信の領域で重要になる技術であり、システム、回路、デバイスにいたるまでこのコンセプトで設計すべきである。本報告書がこの新領域の発展のための１資料になることを期待する。

文献　　本資料の１ページから５ページにまとめている

光ファイバを用いたミリ波サブキャリア伝送技術の研究

目次

概要

本報告は平成２年１月から平成５年２月までの期間中に行なわれた研究結果をまとめたものである。本研究の主な目的は、光ファイバリンクでミリ波信号を伝送するための伝送技術、回路技術、デバイス技術を確立することである。光ファイバには超広帯域性、低損失性、軽重・小型等の特長があり、移動体通信で検討されているエリアが数百ｍのマイクロセルゾーンにミリ波信号を給電するための最も良い伝送媒体と考えられる。上記技術の確立のため以下のグループ体制で研究を進めた。

小川博世主幹研究員	(H2.1～H5.2) ：光ファイバリンク技術全般
竹中　勉研究員	(～H4.3) ：MMICおよびQuasi-Optics
馬場清一研究員	(H2.3～) ：光MMIC
長谷川隆生研究員	(～H3.9) ：多層化MMIC
末松英二研究員	(H4.1～) ：光MMIC
上綱秀樹研究員	(H2.2～) ：光MMIC
松井一浩研究員	(H4.11～) ：Quasi-Optics
David Polifko客員研究員	(H3.4～H4.12) ：光ファイバリンク回路技術
Howard Thomas客員研究員	(H4.5～) ：光ファイバリンクシステム技術
Peter Herczfeld招聘研究員	(H4.11～H4.12) ：Lightwave/Microwave技術全般
Elisabeth Penard客員研究員	(H5.1～) ：Quasi-Optics

本グループは旧MMICグループを引き継いでおり、そのためテーマの継続性のため多層化MMICの研究も引き続き行なった。各研究員の研究成果は各自のテクニカルレポートを参照して頂きたい。本稿では報告者がこれまで担当してきた研究内容を中心に報告する[1]-[116]。

著者の関連する文献

[1] 小川、他, "1990年IEEE MTT-S国際マイクロ波シンポジウムワークショップ出席報告," IEICE技術報告, MW90-66, Jul.1990.

[2] 伊藤、小川、他, "1990年IEEE MTT-S国際マイクロ波シンポジウム報告," IEICE技術報告, MW90-78, Aug.1990.

[3] 赤池、小川, "Analog and digital GaAs MMICs for radio communication equipment," URSI, p.487, 1990.

[4] 小川、他, "光ファイバリンクミリ波パーソナル通信システム," IEICE秋季大会, B-736, Oct.1990.

[5] 竹中、小川, "MMIC多層化スパイラルインダクタ," IEICE秋季大会, C-56, Oct.1990.

[6] 小川、他, "光ファイバを用いたマイクロ波伝送の一検討," IEICE春季大会, B-905, Mar.1991.

[7] 竹中、小川, "L帯アクティブアレーアンテナ用MMIC低雑音増幅器・ダウンコンバータ," IEICE春季大会, C-40, Mar.1991.

[8] 馬場、長谷川、小川, "多層化MMIC伝送線路," IEICE春季大会, SC-2-9, Mar.1991.

[9] 小川、他, "光ファイバを用いたマイクロ波／ミリ波伝送の検討," IEICE技術報告, OSC91-8, May1991.

[10] H.Ogawa et al., "MMIC transmission lines for multi-layered MMICs," IEEE MTT-S Int. Microwave Symp. Dig., pp.1067-1070, Jun.1991.

[11] H.Ogawa et al., "Fiber optic microwave transmission using harmonic modulation and optoelectronic mixing/ optically pumped mixing," IEEE MTT-S Int. Microwave Symp. Dig., pp.593-596, Jun.1991.

[12] 小川、他, "無線通信用光ファイバリンクの検討," IEICE秋季大会, B-274, Sept.1991.

[13] 小川、他, "平衡型レーザ変調器の光ファイバ無線通信リンクへの適用," IEICE秋季大会, B-275, Sept.1991.
[14] D.Polifko and H.Ogawa, "Effects of laser harmonic generation on fiber optic link performance," IEICE秋季大会, B-276, Sept.1991.
[15] 上綱、小川、赤池, "PINフォトダイオードの光入射時の電圧-電流特性," IEICE秋季大会, C-56, Sept.1991.
[16] 長谷川、馬場、小川, "V溝MMIC伝送線路を用いたブランチラインハイブリッド," IEICE秋季大会, C-100, Sept.1991.
[17] 馬場、長谷川、小川, "多層化MMIC伝送線路を用いた超小型ハイブリッド回路," IEICE秋季大会, C-101, Sept.1991.
[18] 小川、他, "MMIC技術の現状と今後の展望," 連合大会S22-5, Sept.1991.
[19] 小川、他, "1991年IEEE MTT-S国際マイクロ波シンポジウム報告," IEICE技術報告, MW91-63, Sept.1992.
[20] D.Polifko and H.Ogawa, "Fiber optic link for microwave/millimeter-wave transmission," MWE'91 Microwave Workshop Dig., pp.127-130, Sept.1991.
[21] 長谷川、馬場、小川, "多層化MMICを用いた多分岐電力分配器," IEICE技術報告, MW91-81, Oct.1991.
[22] T.Hasegawa, S.Banba and H.Ogawa, "Characteristics of valley microstrip lines for use in multilayer MMICs," IEEE Microwave Guided Wave Lett., vol.MGL-1, pp.275-277, Oct.1991.
[23] S.Banba, T.Hasegawa and H.Ogawa, "Multilayer MMIC brancline hybrid using thin dielectric layers," IEEE Microwave Guided Wave Lett., vol.MGL-1, pp.346-347, Nov.1991.
[24] 小川、他, "光ファイバを用いたミリ波信号伝送用フィーダ系の検討," IEICE技術報告, OCS91-65, Nov.1991.
[25] D.Polifko and H.Ogawa, "High-speed modulation characteristics of millimeter-wave fiber optic links," IEICE技術報告, OCS91-66, Nov.1991.
[26] H.Ogawa et al., "Fiber-optic microwave transmission using harmonic laser mixing, optoelectronic mixing, and opticall pumped mixing," IEEE Trans. Microwave Theory Tech., vol.MTT-39, pp.2045-2051, Dec.1991.
[27] 馬場、長谷川、小川, "多層化MMICによる超小型ハイブリッド回路の構成と特性," IEICE技術報告, MW91-109, Dec.1991.
[28] 小川、他, "1991年IEEE MTT-S国際マイクロ波シンポジウムワークショップ出席報告," IEICE技術報告, MW91-120, Dec.1991.
[29] H.Kamitsuna and H.Ogawa, "Novel slow-wave meander lines using multilayer MMIC technologies," IEEE Microwave Guided Wave Lett., vol.MGL-2, pp.8-10, Jan.1992.
[30] 大畑、徳満、高木、厚木、渡辺、小川, "MMICの今後の技術展望・高性能化・高機能化・小型化," IEICE技術報告, MW91-148, Jan.1992.
[31] T.Hasegawa, S.Banba and H.Ogawa, "A branchline hybrid using valley microstrip lines," IEEE Microwave Guided Wave Lett., vol.MGL-2, pp.76-78, Feb.1992.
[32] 小川、他, "光マイクロ波集積回路の構成法," IEICE春季大会, C-94, Mar.1992.
[33] 馬場、上綱、小川, "HEMT光応答特性の基礎検討," IEICE春季大会, C-95, Mar.1992.
[34] 上綱、馬場、小川, "HEMT MMICの光・マイクロ波周波数混合特性とその応用に関する検討," IEICE春季大会, C-96, Mar.1992.
[35] 竹中、小川, "小型・広帯域MMICバランス型アップコンバータ," IEICE春季大会, C-77, Mar.1992.
[36] 小川、他, "ミリ波信号伝送用光ファイバリンクの構成," IEICE春季大会, B-426, Mar.1992.
[37] D.Polifko and H.Ogawa, "Optical modulation method suitable for high carrier frequencies and suppressed carrier transmission," IEICE春季大会, B-427, Mar.1992.
[38] 中條、大滝、小西、上原、藤瀬、竹中、小川, "DBFとMMICを備えた移動体衛星通信用アクティブコンフォーマルアレーの試作," IEICE春季大会, B-52, Mar.1992.

[39] D.Polifko and H.Ogawa, "The merging of photonic and microwave technologies," Microwave Journal, vol.35, pp.75-80, Mar.1992.
[40] 上綱、小川, "受光素子の光・マイクロ波周波数混合特性の光ファイバ無線通信リンクへの適用," IEICE技術報告, MW92-5, Apr.1992.
[41] D.Polifko and H.Ogawa, "Fiber optic link architectural comparison for millimeter wave transmission," Proc. SPIE, Optical Technology for Microwave Applications VI, vol.1703, pp.228-239, Apr.1992.
[42] 小川、他, "ミリ波サブキャリア伝送用光ファイバリンクの検討," IEICE技術報告, MW92-37, May 1992.
[43] S.Banba and H.Ogawa, "Novel symmetrical three-branch optical waveguide with equal power division," IEEE Microwave Guided Wave Lett., vol.MGL-2, pp.188-190, May 1992.
[44] H.Ogawa et al., "Fiber optic millimeter-wave subcarrier transmission links for personal radio communication systems," IEEE MTT-S Int. Microwave Symp. Dig., pp.555-558, Jun.1992.
[45] H.Ogawa et al., "Fiber optic microwave links using balanced laser harmonic generation, and balanced/image cancellation laser mixing," IEEE MTT-S Int. Microwave Symp. Dig., pp.559-562, Jun.1992.
[46] T.Takenaka and H.Ogawa, "Miniaturized MMIC mixers; Image rejection and balanced mixers using multilayer microstrip lines and Line-Unified HEMT modules," IEICE Trans.Electron., vol.E75-C, pp.689-697, Jun.1992.
[47] T.Hasegawa, S.Banba and H.Ogawa, "Multi-branch power dividers using multilayer MMIC technology," IEICE Trans.Electron., vol.E75-C, pp.707-712, Jun.1992.
[48] S.Banba, T.Hasegawa and H.Ogawa, "Novel MMIC transmission lines using thin dielectric layers," IEICE Trans.Electron., vol.E75-C, pp.713-720, Jun.1992.
[49] H.Kamitsuna and H.Ogawa, "Reduced-size double crosstie slow-wave transmission lines for MMICs," IEICE Trans.Electron., vol.E75-C, pp.721-728, Jun.1992.
[50] 馬場、上綱、小川, "マイクロ波・ミリ波デバイスによる光検出の検討," IEICE技術報告, MW92-56, Jun.1992.
[51] D.Polifko, H.Ogawa and T.Kitazawa, "Millimeter-wave optical transmission with combination narrowband EOM and laser modulation," Fourth Optoelectronics Conf. (OEC'92) Tech. Dig.,pp.250-251, Jul.1992.
[52] H.Ogawa et al., "Ka-band FM video subcarrier transmission using monolithic integrated HEMT photodetector," Fourth Optoelectronics Conf. (OEC'92) Post-Deadline Paps. Tech. Dig.,pp.22-23, Jul.1992.
[53] 小川、他, "1992年IEEE MTT-S国際マイクロ波シンポジウムワークショップ出席報告," IEICE技術報告, MW92-68, Jul.1992.
[54] H.Kamitsuna and H.Ogawa, "Fiber optic microwave links using image canceling photodiode mixing," Asia-Pacific Microwave Cof. Proc., pp.309-312, Aug.1992.
[55] T.Takenaka and H.Ogawa, "A miniturized, ultra-wideband MMIC balnced up-converter using a Line Unified HEMT module and multilayer microstrip lines," Asia-Pacific Microwave Cof. Proc., pp.331-334, Aug.1992.
[56] T.Kitazawa, D.Polifko and H.Ogawa, "Analysis of CPW for LiNbO3 optical modulator by extended spectral-domain approach," IEEE Microwave Guided Wave Lett., vol.MGL-2, pp.313-315, Aug.1992.
[57] H.Ogawa et al., "Millimeter-wave subcarrier transmission using optoelectronic mixing and optical heterodyne techniques," Proc. URSI Int. Symp. Sig. Sys. Electron., pp.561-564, Sept.1992.
[58] 小川、他, "1992年IEEE MTT-S国際マイクロ波シンポジウム報告," IEICE技術報告, MW92-72, Sept.1992.
[59] 末松、馬場、上綱、小川, "マイクロ波HBTの光検波器への適用," IEICE技術報告, MW92-76, Sept.1992.
[60] H.Ogawa et al., "Optical/microwave monolithic integrated circuits," MWE'92 Microwave Workshop Dig., pp.191-196, Sept.1992.
[61] D.Polifko and H.Ogawa, "Millimeter-wave fiber optic technologies for cellular personal communications," MWE'92 Microwave Workshop Dig., pp.299-304, Sept.1992.

[62] H.Ogawa et al., "Optical/microwave circuits technologies for microwave and millimeter-wave fiber optic links," Proc. Int. Symp. Antt. Prop., pp.825-828, Sept.1992.
[63] H.Kamitsuna and H.Ogawa, "Fiber optic balanced photodiode mixing links," Proc. Int. Symp. Antt. Prop., pp.829-832, Sept.1992.
[64] 馬場、上綱、小川, "HEMT光応答を用いたMMIC光受信機," IEICE秋季大会, C-73, Sept.1992.
[65] 末松、馬場、上綱、小川, "マイクロ波HBT光検波器," IEICE秋季大会, SC-1-4, Sept.1992.
[66] 上綱、馬場、小川, "HEMT の光・マイクロ波周波数混合に関する一検討," IEICE秋季大会, SC-1-5, Sept.1992.
[67] D.Polifko and H.Ogawa, "Design and characterization of high-speed external modulators for millimeter-wave optical communication," IEICE秋季大会, SC-1-6, Sept.1992.
[68] 小川、他, "レーザダイオードの非線型特性を用いた光ファイバリンクの検討," IEICE秋季大会, SC-1-7, Sept.1992.
[69] H.Thomas and H.Ogawa, "Indoor millimeter wave distribution over fiber optic links," IEICE秋季大会, B-334, Sept.1992.
[70] 北沢、D.Polifko、小川, "光変調器用共平面型導波路の解析," IEICE秋季大会, C-170, Sept.1992.
[71] T.Takenaka and H.Ogawa, "An ultra-wideband MMIC balanced frequency doubler using Line-Unified HEMTs," IEEE Trans. Microwave Theory Techn., vol.MTT-40, pp.1935-1940, Oct.1992.
[72] H.Ogawa et al., "Millimeter-wave fiber optics systems for personal radio communications," IEEE Trans. Microwave Theory Techn., vol.MTT-40, Dec.1992.
[73] H.Ogawa et al., "Fiber optic microwave links using balanced laser harmonic generation, and balanced/image cancellation laser mixing," IEEE Trans. Microwave Theory Techn., vol.MTT-40, Dec.1992.
[74] 小川, "光ファイバミリ波伝送技術," 電気学会ミリ波調査専門委員会, MD-15-2, Dec.1992.
[75] 北沢、D.Polifko、小川, "拡張されたスペクトル領域法による光変調器用共平面型導波路の解析," IEICE技術報告, MW92-, Dec.1992.
[76] H.Ogawa et al., "Fiber optic microwave subcarrier transmission links using laser diodes as receiving mixer," IEICE Trans. Electron., vol.E76-C, Feb.1993.
[77] T.Kitazawa, D.Polifko and H.Ogawa, "Simplified analysis of coplanar waveguide for LiNbO3 optical modulator by variational method," IEICE Trans. Electron., vol.E76-C, Feb.1993.
[78] H.Kamitsuna and H.Ogawa, "Fiber optic microwave links using balanced/image canceling photodiode mixing," IEICE Trans. Electron., vol.E76-C, Feb.1993.
[79] D.Polifko and H.Ogawa, "Comparison of traveling wave external modulator microwave mixers," IEICE Trans. Electron., vol.E76-C, Feb.1993.
[80] 小川, "ミリ波と光ファイバ," オプトエレクトロニクス, 38-2, Feb.1993.
[81] 小川、他, "光ファイバを用いた50GHz帯FM信号伝送実験," IEICE春季大会, Mar.1993.
[82] 馬場、上綱、末松、小川, "HEMT光検出器の雑音特性," IEICE春季大会, Mar.1993.
[83] 末松、馬場、上綱、小川, "MMIC HBT光検出器の周波数応答特性," IEICE春季大会, Mar.1993.
[84] 上綱、馬場、小川, "MMICプロセスを用いたモノリシックイメージ抑圧型光・マイクロ波周波数アップコンバータ," IEICE春季大会, Mar.1993.
[85] 松井、Polifko、小川, "導波路型ミリ波光変調器のオンウエハ評価方法の提案," IEICE春季大会, Mar.1993.
[86] 北沢、小川, "光変調器用電極の解析," IEICE春季大会, Mar.1993.
[87] H.Kamitsuna and H.Ogawa, "Characterization and application of lumped double crosstie slow-wave transmission lines," IEICE Trans. Electron., vol.E76-C, Jun.1993.
[88] H.Ogawa et al., "A comparison of noise performance between a PIN diode and MMIC HEMT and HBT optical receivers," IEEE MTT-S Int. Microwave Symp. Dig., Jun.1993.
[89] D.Polifko and H.Ogawa, "Design and on-wafer testing of millimeter-wave external optical modulators," IEEE MTT-S Int. Microwave Symp. Dig., Jun.1993.

[90] H.Kamitsuna and H.Ogawa, "Monolithic image rejection optoelectronic up-converters using the MMIC process," IEEE MTT-S Int. Microwave Symp. Dig., Jun.1993.
[91] T.Kitazawa, D.Polifko and H.Ogawa, "Analysis of LiNbO3 optical modulator using coplanar-type electrode," IEEE MTT-S Int. Microwave Symp. Dig., Jun.1993.
[92] H.Ogawa et al., "Fiber optic 50-Ghz FM subcarrier transmission using HBT device," URSI Meeting, Sept.1993.
（投稿中）
[93] D.Polifko and H.Ogawa, "Broadband frequency mixing with traveling wave external mixer," submitted to J. Lightwave Technolo.
[94] H.Kamitsuna and H.Ogawa, "Ultra-wideband MMIC active power splitter with arbitary phase relationship," submitted to IEEE Trans. Microwave Theory Tech.
[95] E.Suematsu and H.Ogawa, "Frequency response of MMIC HBT photodetectors," submitted to IEEE Microwave and Guided Wave Lett.
[96] H.Thomas and H.Ogawa, "Indoor millimeter wave PCN/LAN experiment based on direct MMW distribution over optical fiber and multipath robust spread spectrum modulation," submitted to VTC'93.
（特許）
[97] 小川, "光ファイバ無線通信方式," 特願平02-136679, May1990.
[98] 小川, "光リンク無線通信方式," 特願平02-158956, Jun.1990.
[99] 小川, "無線装置," 特願平02-217384, Aug.1990.
[100]上綱、小川, "光制御マイクロ波集積回路," 特願平02-278515, Oct.1990.
[101]竹中、小川, "共平面アンテナ," 特願平02-319917, Nov.1990.
[102]小川, "ファイバ無線機," 特願平03-056228, Jan.1991.
[103]小川, "ファイバ無線," 特願平03-056253, Jan.1991.
[104]神谷、小川, "アンテナ給電用光伝送システム," 特願平03-043489, Mar.1991.
[105]小川、他, "無線リンク用光伝送システム," 特願平03-115734, May1991.
[106]小川, "無線リンク用光伝送システム," 特願平03-164258, Jul.1991.
[107]D.Polifko, 小川, "光ファイバリンク," 特願平03-175057, Jul.191.
[108]竹中、小川, "モノリシックマイクロ波集積回路," 特願平03-221550, Sept.1991.
[109]小川, "移動体無線通信システム," 特願平03-300230, Nov.1991.
[110]小川、他, "高周波信号用伝送リンクシステム," 特願平03-310576, Nov.1991.
[111]竹中、小川, "マイクロ波周波数逓倍回路," 特願平03-344441, Dec.1991.
[112]上綱、小川, "マイクロ波遅波回路," 特願平04-046783, Mar.1992.
[113]上綱、小川, "マイクロ波遅波回路," 特願平04-123723, May 1992.
[114]上綱、小川, "光マイクロ波混合回路," 特願平04-180949, Jul.1992.
[115]D.Polifko, 小川, "周波数ミキサ装置," 特願平04-284249, Oct.1992.
[116]上綱、小川, "マイクロ波信号分配回路," 特願平04- , 1993.

1. はじめに

本章では、ミリ波と光ファイバがマイクロセルを用いた超小型携帯機用移動通信において不可欠であることを述べる。さらに、簡単な光ファイバリンク例を紹介して、サブキャリ周波数がどのように伝達されるのかを明らかにする。

1.1 なぜミリ波か？

第1.1図を見て頂きたい。この図はある都市における近未来の移動通信の１つの形態を示している。携帯電話は腕時計サイズまで小型化され、道路においても、建物の中でも通信ができる。さらに、携帯機は音声だけでなく、画像、データ等の広帯域情報も運ぶことができ、人間活動に大きな影響をもたらしている。このようなシステムでは膨大な数の携帯機、しかも画像等の信号も扱うため、無線基地局（例えばＮＴＴの鉄塔のある建物等にある）と端末間の無線周波数帯には広帯域性が要求される。例えば、極端に簡単化した例で示すと、テレビで見ている動画像で無線の周波数を直接周波数変調（ＦＭ）した場合に必要とされる周波数帯域は約40MHzであり、もしこの帯域を１つの端末に割り当てて１つの無線基地局で100端末を収容した場合の無線周波数帯域は4GHzとなる。ところで、現在の自動車・携帯電話に割り当てられている周波数はＮＴＴの場合片方向たかだか15MHzであり、直接周波数変調の場合１つの動画像も送れないことになる。また、現在のシステムで使用している無線周波数は900MHz帯であり、この周波数帯で多数の画像信号を伝送するのは困難である。これを解決できる１つの方法として、無線周波数にミリ波を用いることである。例えば、無線周波数に50GHzを用いた場合、先の4GHzは比帯域（＝帯域幅／無線周波数）にして８％、60GHzにすると７％であり、これらは現状のミリ波回路では実現し得る帯域である。これが近未来の移動通信にミリ波を用いる１つの理由である。

もう１つの理由はミリ波の伝搬する到達距離が短いことである。ミリ波は大気中の分子（酸素、水蒸気等）、降水（雨、雪等）により減衰する。例えば、無線周波数を60GHz帯に選ぶと酸素による吸収が顕著になり、約16dB/km減衰する。この特徴は逆に無線ゾーンを構成するときに利用できる。すなわち、収容する端末数が飛躍的に増大することが考えられるため、同一の無線周波数を繰り返して使用するマイクロセルゾーン（半径が数１００メートル程度の無線ゾーン、現在の自動車電話の首都圏における無線ゾーン半径は数キロメートル以内である）の検討が進められているが、上記減衰特性は信号の混信や干渉を軽減できるように利用でき、無線周波数を効率良く用いたシステムになる。また、無線ゾーンが小さくなれば、携帯端末の送信電力を低下させることもでき、このためさらに端末を小型化できるメリットもある。

このようなミリ波分配ネットワークが近未来通信の形態として有望であることが理解して頂けたかと思われるが、それでは次に問題となるのはいかにしてミリ波を無線基地局まで伝送するかである。同軸線路か、導波管か、あるいは無線で給電するのか。しかしながら、これらは非常に可能性が低いと考えられる。同軸線路の伝送損失は周波数のルートに比例して増大する。例えば、40GHzでは１メートルあたり約2.9dBであり、同軸でミリ波給電は非現実的である。一方、導波管では周波数に逆比例して減衰定数が小

さくなる伝搬モードがあり、ミリ波の伝送に適している。しかしながら、導波管分配網を都市内に配置するのも導波管の形状等を考慮した場合非現実的である。最も簡単な方法は無線で無線基地局にミリ波を給電することである。無線基地局の数が少なければよいが、マイクロセルゾーンのような多くの無線基地局数を必要とする場合には、多くの無線周波数を給電用に使用せざるを得なくなる。上述のようにミリ波は超短距離通信でその特徴をいかんなく発揮できるので、ミリ波を給電線に使用することは距離、周波数の干渉等いろいろと問題がある。それでは、何が最適な伝送媒体に成り得るのか。

1.2 なぜ光ファイバか？

光ファイバは長距離・大容量通信実現のための伝送媒体として用いられ、最近ではCATV等の光分配システムへの応用も盛んである。光ファイバの構造は図1.2に示すように、直径が約10μmのコア（屈折率n_1）と直径が約125μmのグラッド（屈折率n_2）から成る。材料は軽量な石英系ガラス等である。もしn_1がn_2よりも大きく、なおかつ入射角が特定の条件を満足すれば図のように光は全反射して光ファイバ中を伝搬する。屈折率の大きさの違いは比屈折率差と定義され、単一モードファイバの場合約0.3前後である。なお、光ファイバのパラメータの定義、伝搬モード等についての詳細は文献３を参照。このように、光ファイバの構造は他の線路に比し細径であり、そのため小型かつ軽量である。したがって、導波管よりもはるかに設置性に優れ、信号分配ネットワーク形成には適した伝送媒体と言える。

光ファイバの他の大きな特長は低伝送損失と広帯域性である。波長1.3μmで標準的に0.5dB/km以下が得られており、これは設置性に優れた同軸線路の伝送損失よりもはるかに低い値である。このため、システムの制御を行なう制御局と無線基地局の間の距離の自由度が大きくなり、数十ｋｍの伝送距離の確保も可能である。波長1.3μmは周波数約230THzに相当し、例えば60GHzは光の周波数の約0.03%であり、光の帯域ではミリ波の帯域は全く問題とならない。このため、ミリ波を多重化した信号も光ファイバで伝送できることになる。このように、光ファイバは多数のミリ波信号を低損失で所望の場所に伝送してマイクロセルゾーンを形成することのできる伝送媒体として非常に有望である。

1.3 サブキャリアとは何か？

それではミリ波をどのような伝送リンクで送ることが出来るのか。その前にこれから何回も使われるサブキャリアの用語の定義を与える。キャリアは変調信号を伝送するための搬送波として無線通信では使われているが、光ファイバを伝送路として用いる場合キャリアは1.3μm等の光になる。ミリ波信号は光キャリアを変調するための変調信号になるが、光レシーバーで検出後無線ゾーンに放射され、今度はミリ波がキャリアとなって端末機に変調信号を供給することになるため、サブキャリアと言われている。複数のミリ波信号（マイクロ波も含む）を多重化して光ファイバで伝送するシステムのことをSCM(Subcarrier Multiplexing)と呼ばれているのはこのためである。

まえおきが長くなってしまったが、ミリ波伝送用光ファイバリンクの基本構成例を図1.3に示す。他にも種々の構成のリンクが提案されているが、本稿では最も簡易化され

た例を示す。なお、ミリ波を直接伝送しないで低周波を伝送し、光レシーバー側でミリ波に変換する構成ももちろん考えられるが、ここでは省略する。ダウンリンク（制御基地局から無線基地局へのリンク）の基本構成要素は、光キャリアを発生する光源（LD: Laser Diode）、光キャリアをミリ波で強度変調する光外部変調器（EOM: External Optical Modulator）、光キャリアを伝送する光ファイバ、光キャリアから変調信号（ミリ波）を検出するための検波器（PD: Photodetector）である。その他の電気回路としては、ミリ波信号合成器、ミリ波増幅器、ミリ波放射器等である。また、無線基地局から制御基地局へのアップリンク例も図1.3に示しているが、端末からのミリ波信号レベルは一定ではない。もし、これらの受信信号で直接光を変調すると受信レベルの高い信号が歪んでしまう可能性が高い。そこで、受信レベルを一定にするため従来の無線装置で良く用いられているヘテロダイン方式でミリ波信号を低周波に周波数変換して受信レベルを一定にする。この信号で光の強度変調を行なえばよいが、周波数が低くなったために外部変調器を用いる必要がなく、LDの直接変調で低周波サブキャリアを制御基地局に伝送できるメリットがある。

1.4 ミリ波サブキャリア伝送特性

ここでは図1.3で示した伝送リンクを用いて画像信号がどのように伝送されるのかを示す。画像信号は図1.4に示す映像スペクトルを有するNTSC信号（ベースバンド帯域幅は約4MHz）であり、これをミリ波周波数変調器でミリ波帯に変換する（図1.4のスペクトラム１）。ここで示すサブキャリア周波数は26GHz帯である。このスペクトラムで光キャリアの強度変調を行なうが、使用した変調器はLiNbO3上に製作した進行波導波路型変調器である。なお、導波路型変調器については文献参照。サブキャリアを運んできた光信号は光検出器でサブキャリアに変換される。ここでは、超高速PINフォトダイオード（受信感度0.48mA/mW）を使用した。光検出器に関しては文献参照。フォトダイオードの検波出力スペクトラム２も図1.4に示したが、EOM入力からPD出力間には約70dBのリンク損失があり、そのため出力レベルが低下している。

図1.5はEOM-PIN間の伝送周波数特性を示す。参考のためLDの周波数特性も示しているが、低周波域において低いリンク損失が得られてる。FM伝送路の評価は信号対雑音比（SNR: Signai-to-Noise Ratio）を用いて行なわれているが、評価SNRとして約63dBの高い値を光ファイバリンクを用いても得られている。

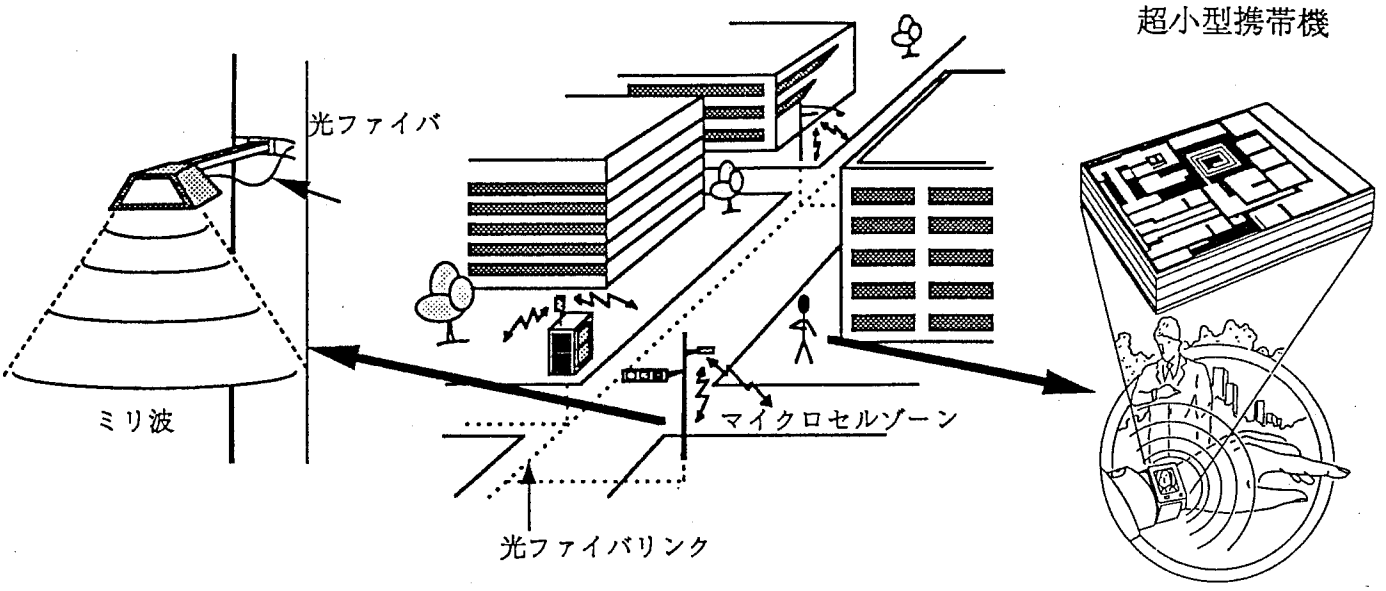

図 1.1　光ファイバリンクを用いたマイクロセルミリ波移動通信システムイメージ

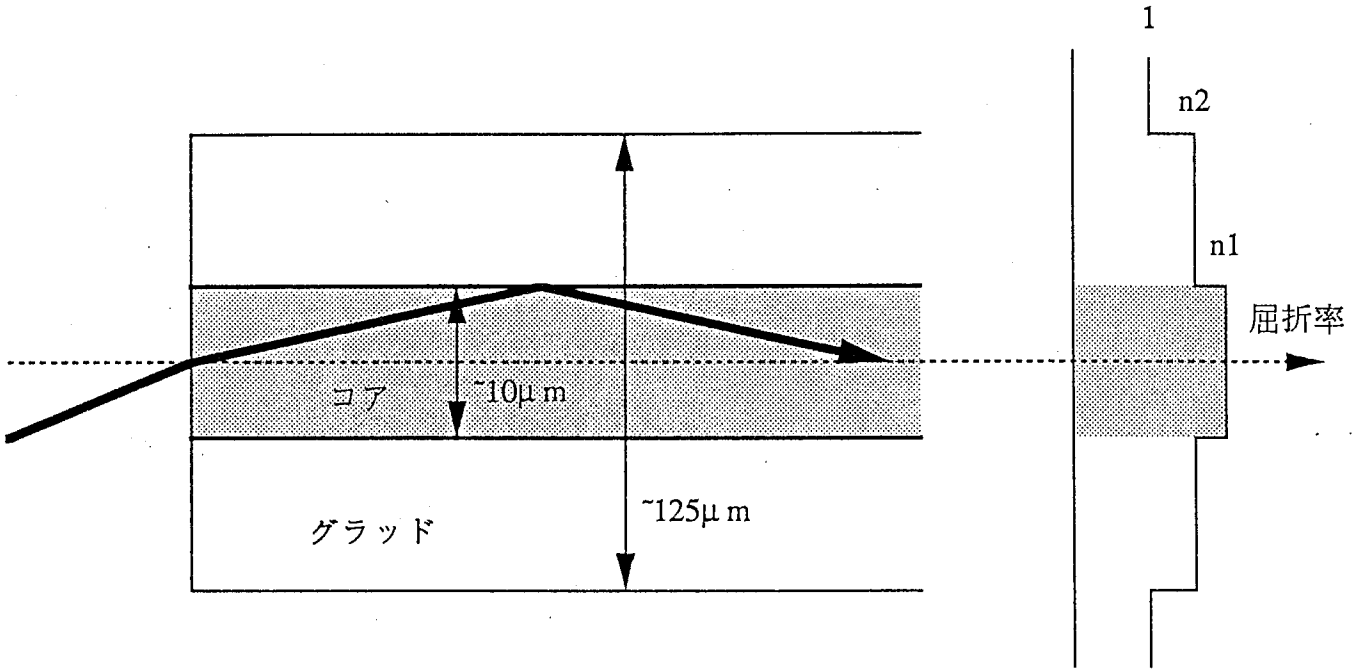

図 1.2　光ファイバの断面と光キャリアの伝搬

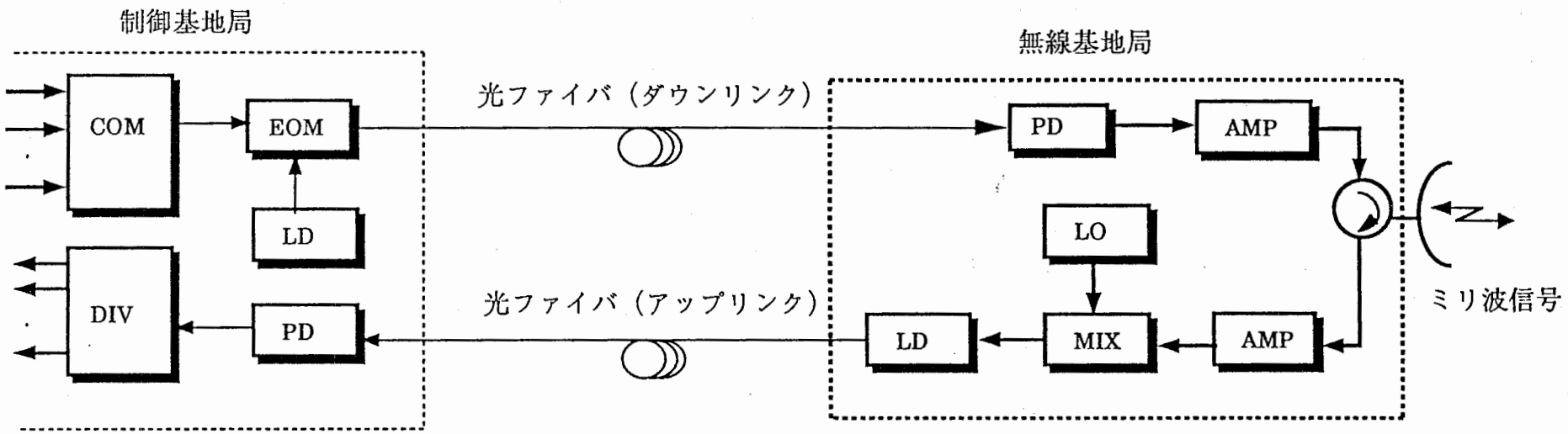

図 1.3　光ファイバリンクの基本構成
LD: レーザダイオード、PD: フォトダイオード、EOM: 外部変調器、
LO: 局部発振器、MIX: 周波数変換器、AMP: 増幅器、COM: 合成器、DIV: 分配器

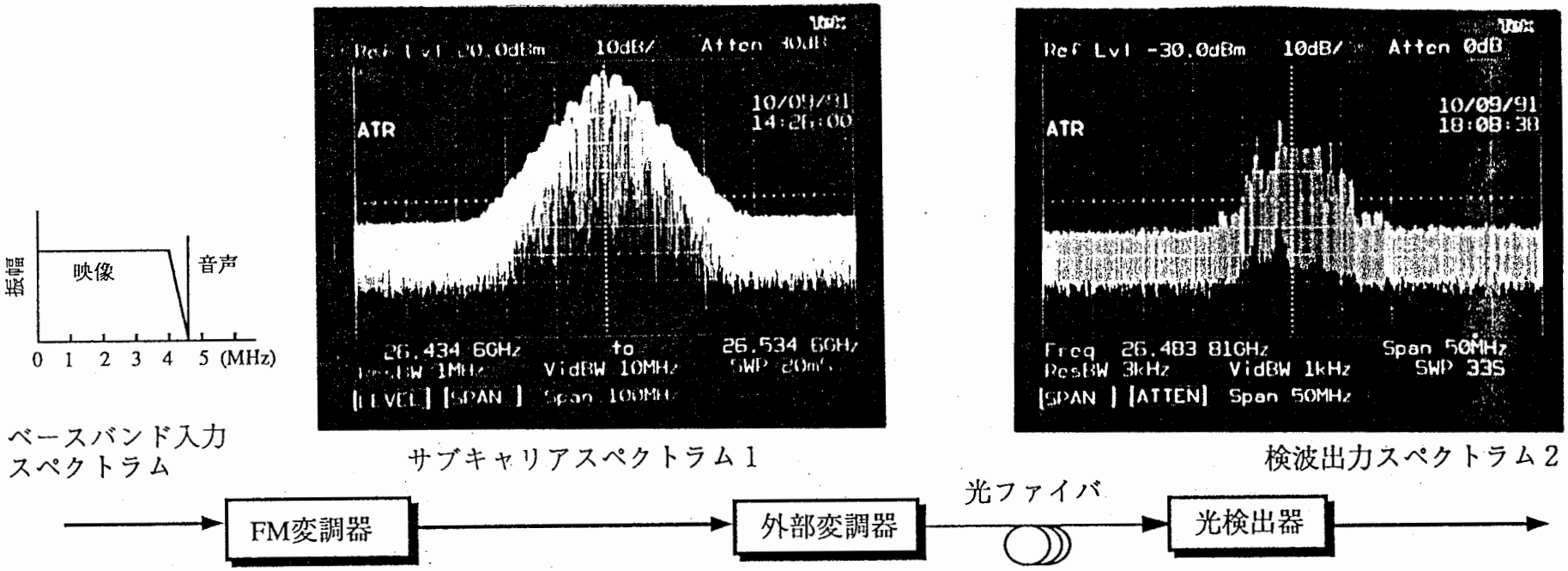

図 1.4　光ファイバリンクにおける映像信号スペクトラム
サブキャリア周波数は26GHz帯を使用

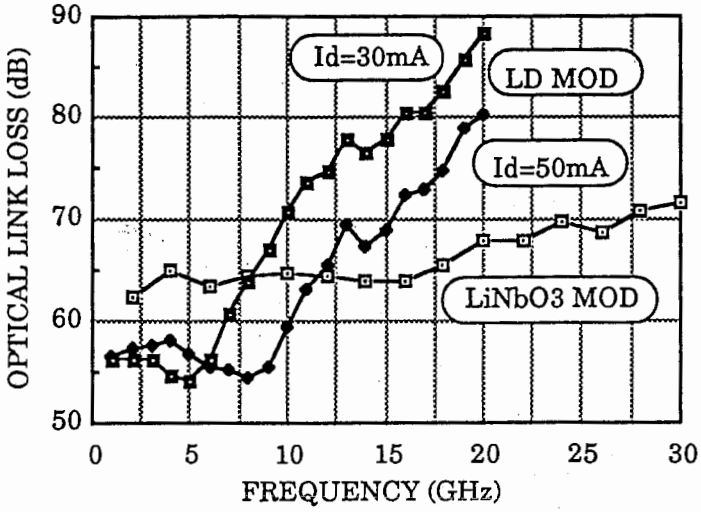

図 1.5　光外部変調器と光検出器間のリンク損失周波数特性。Idはレーザダイオードのバイアス電流であり、周波数特性はバイアス電流に影響される。

2. 光ファイバミリ波分配ネットワーク構成法

本章では、第１章で述べたシステムの概要について光ファイバリンクの構成法も含めて議論する。

2.1 MILLIMETER-WAVE FIBER OPTIC FEED CONCEPT

The system concept of the fiber optic millimeter-wave subcarrier transmission link is shown in Fig. 2.1. A large number of modulated millimeter-wave subcarriers are combined electrically by power combiners. The optical carrier is intensity modulated by this composite signal, transmitted by single-mode fiber, and is then optically divided at each radio base station. The tapped optical signal is directly detected by a high-frequency photodetector and amplified by MMIC amplifiers. The amplified millimeter-wave signals are subsequently radiated into the microcell zone (down link) and received by portable communication terminals.

Each radio base station also receives millimeter-wave signals from the portable terminals and down-converts them to RFs by using a frequency converter and local oscillator signal. The down-converted signals are used to intensity modulate a relatively inexpensive and low frequency laser diode. The optical signals from each radio base station are combined and then transmitted back to the central base station over singlemode fiber. The received optical signals are detected, amplified and demultiplexed (up link).

Because of the site-specific location of each radio base stations (e.g. light posts, telephone boxes, sides of buildings, etc.) they must be small and should broadcast over limited (less than several 100 meters) and well defined areas (within a city block or within one floor of a building for example). To avoid frequency interference between adjacent zones, different millimeter-wave subcarrier frequencies are utilized within two adjacent zone. Simultaneous use of fiber optic distribution links and millimeter-wave frequencies provide the following advantages within microcellular systems:

1. Fiber optic transmission lines have practically zero loss for lengths less than one kilometer. Thus cell spacing is limited only by the millimeter-wave radio signal transmission range, propagation effects such as multipath fading, and attenuation due to rain. Additionally, the technology for fiber optic communication is maturing to the point of being financially and technologically competitive with all electrical broadcast systems.

2. Millimeter-waves are essentially broadband frequencies which can transmit a large number of video/voice subcarriers. For example, an FM-modulated 4.2 MHz NTSC video signal requires a 36 MHz transmission bandwidth. If the channel separation is 40 MHz with 100 channels being

transmitted, the resultant radio frequency bandwidth is 4 GHz. At a 60 GHz subcarrier frequency, the relative bandwidth is only 7 percent.

3. Millimeter-waves are readily absorbed by oxygen and water molecules. At 60 GHz there is an absorption peak (16 dB/km) due to atmospheric oxygen. At a transmission frequency of 60 GHz for example, this absorption effect can be selectively exploited to limit signal propagation beyond the microcell boundaries. However, local regulations governing frequency usage need to also be considered in choosing subcarrier frequencies in the final system implementation.

4. The system control functions, such as frequency allocation and a modulation/demodulation scheme, can be located within the central base station. This simplifies the design of the radio base station, more so if the subcarrier frequency is distributed from the central base station. The primary functions of the radio base stations are optical/RF conversion, RF amplification, RF down conversion, and RF/optical conversion. Because all of the components required for these functions are analog devices, monolithic integration technologies can be adopted to configure radio base station hardware.

2.2 ARCHITECTURAL CLASSIFICATION

It is generally assumed that the typical signal format for a very high-speed fiber optic link will be a baseband data signal modulating a microwave/ millimeter-wave (MMW) carrier reference. We can also assume that the data format is irrelevant and that the data bandwidth is the primary concern for most applications. Typically, F.O. link architectures are designed to be broadband. Alternatively, by designing for narrowband operation, improved performance can be realized, especially at millimeter-wave frequencies. Frequently, the extent of the carrier frequency is considered the most important criteria in selecting opto-electronic devices. Thus, in establishing a common basis on which to compare several microwave F.O. links, we realize that the ultimate goal should be to deliver as much undistorted information as possible over a specified distance at a given carrier frequency.

The twelve F.O. link architectures under consideration are shown in Fig. 2.2. The length of each optical fiber is application-dependent and can span from several meters to a few kilometers (<3 at 50GHz - single mode). Likewise, each amplifier and mixer has characteristics particular to the bandwidth and gain needs for its architecture. Architectures 1 through 6 are of the direct modulation types and architectures 7 through 12 are considered externally modulated links. For two-way communication links, two separate F.O. links would be required. Within the scope of this study, only unidirectional communication is considered for each architectural format. The architectures are named and described as

follows:

1. Local data mixing, direct modulation
2. Dual fiber remote data mixing, direct modulation
3. Laser diode mixing
4. Photodiode mixing, direct modulation
5. Remote LO control, direct modulation
6. Single fiber remote data mixing, direct modulation
7. Local data mixing, external modulation
8. Dual fiber remote data mixing, external mod.
9. Photodiode mixing, external modulation
10. Single fiber remote data mix., dual modulation
11. Dual modulation, amplitude modulation
12. Dual modulation with carrier suppression

2.2.1 Directly Modulated F.O. Links

Link No.1 is a conventional F.O. link in which the data signal is up-converted by the MMW carrier reference before laser bias current modulation. Of the twelve architectures, this one in principle is the most elementary to design, fabricate, install and maintain. However, when operated at MMW frequencies, this architecture suffers numerous limitations. The foremost limitations are high insertion loss, high noise figure, and poor dynamic range. The later two problems arise from the proximity of the MMW carrier frequency to the relaxation oscillation peak of the laser diode. The link insertion loss is a function of device responsivity, impedance mismatch and light coupling. Additional concerns over operational reliability are introduced when the value of the laser diode's bias current is driven high to obtain the desired bandwidth response by extending the diode's relaxation oscillation frequency. Even with reactive impedance matching of the devices and good light coupling, insertion loss can still be as large as -35dB with a noise figure of about 65dB near 20GHz for a 3 percent bandwidth6. In this design, there is a notably large trade-off between simplicity and system performance. The laser diode is the limiting factor of system performance in this architecture.

Architecture No. 2 is a well known alternative to link architecture No. 1. By transmitting the data signal and carrier reference separately over different F.O. links, the performance of each link can be optimized for each particular frequency and bandwidth. Separation of these signals can significantly increase dynamic range. Up-converted system insertion loss can be reduced to zero, if high gain data links and a carrier reference post detection amplifier are used as shown in the figure. This would require a data link gain equal to the mixer conversion loss, a

situation previously demonstrated. Once again, the laser diode in the carrier reference link is the limiting component that prohibits ultra-wideband performance. Using a sub-harmonically injection-locked oscillator in the carrier reference link could also extend the bandwidth considerably, but this would make the link complex and increase the cost.

By using the optical diode as a MMW mixing element, architectures Nos. 3 and 4 can be implemented. J.J. Pan has demonstrated laser diode mixing properties that show potential for efficient mixing in both an up and down conversion configuration in the lower microwave bands20. D.K. Donald et al., however, not only showed good mixing efficiency, but also demonstrated extended bandwidths of the photodiode up to 80GHz. Once again, arguments similar to the first two apply to links 3 and 4, with respect to the mixing location. Injecting a high frequency up-converted data signal into the laser is not as beneficial as optimizing separate links and then mixing after the two signals are detected in separate photodiodes. Of the two architectures, poorer performance is therefore expected from the laser diode mixing architecture at MMW frequencies. Additionally, the photodiode is well suited to MMW mixing, being less sensitive to the high LO power than the laser diode. The possible benefits of these two configurations lie within the simplicity of their circuit designs. Essentially, MMW mixers are not needed, reduced local oscillator power can sometimes be used in the mixing process, and conversion gain is possible.

Architecture No. 5 is unique in that no MMW signals need to be transmitted by fiber. This eliminates the need for high speed lasers and photodetectors. Numerous stable, high-power output, miniature MMW oscillators are commercially available. The price, reliability, and frequency ranges are typically better than those for high-speed laser diodes. Low-frequency control signals or even crystal time-base signals for the remote oscillator can be sent over the same fiber by the same low-speed (a few GHz bandwidth) laser diode that transmits the data signal. For antenna remoting applications and personal communication cellular distribution networks, this configuration is quite beneficial. Signal distortion and noise arising from the laser are reduced by using low-frequency distributed feedback (DFB) lasers with low RIN. Alternatively, very low-frequency microwave signals can be sent to the optical receiver to be used for subharmonically injection locking the remote oscillator. For directly modulated links, this architecture has virtually unlimited high-frequency potential. It is interesting to note that this link architecture could be used in an externally modulated configuration. However, the additional cost and bulk required make this option less attractive.

The final directly modulated F.O. link architecture, No. 6, is very similar to

links 2 and 5. The major differences lie within a signal separating circuit at the electrical output of the photodetector. Filtering and amplification of the carrier reference are required. Subsequently, the amplified data and carrier signals are mixed in a conventional MMW mixer. More complicated methods that use the photodiode as a mixer in this configuration are also possible by applying feedback, thus eliminating the need for the external mixer. This architectures major benefit is that the laser diode is modulated with relatively low power levels, thus distortion is minimized and only one fiber is required. This scheme is also more economical than that of link No. 5 because the carrier reference is centrally located, and thus multiple remote oscillators are not needed for diverse systems. Using a sub-harmonically injection-locked oscillator in the carrier reference link, as suggested in architecture No. 2, could extend the bandwidth. In architecture No. 6, however, since only one laser and one photodiode are used, adding the additional circuitry would be more economical.

2.2.2 Externally Modulated F.O. Links

Link Nos. 7, 8 and 9 can be compared with their direct modulation counterparts, Nos. 1, 2 and 4. Within these externally modulated links, the laser (either diode or solidstate) is operated in a cw mode and therefore does not experience frequency chirping or produce additional link distortion. Linearity and power consumption of the external modulator become the primary concerns when implementing these architectures. Best performance, irrespective of the external modulator, is obtained when low-noise and high-power solidstate lasers are incorporated, which can significantly lower the noise figure and increase gain and dynamic range.

As in the architectures requiring two separately optimized links, architecture Nos. 8 and 9 also benefit from separately optimized modulators. Unfortunately, the need for dual fibers, lasers, photodiodes and modulators makes these configurations costly and bulky. However, in configuration 9, the data signal EOM could be removed, allowing the laser (diode) source to be directly modulated and thus slightly decreasing the number of components and the cost.

The improved configuration of link No. 10 utilizes only one photodiode and fiber with a filter to separate the carrier and data at the output of the photodiode. Similar to link Nos. 7, 8 and 9, link distortion is dependent on the external modulators. However, in link No. 10, either the data or the carrier signal can be produced with the laser diode, and the remaining signal can be generated by the external modulator. This allows the designer to utilize the optimal components for each particular purpose. For example, a laser diode optimized for data frequency transmission could produce modulated data output, while a high-frequency, narrowband external modulator could be used to supply the carrier frequency

reference. In this example, the bandwidth of the external modulator can be as narrow as possible, thus reducing the driving voltage and improving the gain of the overall link.

Simplified versions of link No. 10 are given by link Nos. 11 and 12. Here, only one laser diode, one fiber and one photodetector are utilized. By injecting the directly modulated laser light into the external modulator, both signals emerge from the photodetector in addition to the up-converted data signal. A post-detection filter is all that is needed to choose the desired signal. In architecture No. 12, a short piece of fiber is used to feed-forward the original laser diode carrier signal. When that signal and the one from the EOM are combined, total cancellation of the original carrier occurs. Therefore, the photodiode only receives the up-converted sidebands and post-detection filtering is further simplified.

Unfortunately, architecture No. 12 can only reach frequencies within the bandwidth of the particular laser diode. Thus, unless laser diode harmonics are used, millimeter-wave frequencies are difficult to obtain. Architecture No. 11 is not limited by the laser diode's frequency response when the carrier frequency is applied to the EOM. This combination directly/externally modulated link shows the most promise for reaching MMW frequencies and does not limit the bandwidth of the data signal.

All which is required is a single frequency, resonant type high frequency EOM to obtain the desired carrier reference. The bandwidth of the laser diode determines the maximum bandwidth of the data signal. Also, cellular type distribution networks incorporating this architecture are very economical because the MMW source is centrally located. The EOM output power can be further divided and/or amplified in the optical domain to service a multitude of locations using the same transmitter. Therefore fewer oscillators are required per zone. This architecture is simple and economical and demonstrates a very high frequency potential.

2.3 ANALYTICAL COMPARISON METHOD

For this study, commercially available optical transmitters and optical receivers are used in each architecture. In configurations where two links are required (No.s 2, 4, 8, and 9), the second link is replaced by a direct coaxial connection. Any degradation in gain or noise performance due to the absence of the second link is taken into consideration. In this study only up-conversion configurations are discussed. Alternately, with the proper injection of signals, some of the links can be operated in a down-conversion configuration.

In all other studies analyzing directly and externally modulated F.O. links, parameters such as gain, noise figure, dynamic range, and linearity were

measured or calculated from the laser's input to the photodetector's output. Since many of the architectures being considered in this paper include several diodes, fibers or links in general, these parameters are redefined.

F.O. link gain is defined over the whole system, i.e. from the input data signal level to the output of the up-converted signal level. Thus, for example, conversion loss of external mixers or filter insertion loss, if present, is also included in the gain definition. This provides a better system comparison than the individual optical link gain (from laser input power to photodiode output power) because the F.O. links within each architecture could have potentially different RF gains when optimized for specific applications. Other figures of merit such as noise figure, linearity, bandwidth and conversion loss (or system gain) are also described in terms of the whole system architecture.

Each of the F.O. links is characterized with respect to gain, noise figure, dynamic range, and linearity for frequencies within the opto-electronic device's operating bandwidths. All values obtained are considered representative for generally available devices and are the foundation of this study. Additionally, a separate analysis is performed which considers the many possible system improvements and the incorporation of state-of-the-art devices. These results are considered to indicate the optimal performance that can now be accomplished. Finally, each link is evaluated on the basis of its millimeter-wave performance potential.

2.4 EXPERIMENTAL SYSTEM COMPONENTS

Commercially available transmitter and receiver modules from Ortel are used. The 1.3um laser diode packages have SMA connectors for RF signal input, and light is output through pigtailed 9/125um fibers. Broadband matching is employed through a series 47 Ohm resistor. Threshold currents range from 16 to 21mA, and the diode's 3dB electrical bandwidths are approximately 5GHz (at 3Ith with a corresponding 2.9mW optical output power) and 10GHz (at 4Ith with a corresponding 7mW optical output power). The InGaAs PIN diodes have responsivities of approximately 0.9mA/mW and 3dB electrical bandwidths of 11GHz. The detector is a also broad-band resistively matched, and a short length of single mode fiber is pigtailed to the module. A short length of single mode fiber connects the two optical modules and careful attention is given to insure minimal reflection from the fiber optic connectors. For calibration and verification, 40GHz, 1.3um photodetector modules from New Focus are also used. Sumitomo Cement Corp. traveling wave LiNbO3 Mach-Zehnder modulators are used for the externally modulated links. They have usable bandwidths of 25GHz and optical insertion losses of approximately 6 dB. Operating voltages are 7-8Volts with

extinction ratios approaching 20dB.

A standard diode mixer with a conversion loss and noise figure of 8dB at 10GHz is used for link configurations 1, 2, 5, 6, 7, 8 and 10. A local oscillator power of approximately 10dBm is needed to drive the mixer efficiently. For link configurations 3, 5, and 6, the data and carrier signals are combined in a 0-40GHz microwave power combiner and are then supplied to the laser diode. In configuration 4, the local oscillator signal is supplied to the photodiode through a three port microwave circulator at port one. The photodiode is located at port two and the up-converted output is taken from port three. Wideband (0.5 to 26.5GHz) amplifiers from Hewlett Packard are used when required. Optical fiber losses are considered negligible.

An IF (data frequency) of 500MHz was chosen. As previously stated, all link configurations are operated in an up-conversion configuration. Similarly, the links could be used in a down-conversion configuration, but it has been observed that the optical devices, when used as mixers, are not as efficient under these conditions. This can be explained by the laser's decreased responsivity in transmitting signals around the relaxation oscillation frequency. Likewise, the photodiode exhibits reduced responsivity in detecting high-frequency signals because of package parasitics and carrier transit time limitations.

2.5 DISCUSSION OF RESULTS

Table 2.1 shows the summarized results of the twelve architectures. The comparison is divided into several areas explained as follows:

- **Carrier Frequency** - The frequency to which the data signal is up-converted. This number, for the present, represents what can typically be accomplished in laboratories. It is not necessarily the best ever obtained, but it is a repeatable value. For the future, it represents what could be achieved with expected advances and refinements in optical and electrical link components.

- **Gain at Carrier Frequency** - The link gain, or more typically the link insertion loss. This is defined from input data signal level to output level of the up-converted sidebands.

- **Noise Figure and Dynamic Range** - Both of these figures of merit are presented in a relative manner. Both numbers are highly dependent on the optical source and are compared by using the best and most appropriate optical source for each particular architecture. A low noise figure is considered less than 30dB, whereas medium and high noise figures are 30-45dB and >45dB respectively.

Dynamic range (either spurious free or compression) is a function of the system gain, noise, and linearity. It is more difficult to estimate given the wide range of the system variables, but as a reference, the largest spurious signal-free dynamic range reported to date by Ackerman et. al. is 117dB•Hz2/3.

Overall, the system performance limitations of each architecture have been found to depend on either the optical source or the external modulator. Laser bandwidth, RIN and nonlinearity are three factors which limit the maximum carrier frequency and other characteristics. These factors are functions of the bias current and, to a lesser extent, the modulation index. Only in the case of the laser mixer is nonlinearity beneficial. Thus, when laser diodes are used, the bias point greatly affects performance and should thus be carefully chosen to exploit the optimal laser characteristics. When solidstate sources are used, typically the noise (RIN <-165dB/Hz) is very small. In this case the optical output power and the external modulator switching power are important.

The photodiode bandwidth or nonlinearity is not a matter of concern, considering the commercial availability of 60GHz detectors. Optical illumination power must be chosen carefully so as not to saturate the detector, thus limiting the gain and dynamic range of externally modulated architectures (gain column,Table 2.1).

Use of laser or photodiode harmonics is one way to achieve high-frequency operation without the need for high bandwidth lasers and photodetectors. This reduces system complexity and cost, but can sometimes compromise the reliability of the devices as well as degrade system performance through the addition of noise and additional nonlinearities. This is particularly true of the laser diode mixer whose potential in the millimeter-wave bands is limited.

The system gain of most of the architectures can be significantly improved with such methods. Most of these capabilities now exist and require minor modification of design techniques. In this study, it has been shown that carrier frequency extension is primarily dependent on the development of narrowband external modulators. LiNb03 design processes are mature and should continue to yield higher operating frequencies. Although, the use of alternate materials, such as nonlinear optical polymers (NOP) or semiconductor substrates have much potential and should also be considered. A recent NOP modulator has been fabricated and has demonstrated 3dB bandwidths greater than 40GHz. As shown in Table 2.1, carrier frequencies approaching 60GHz are feasible within the next several years.

- **Complexity** - The number of general components (mixers, power combiners,

etc.), power supplies, MMW sources, filters and optical components (lasers, photodetectors, fibers, etc.) are compared to give a relative measure of system complexity. Additionally, the extent of the control circuitry, as in architecture No. 5, is considered to increase the complexity by requiring data processing elements to control the local oscillator frequency, phase and amplitude.

- **Relative Cost** - The primary consideration in evaluating cost is the optical source and/or external modulator. Additionally, the required device bandwidths, number of amplifiers, MMW sources and other costly components contribute to this measure.

A major difference between the architectures presented is using one or two fibers to transmit the various signals. Obviously choosing only one laser, fiber and detector is preferable for simplicity and reliability. Cost is also an important issue for commercial applications of F.O. links. In diverse systems such as personal communication cellular distribution networks, costs quickly escalate when many links are implemented. The price of high-speed components is still prohibitively high, and in many cases, they are still commercially unavailable. Methods used in architecture Nos. 5 and 11 which only require 1 fiber however, demonstrate the potential for single-fiber systems which compare with or outperform their dual fiber counterparts.

Consideration must also be given to packaging the optical and electrical portions of the transmit and receive modules. Research has been performed by others that shows improved system performance by the integrating the optical and electrical portions of the modules. Reduced parasitics as well as overall reductions in size have been accomplished. Future trends will be based on the miniaturization of the optical hardware and replacement of hybrid circuitry with MMICs. This will reduce system complexity and cost and improve reliability.

- **Millimeter-wave Potential** - This percentage reflects the potential of the particular architecture to achieve millimeter-wave data transmission.

Given the obvious limitations of the laser diode modulation bandwidth (currently and in the near future), it is not foreseen that direct laser current modulation at fundamental frequencies will be feasible at millimeter wave frequencies. Although quantum well lasers are promising, adequate performance has not yet been demonstrated. Also, diode parasitics will continue to restrict the useable frequency response. Thus, architectures such as Nos. 2, 4, and 6-12 are prospective alternatives which, through either fundamental modulation,

harmonic generation, or external modulation, can provide the needed carrier reference frequencies.

The best of these alternatives (other than No. 5, which doesn't require direct MMW signal transmission) are the architectures using low noise laser sources and high-frequency external modulators. Laser diode chirp and high distortion in these architectures is essentially reduced due to the low modulation frequency. Likewise, performance is further enhanced in architectures such as No. 8, because of the ability to separately optimize each sub-link.

The best compromise between simplicity and performance though, occurs in architecture No. 11, where the data signal modulates the laser diode. In this architecture, a minimum number of components are required. Also, the availability of high power, low RIN and low bandwidth laser packages with optical isolators has increased. The remaining carrier frequency limitation depends solely on the EOM. Up-conversion performance for this architecture is data-bandwidth independent. This link is further analyzed to demonstrate its potential.

In the first experiment, the EOM carrier frequency is varied from 1 to 20GHz while the data signal (a 0.5GHz sinusoid) modulates the laser diode. Laser diode bias current and EOM bias voltage are optimized to obtain the highest up-converted power levels. Fig. 2.3 shows the resulting electrical power measured at the photodiode output. Data signal gain for this un-optimized link is approximately -43dB.

In the second experiment, shown in Fig. 2.4, video data at a sub-carrier frequency of 91.26278MHz directly modulates a low noise laser diode. The laser output is up-converted by the EOM to a microwave carrier frequency. The microwave carrier is incremented from 2-25GHz with the resulting system performance evaluated every GHz. Since the up-converted video signal power remains virtually at the same level across the EOM bandwidth, errorless signal transmission is obtained until 25GHz. It is concluded that if a narrow-band MMW modulator were available, similar performance would be obtained. We are currently designing such modulators with operating frequencies greater than 40GHz.

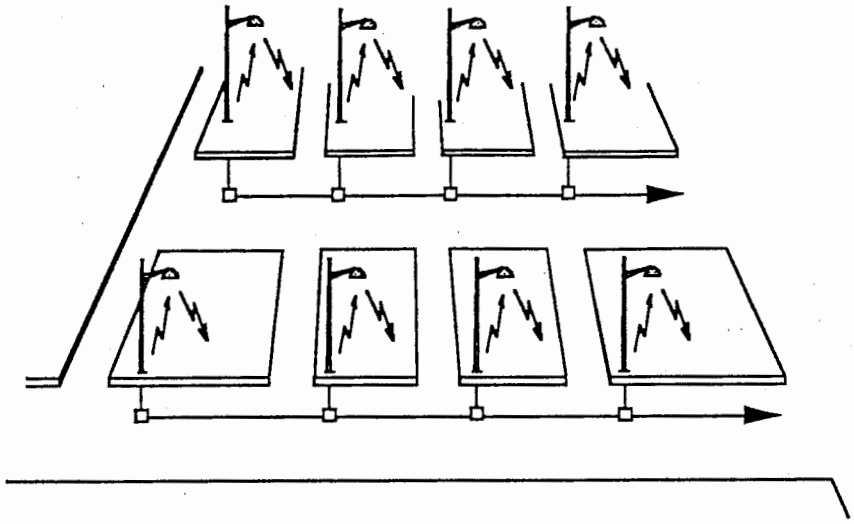

Outdoor Microcell Concept

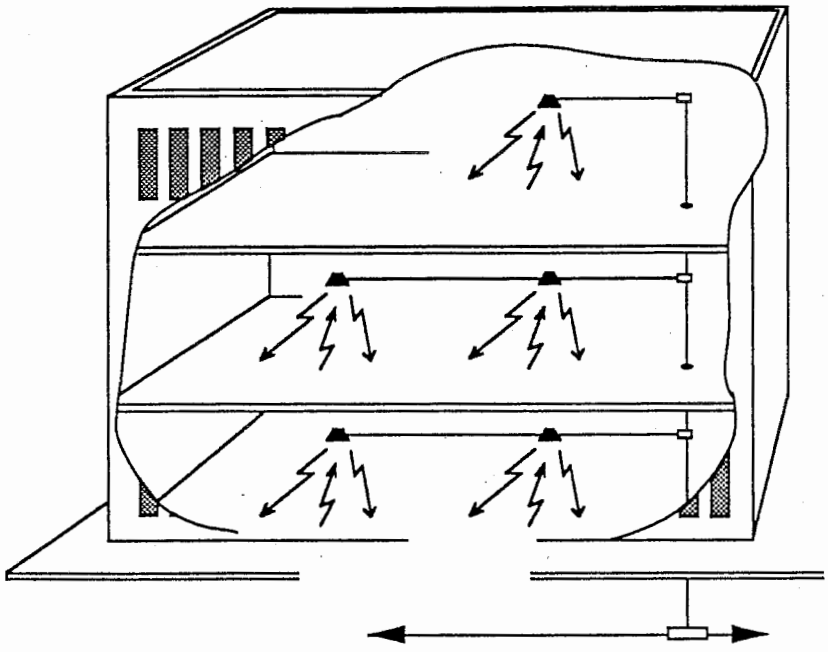

Indoor Microcell Concept

図2.1　光ファイバリンクを用いたミリ波分配ネットワーク概念図

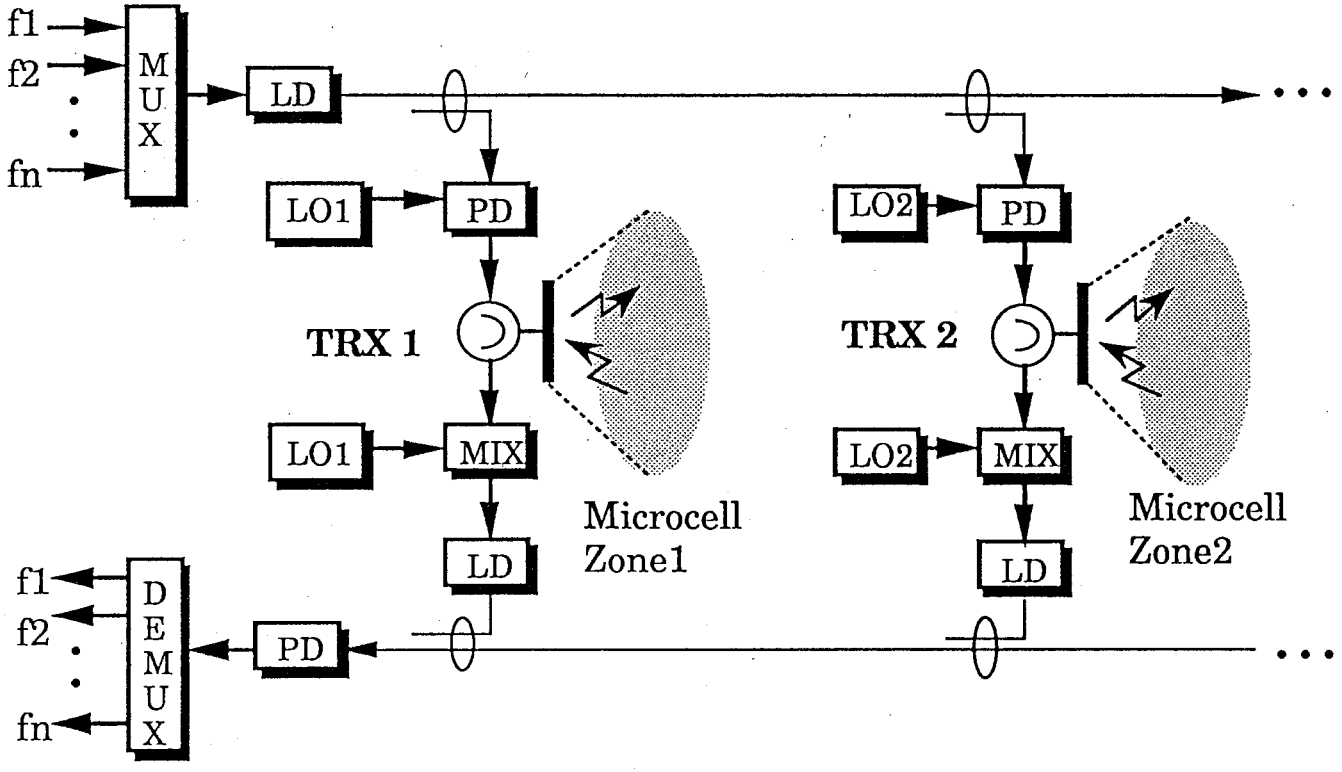

図2.1　光ファイバリンク構成図（続き）

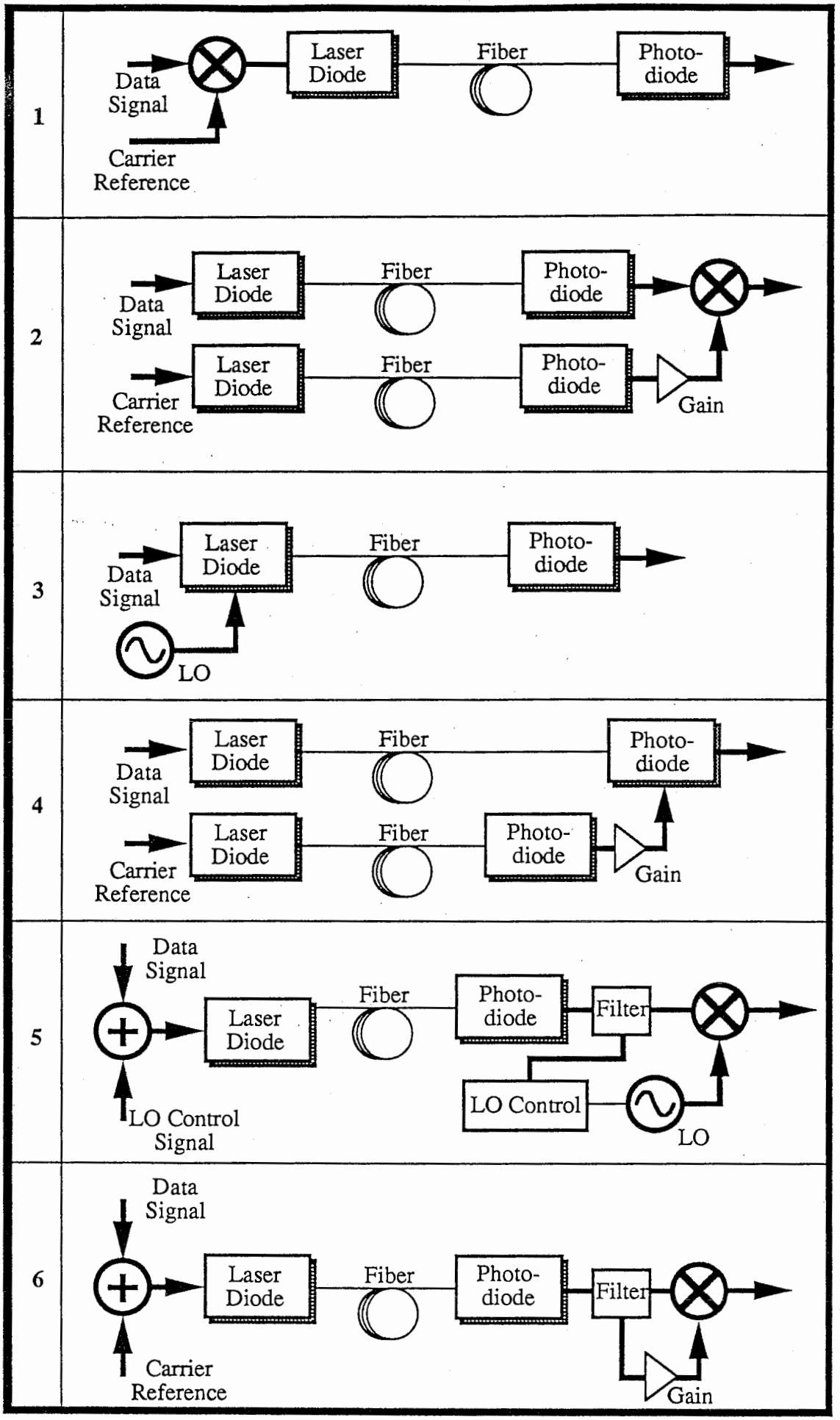

図2.2　ミリ波伝送用光ファイバリンクの構成

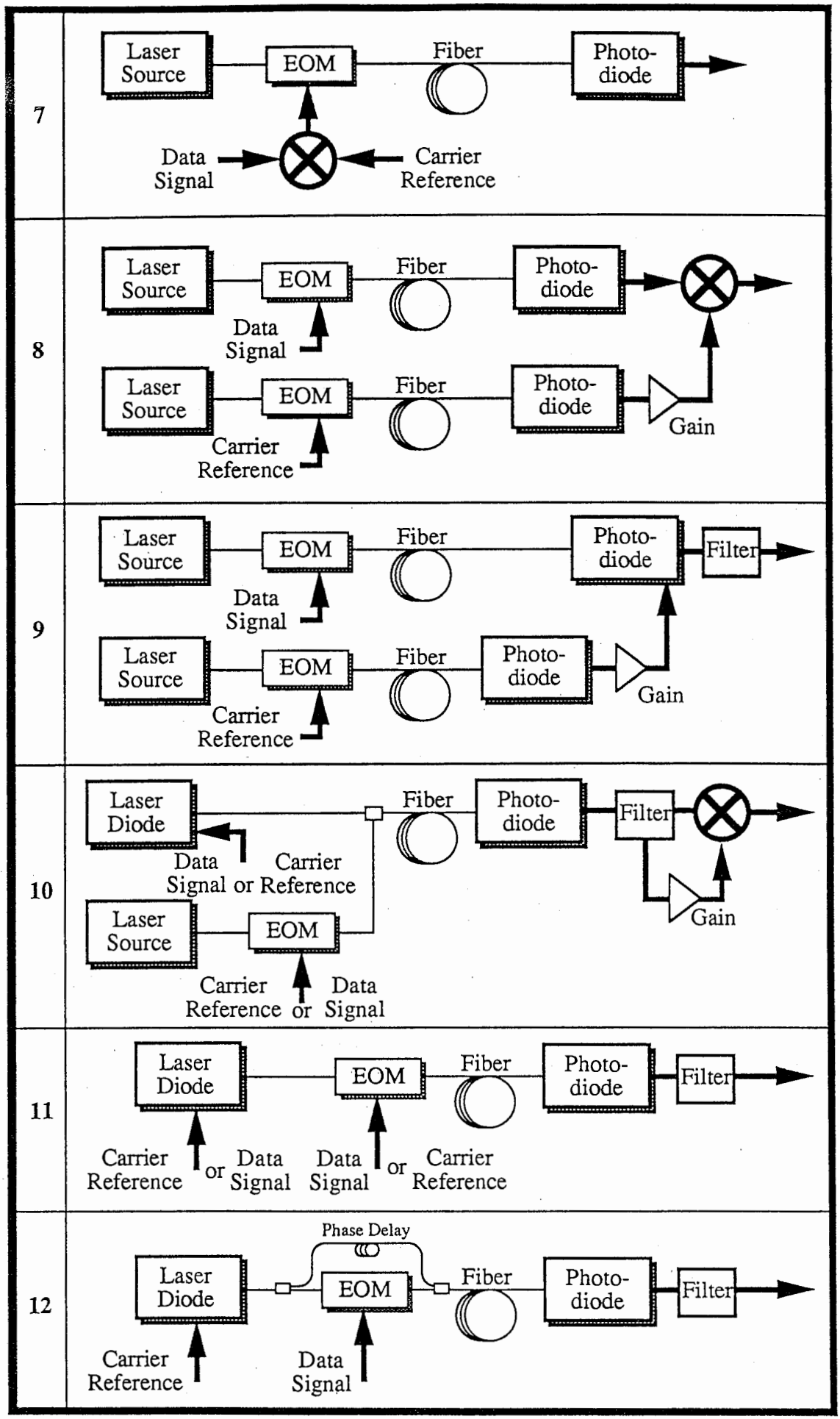
7
Laser Source
EOM
Fiber
Photo-diode
Data Signal
Carrier Reference
8
Laser Source
EOM
Fiber
Photo-diode
Data Signal
Laser Source
EOM
Fiber
Photo-diode
Gain
Carrier Reference
9
Laser Source
EOM
Fiber
Photo-diode
Filter
Data Signal
Laser Source
EOM
Fiber
Photo-diode
Gain
Carrier Reference
10
Laser Diode
Fiber
Photo-diode
Filter
Data Signal or Carrier Reference
Laser Source
EOM
Gain
Carrier Reference or Data Signal
11
Laser Diode
EOM
Fiber
Photo-diode
Filter
Carrier Reference or Data Signal
Data Signal or Carrier Reference
12
Phase Delay
Laser Diode
EOM
Fiber
Photo-diode
Filter
Carrier Reference
Data Signal

図2.2　続き

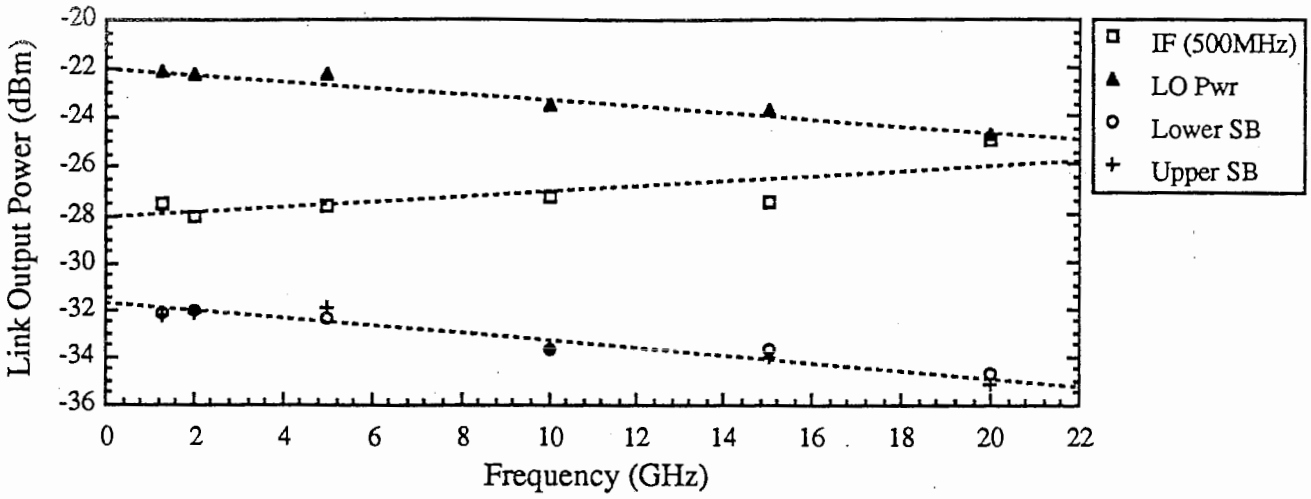

図2.3　Architecture No.11の出力周波数特性

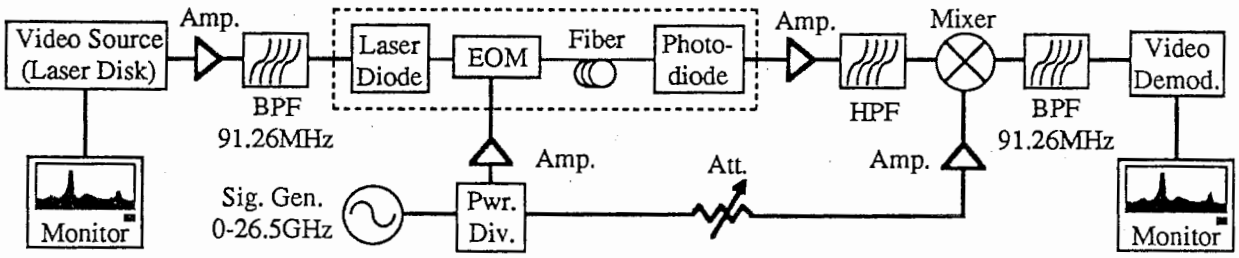

図2.4　Architecture No.11の画像伝送実験系

Table 2.1. Comparison of Potential Millimeter-wave Fiber Optic Links

Arch. No.	Carrier Frequency	Gain at Carrier Frequency	Noise Figure	Dynamic Range	Complexity (# Components)	Relative Cost	MMW Potential +	
			L-low M-med H-high	L-low M-med H-high	L-low M-med H-high	L-low M-med H-high		
	GHz	dB					%	Units
1	20 □	-27	H ●	L	L	M	40	Present
	25-35 □	-35 to -25	H ●	L	L	M		Future
2	20 □○	-3 to +8	M	M	M	H	60	Present
	25-35 □○	>+10	M	M	M	H		Future
3	20 □	-35	H ●	L	L	M	30	Present
	25-35 □	-25 to -35	H ●	L	L	M		Future
4	20 □○	-30	M	M	M	M	70	Present
	25-35 □○	-35 to -25	M	M	M	M		Future
5	Unlimited	-4 to +7	L	H	H	M	100	Present
	Unlimited	>+10	L	H	H	M		Future
6	20 □○	-25	H	M	M	M	60	Present
	25-35 □○	-35 to -25	M	M	M	M		Future
7	40	-40	M ■	M	L	M	80	Present
	45-50	-40 to -30	M ■	M	L	M		Future
8	40	-5 to 0	L ■	H	H	H	100	Present
	40-60	>0	L ■	H	H	H		Future
9	40	-40	L ■	M	H	H	100	Present
	40-60	-45 to -35	L ■	M	H	H		Future
10	40	-20	L ■	H	H	M	100	Present
	40-60	>-20	L ■	H	H	M		Future
11	40	-40	L	M	L	L	100	Present
	40-60	-45 to -40	L	M	L	L		Future
12	20 □	-35	H ●	L	M	M	60	Present
	25-35 □	-45 to -30	H ●	M	M	M		Future

Notes: □ Laser diode bandwidth limited
○ Carrier frequency can be extended by laser diode harmonics
■ Dependent on optical source responsivity and/or noise
● Laser diode RIN limited
+ MMW Potential (Millimeter-wave carrier frequency potential)

Present - best estimate of current technological capabilities
Future - best estimate of technological capabilities within span of several years

3. 光／マイクロ波集積回路（OMMIC）の光ファイバリンクへの適用

本章では、ミリ波分配用光ファイバリンク実現において重要である、無線基地局用デバイス技術の提案、およびこれを用いたミリ波サブキャリア伝送実験結果について述べる。

3.1 光／マイクロ波集積回路（Optical/Microwave Monolithic Integrated Circuits）

Optoelectronic Integrated circuits (OEICs) have received much attention since monolithic integration offers significant advantages in cost reduction, compactness and performance improvement. The GaAs-based OEICs are developed for short wavelength systems such as optical LAN and CATV networks, while the InP-based OEICs for long-haul and large-capacity transmission systems using long wavelength carrier. There have been proposed many kinds of OEICs which use different devices and different fabrication process. The performance of these devices becomes comparable to that of hybrid integrated circuits (HICs). However, despite many potential advantages of monolithic integration, OEICs have yet to outperform HICs because of their complicated fabrication process. In this paper, we are going to introduce the use of electronic devices (HEMT, HBT) as photodetectors which are made by monolithic microwave/millimeter-wave (MMW) integrated circuit (MMIC) process. The purpose of this work is not optimization of photodetector devices but monolithic integration of photodetector with MMW circuits on a single chip using the conventional MMIC fabrication process. This kind of MMICs is named as "Optical/Microwave Integrated Circuits" in this report.

MMIC technology has the potential to reduce the size and cost of electrical transceivers. Many MMW circuit functions have been realized by MMICs, and design, fabrication and measurement technologies for MMICs are becoming matured. These components are being utilized to configure not only MMW transceivers for radio but also optical/MMW transducers for fiber optic subcarrier transmission links. One of hardware alternative of optical/MMW transducer is an utilization of OEICs. However, the frequency range is limited below 10GHz. To overcome the above frequency problem, high-speed photodetectors can be integrated with MMW components in hybrid (HIC). In spite of the performance improvement by HIC technologies, they have cost, size and performance limitations due to the essential differences between the MMIC and discrete device fabrication process. Thus if the photodetection circuits can be fabricated by the current MMIC process, this technology is most promising to realize compact and cost-effective optical/MMW transducer.

In the following sections I will review photodetector technologies which can integrate other MMW devices. We will also describe the optical response of

MMIC-based photodetectors (HEMT, HBT), and show the experimental results of subcarrier transmission using LiNbO3 optical external modulator (EOM).

3.1.1 Monolithically Integrated Photodetecotrs

There have been a number of attempts to integrate photodetectors with amplifiers. The high-speed photodetector devices are classified into two groups, i.e. two terminal devices (diode) and three terminal devices (transistor). Two terminal devices are PIN diodes, Schottky barrier diodes (SBD), photoconductors (PCD), and metal-semiconductor-metal photodiodes (MSM-PD). Since PIN diodes are basically vertical structural devices, the fabrication process becomes more complicated than planar structural devices such as SBDs, PCDs and MSM-PDs. Although the PCDs have a large photocurrent gain, the available frequency bandwidth is lower than that of other SBDs and MSM-PDs. These two devices have demonstrated a 3-dB bandwidth in excess of 100GHz. Integration of MSM-PD with monolithic amplifiers are investigated for optical receiver applications.

As for the three terminal devices, HPT, MESFET, and HEMT have been studied for photodetectors. These devices except HPTs can realize not only photodetection functions but also MMW amplification or frequency mixing. Since all receiver components can be fabricated by the same MMIC process, monolithically integration of compact and cost-effective optical/MMW transducer is possible. HPTs have not been developed for MMW devices so far, it is difficult to produce optical/MMW transducer by HPT process. However, HBT devices are being developed for high-speed digital and high-frequency analog devices as electronic devices. If these electronic process-based HBTs can operate as photodetectors, HBT-based monolithic optical/MMW transducer is feasible. This will be discussed in following section. Other two devices, MESFET and HEMT are widely used in the commercial equipment and the performance of these devices is continuously improved using new material, new process and new circuit design methods. A lot of results are appeared in Ref.[5]. In addition to the application of MESFET and HEMT as MMW devices, these devices can be used as MMW optoelectronic devices which utilize the high-speed and high-frequency characteristics in the electrical domain.

3.1.2 Basic Performance of HEMT Photodetectors

The basic performance of HEMT and HBT photodetectors are evaluated using 0.83-μm wavelength carrier and LiNbO3 external optical modulator (EOM). Fig.3.1 shows the experimental setup for MMIC devices. Since the devices are fabricated on a GaAs wafer, we use an on-wafer probe station to measure the optical response. The input optical beam is focused within a spot diameter of

10μm. Fig.3.2 shows the schematic configuration of HEMT photodetector composed of three electrodes. A n-AlGaAs/InGaAs HEMT with a cutoff frequency of approximately 40GHz has a gate length of 0.25μm and gate width of 100μm.

A LiNbO3 EOM is used as the optical transmitter. Optical insertion loss is about 9dB and Vp for 100% modulation is 2.3V. Although a 3-db bandwidth of the EOM is 4GHz, the increase of the link loss is less than 10dB in the frequency range up to 20GHz. An ultra-wideband PIN photodiode (New Focus 1001) whose 3-dB bandwidth and responsivity are 40GHz and 0.52mW/mA, respectively, is used for comparison of HEMT detectors. Fig.3.3 shows the frequency response of HEMT detector as well as PIN device. At zero gate bias, the HEMT detector has a responsivity of 2.1mA/mW. Due to the difference of responsivity, the link loss of HEMT is 12-dB smaller than that of PIN. However, the experimental result shows 22-dB link loss improvement at 1-GHz subcarrier frequency. This large improvement is attained by the internal gain which decreases as frequency increases. At the frequency range above 15GHz, the link loss of HEMT becomes larger than that of PIN device. This frequency depends on the coupling efficiency which is defined how much optical power is supplied into GaAs layer. The electrode structure of HEMT is not suitable for optical beam input because of the straight pattern. Since the frequency response of MMW HEMT detector is not yet analyzed in detail, further investigation is required for realizing MMW photodetector.

3.2 Fiber Optic Data Link Performance

In order to demonstrate the principles of millimeter-wave subcarrier transmission over fiber optic links, we configured the link shown in Fig.3.4 with both 0.83μm and 1.3μm optical devices. The fiber optic link's performance is characterized both in terms of digital and analog signal transmissions as shown in the experimental setup in Fig.3.4(a). All system impedances are 50 Ohms. A bit error rate (BER) measurement is used to characterize both the directly modulated IF link and the externally modulation RF link. An FM analog modulation scheme is also used to evaluate both links. In all measurements, the Tx (transmitter) consists of amplifiers and filters, and where appropriate, an up-converter, all optimized to the frequency in use. The Rcvr. (receiver) contains similar components.

3.2.1 IF Link Evaluation

The IF data portion of the link is first evaluated, using 70 MHz (QPSK) and 300 MHz (FM) subcarriers. The QPSK IF data link portion consists of 1.3μm optical devices. The clock frequency of QPSK modulator is 6.312 MHz with the IF

frequency 70 MHz. The detected IF data signal is amplified and then supplied to the demodulator through the noise and interference measurement test set (HP3708A). The BER performance is shown in Fig. 3.5(a). A CNR degradation from the theoretical value is within 1.5 dB at an error rate of 10-4. Because the data with the fiber optic link is the same as that without (direct transmission - all electrical), no CNR degradation is caused by the fiber optic link.

The FM IF data link portion is composed of 0.83μm optical devices and a HEMT detector. The base-bandwidth and required RF bandwidth of the FM modulator are 4.2 MHz and 36 MHz, respectively. Fig.3.5(b) shows the weighted SNR performance of this IF link vs. IDS. The link performances for a MMIC MESFET detector and PIN photodiode are also shown in the same figure for comparison. A weighted SNR of 62.5dB is achieved by a PIN photodiode. The average weighted SNRs by HEMT and MESFET detectors are about 60 dB and 59 dB, respectively. The difference of the weighted SNR of the HEMT and MESFET detectors arises from the device's transconductance. Although a SNR fluctuation is observed in the experiment due to a large forward current IDS, a high SNR is attained by the MMIC HEMT detector. This fluctuation can be decreased by reducing the input optical power, as shown in Fig.3.5(c). In this figure it is shown that as the optical input power is reduced, the magnitude of the SNR fluctuations decrease. It should be noted that at these same frequencies, the HEMT detector has higher responsivity than the PIN photodiode. However, as observed by the SNR, the HEMT noise floor is much higher than that of the PIN photodiode, hence the similar SNRs.

3.2.2 RF Link Evaluation

The RF portion of the fiber optic link is characterized by a 26 GHz subcarrier which transmits either QPSK or FM signals. Availability of the 26 GHz modulators is the primary reason this frequency is used. The LiNbO3 external modulators described in the previous section are also used in this experiment. Ideally, frequencies much higher could be used as long as the external optical modulator met the bandwidth requirement.

The 1.3μm optical links are evaluated using both digital and analog signals. Fig.3.6 shows the BER and weighted SNR performance of links employing a PIN photodiode. The external modulator is modulated by the 26 GHz subcarrier signal. The BER performance is measured using the same QPSK modulator/demodulator as was used in the IF link. CNR degradation from the theoretical value is within 2 dB and the value is the same as that obtained without the fiber optic link (Tx-Rcvr.), showing no degradation from link insertion. The BER versus the received optical power is shown in Fig.3.6(b) for a modulation index of m=0.66,

0.33, 0.17 and 0.08. The modulation index is a function of the subcarrier amplitude and Vp of the external modulator [34]. The required optical power at the receiver is inversely proportional to the subcarrier input power.

Fig.3.6(c) shows the weighted SNR versus the modulation input power (Tx output power). The SNR is first measured by a direct connection of the transmitter (Tx) and receiver (Rcvr.) and then subsequently measured using the fiber optic link inserted. The average weighted SNR of the Tx-Rcvr. link is approximately 64 dB, while that of the fiber optic link is 63 dB at a modulation input power of 12 dBm. The frequency spectrums of the 26 GHz band subcarrier signals are shown in Fig.3.6.

The RF link composed of HEMT detectors is next characterized with the 26 GHz band subcarrier using the experimental setup shown in Fig.3.4(b). The direct Tx-Rcvr. link and the fiber optic link which has a PIN photodiode as a detector are first measured. Next, the link with a HEMT detector is evaluated. The CNR degradation from the PIN photodiode link is less than 0.5dB and 1 dB at error rates of 10-4 and 10-8, respectively as shown in Fig.3.7(a). These results as well as those obtained with the IF link indicate that MMIC HEMT photodetectors are noisier than PIN photodiodes primarily because of the relatively high forward current in the HEMT.

The link described above is further investigated in terms of analog signal. A 25-GHz FM modulated signal with baseband width of 4.2 MHz and required RF bandwidth of 36MHz is supplied to the EOM. Two amplifiers whose total gain is 51.3dB at 25-GHz band are connected to the HEMT detector output to amplify the low detected power level. The optical input power of the detector is -5.7dBm. The SNR larger than 50dB was attained at a drain bias voltage of 5V because the signal level is improved by an increase of the drain voltage. The signal level is not strongly dependent on the gate bias voltage. The SNR fluctuated within 1dB due to the instability of the laser diode output power and the optical beam vibration. Fig.3.7(b) shows the weighted SNR versus the optical input power of HEMT. The weighted SNR is proportional to the input power of EOM and is not saturated at an input power of 15dBm. Higher input power of EOM can improve the SNR. The PIN used is the same as that in Fig.3.3. The averaged SNR at an optical input power of -6dBm is 55dB by PIN and 49dB by HEMT. Because the detected amplitude difference of two detectors at 25-GHz band is approximately 9dB, 3-dB noise degradation by PIN detector could be observed in the experiment. In spite of the poor coupling efficiency of HEMT devices, the high SNR value was achieved by HEMT.

3.3 50GHz帯サブキャリア伝送実験

本節では光外部変調器を用いたミリ波伝送用光ファイバリンクの構成について述べる。図3.8に光ファイバリンク（ダウンリンク：制御局から無線基地局へ）の構成を示す。図3.8(a)は外部変調器を用いた最も基本的な構成である。光源には変調機能は必要ではなく、Nd:YAGレーザ等の出力パワーレベルの高いものを用いることが出来る。ただし、50GHz帯のFM変調波を直接外部変調器に印加するので、50GHz帯FM変調器またはIF帯FM変調波を50GHz帯に変換するためのアップコンバータが必要である。図には50GHzFM直接変調器の例を示す。図(b)では光源にレーザダイオードを用いて、光源に対しても変調機能を持たせ低周波帯のFM変調波をLDに印加し、このLD出力をEOMに入力させる。EOMのバイアスは半波長電圧の中心部に設定して動作させるが、電圧を適当に調整することにより高い非線型性を持たせることができる。この状態に50GHz帯のCWをEOMに加えると、LDを強度変調させたIF変調波とCWとの間にミキシンを行なわせることができ、IF変調波を50GHz帯にアップコンバートできる。これを受光器側で検波しフィルタで選別することによりミリ波信号をRF受信機に伝送できる。本構成は光送信機の特にRFの構成を簡易化できる利点がある。図3.9は無線基地局から制御局へのアップリンクの構成を示す。無線ゾーンを用いた移動通信では各端末からの無線信号の受信レベルが一定ではなく、使用条件では大きく変わる。そこでアップリンクでは受信ミリ波周波数を低周波に変換して受信レベルを一定化後、LDの強度変調を行なって伝送する。ミリ波局発を必要とするが、ダウンリンクに図3.8(b)を用いた場合、50GHzのLO成分もPDで検出できるのでこれを図3.9のMMW LOとして再利用できる大きなメリットがある。

画像伝送用50GHz帯無線装置、YAGレーザ（出力29nW）、EOM、PD（3dB帯域幅40GHz）の各デバイスを用いて図3.8(a)のリンク構成で伝送実験を行なった。評価パラメータとしてはFM伝送で用いられている評価SNRを採用した。図3.10(a)はPDの光入力レベル依存性、図3.10(b)は50GHz帯受信機のRF入力レベル依存性を示す。EOM INからPD OUTまでの間のリンク損失は64dBであった。図より評価SNR値が58dBの高い値を光ファイバリンクを通しても得られることを明らかにした。最近、HBTを用いて50GHz帯サブキャリア伝送実験を行ない、評価SNR値が45dBで伝送できることを明らかにした。

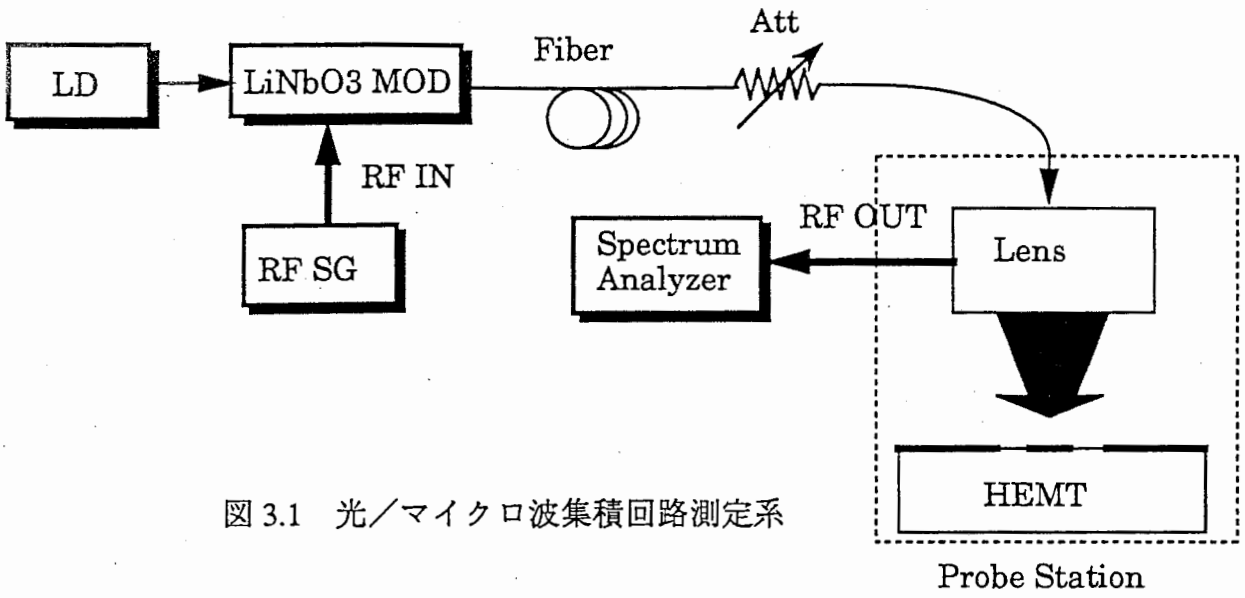

図 3.1　光／マイクロ波集積回路測定系

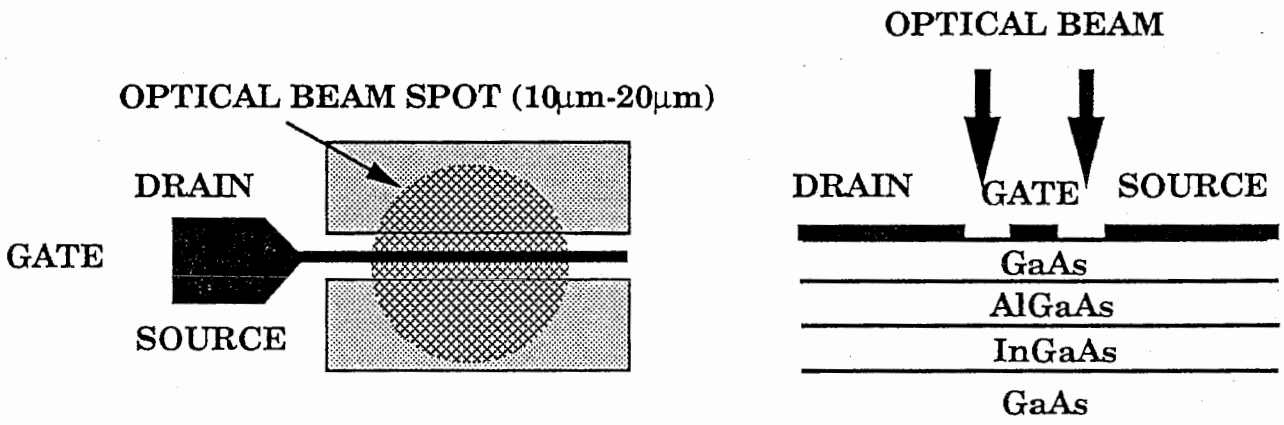

図 3.2　HEMT光検出器

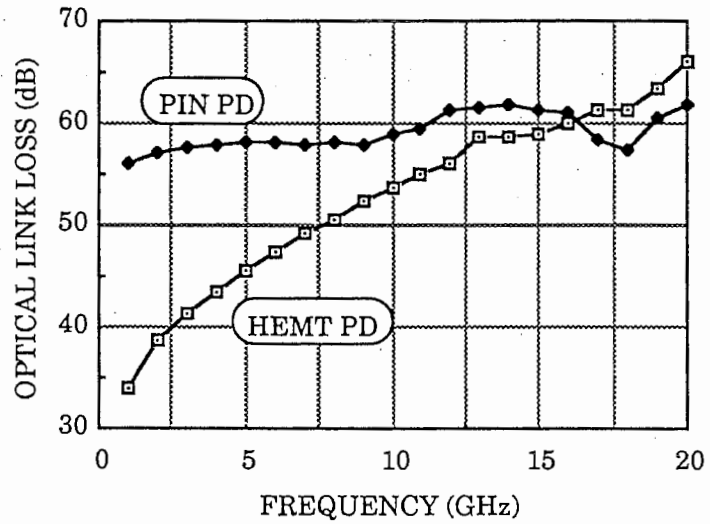

図 3.3 HEMTおよびPIN光検出器の周波数特性

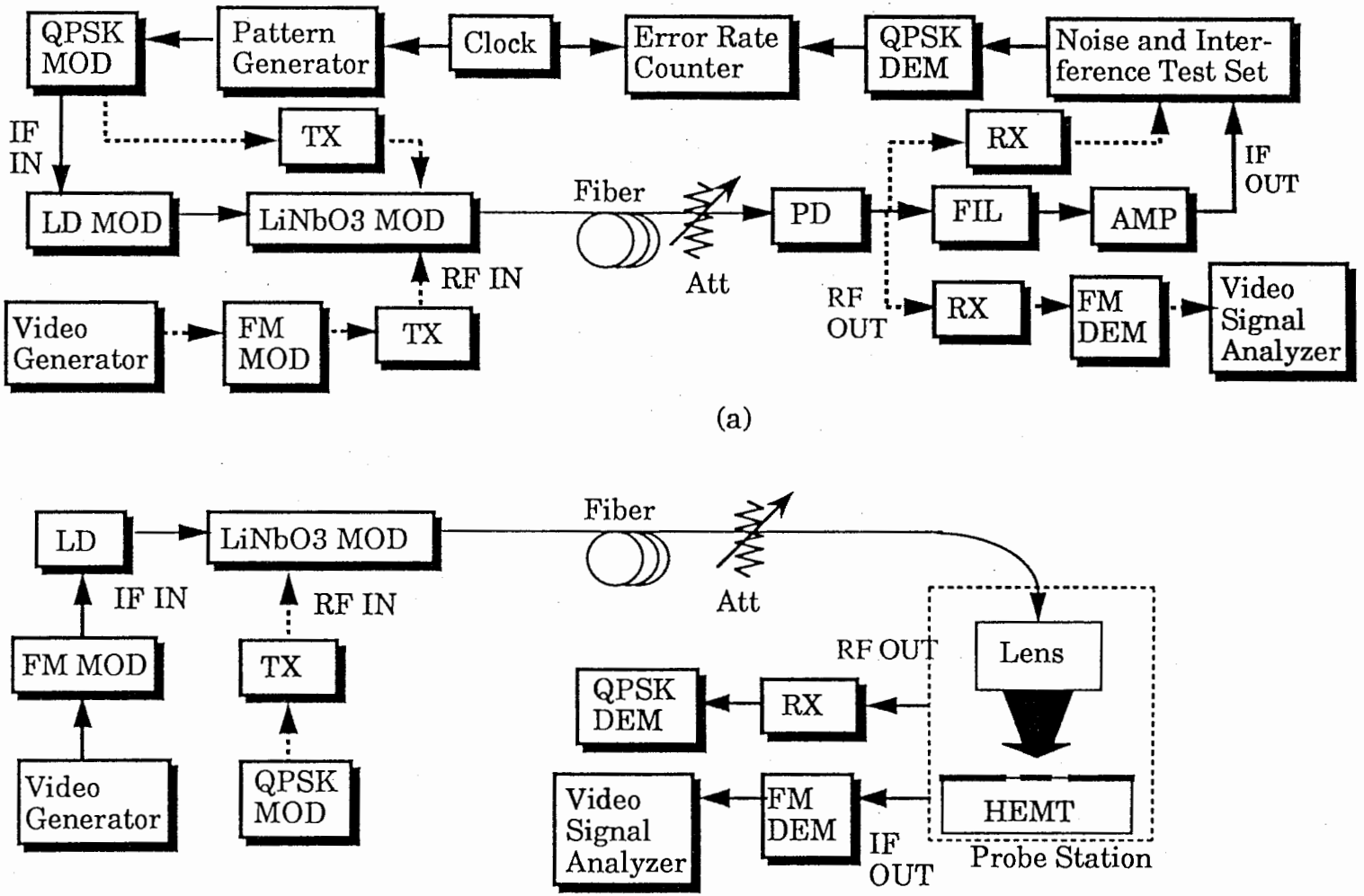

Fig.3.4. Experimental configurations for analog and digital signal transmission analysis by fiber optic link. (a) 1.3μm link configuration of laser diode direct modulation and LiNbO3 external modulation. (b) 0.83μm HEMT detector evaluation link using modified electrooptic on-wafer probe station.

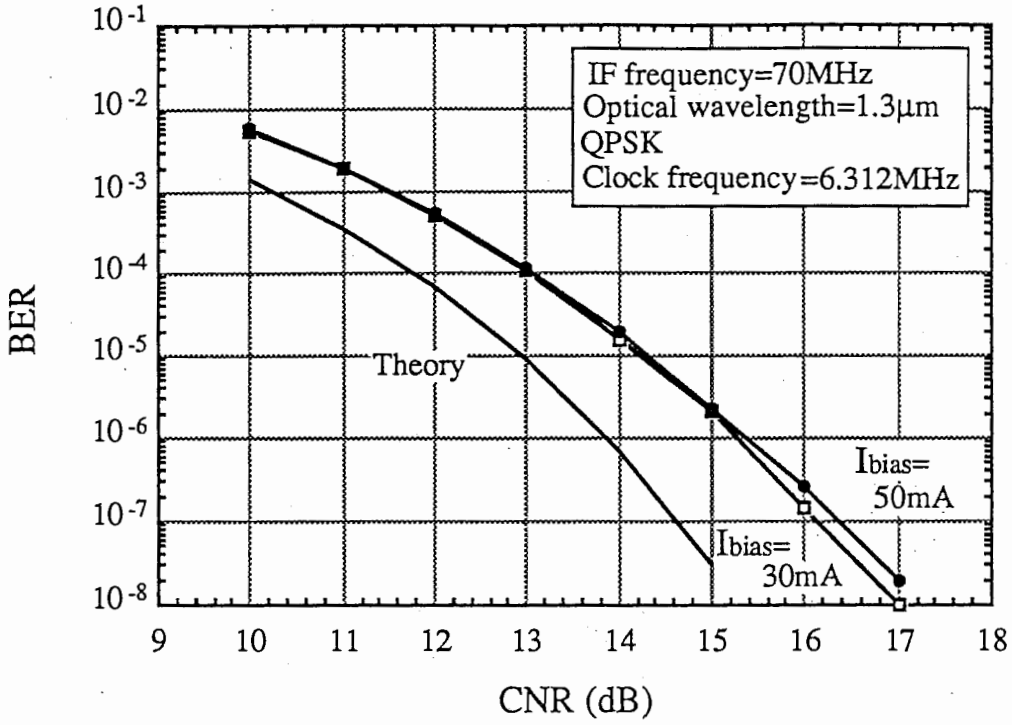

Fig. 3.5 (a)

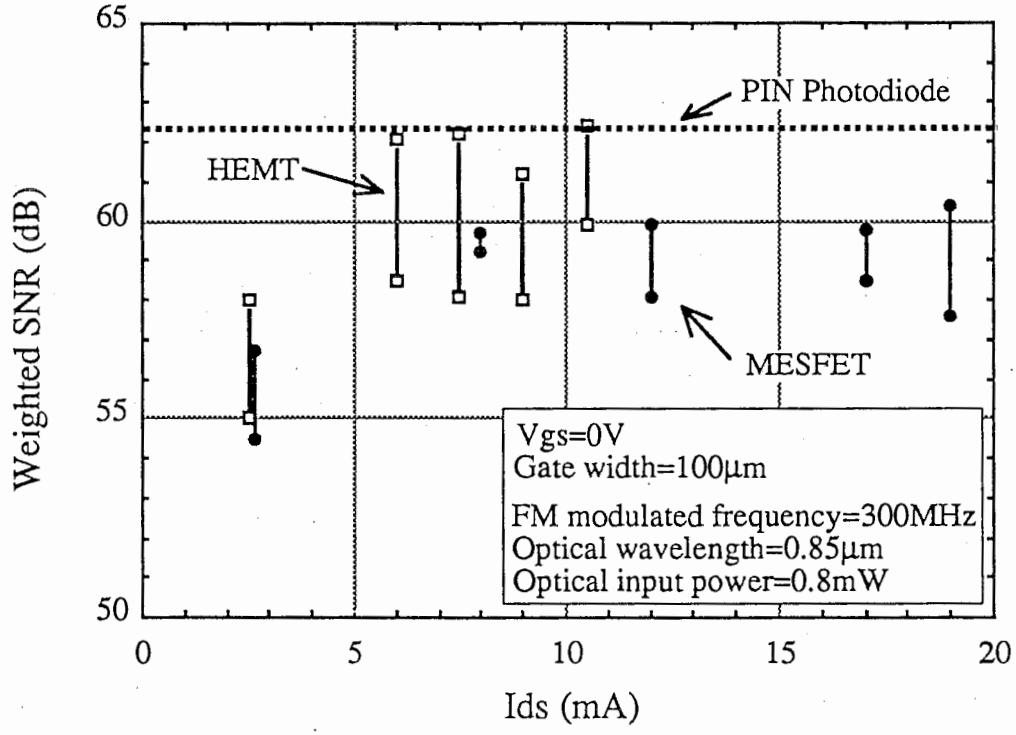

Fig. 3.5 (b)

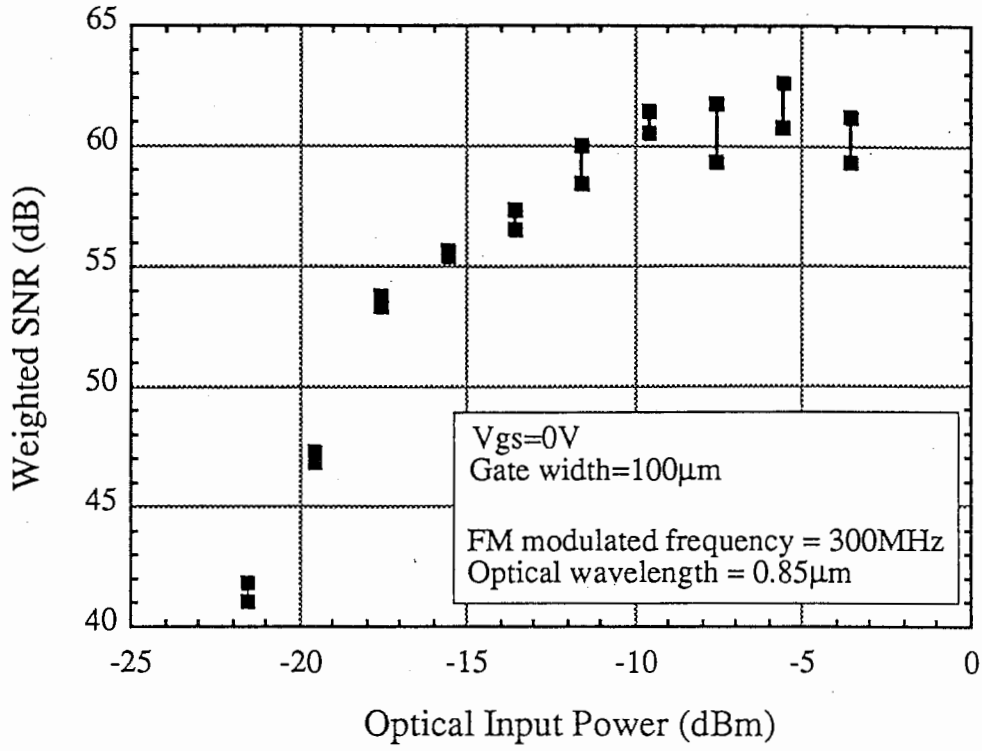

Fig. 3.5(c)

Fig.3.5 IF Link performance. (a) QPSK BER results of 1.3μm, 70MHz IF link. (b) Weighted SNR results of 0.83μm, 300MHz IF link using MMIC HEMT photodetector. (c) Weighted SNR versus optical input power of link in 3.5(b).

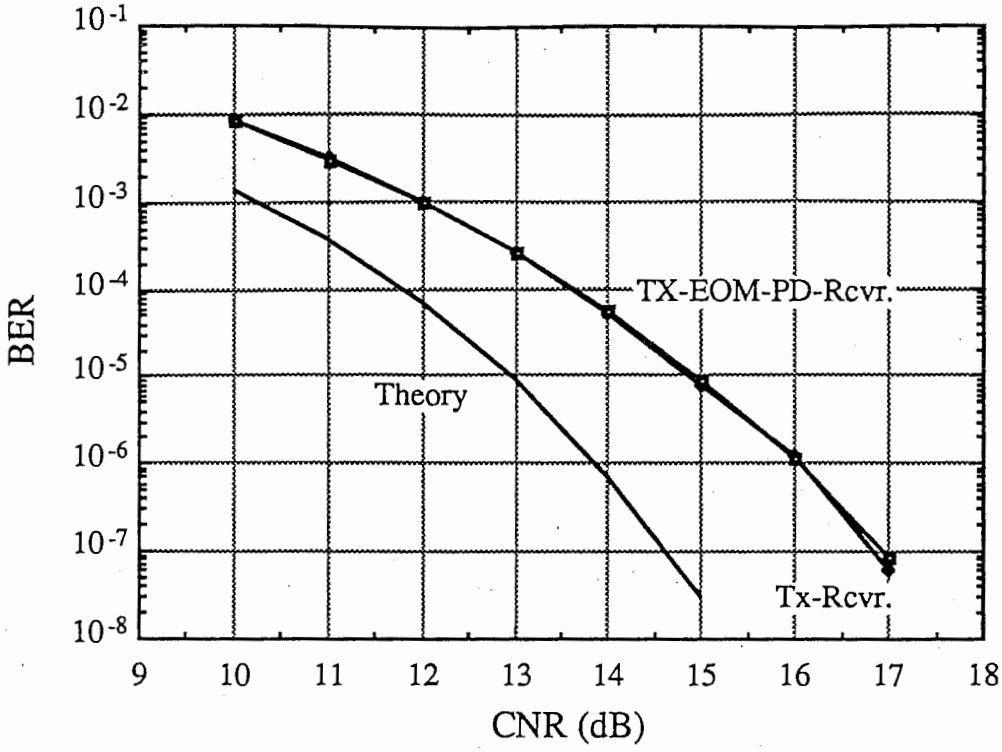

Fig. 3.6 (a)

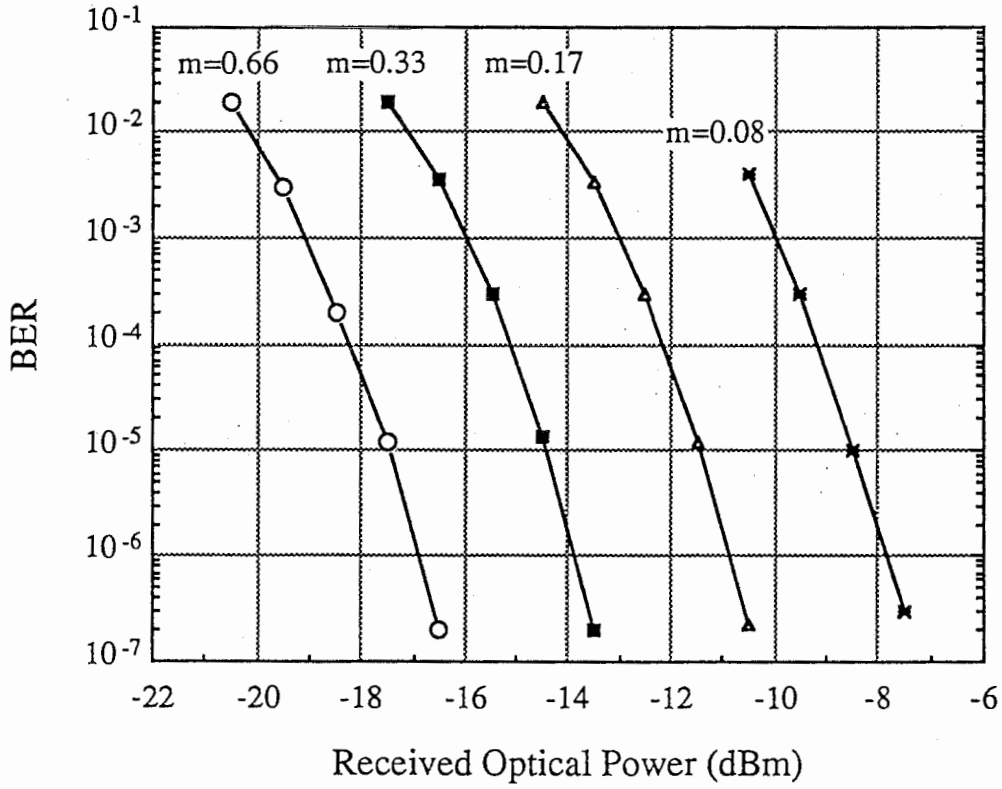

Fig. 3.6 (b)

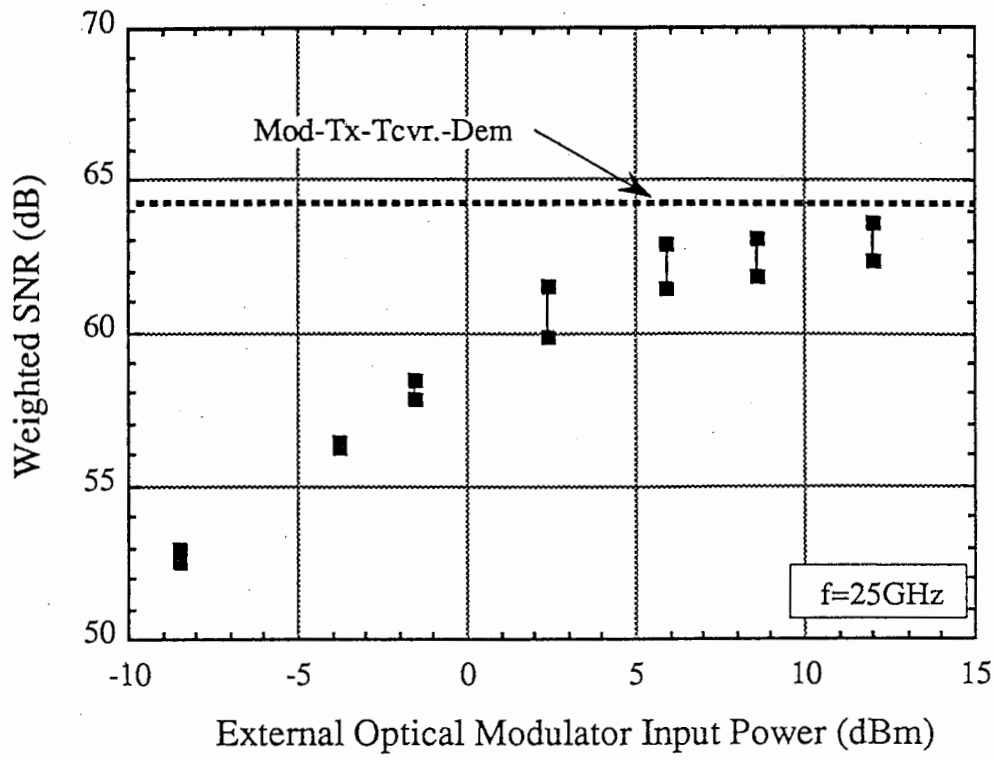

Fig. 3.6 (c)

Fig.3.6. Link performance of 1.3μm RF (26 GHz subcarrier) link. (a) BER versus CNR. (b) BER versus received optical input power. (c) Weighted SNR versus modulation input RF power. Dotted line is the weighted SNR without fiber optic link. Maximum and minimum values are represented by black squares.

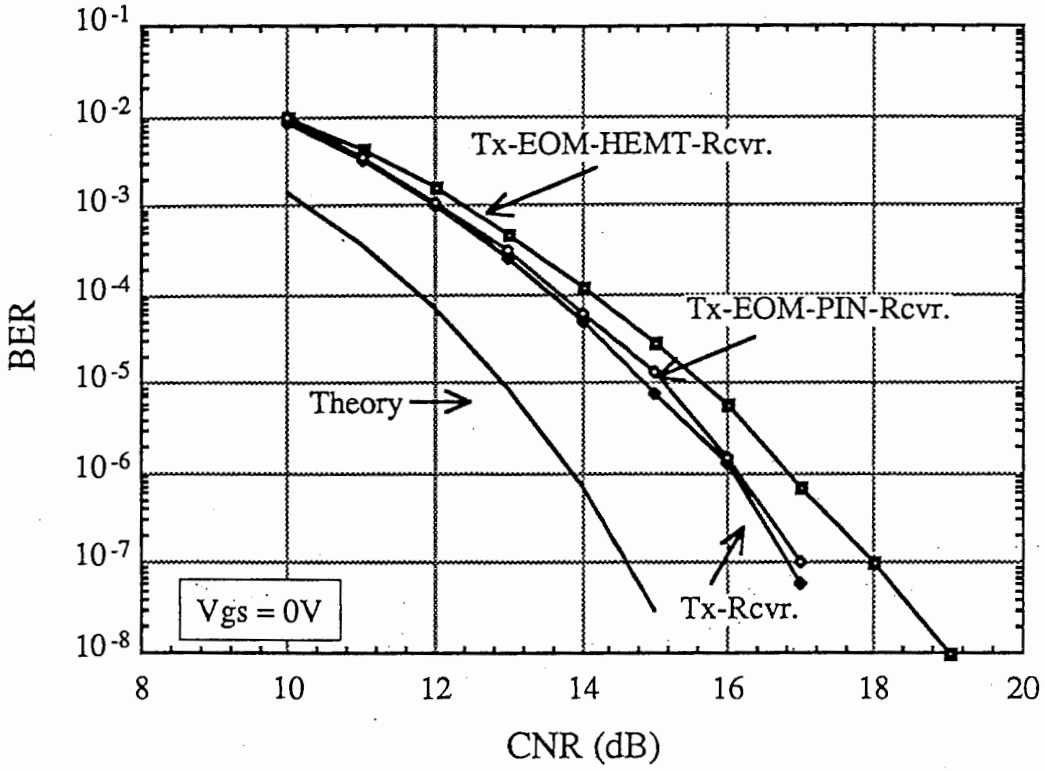

(a)

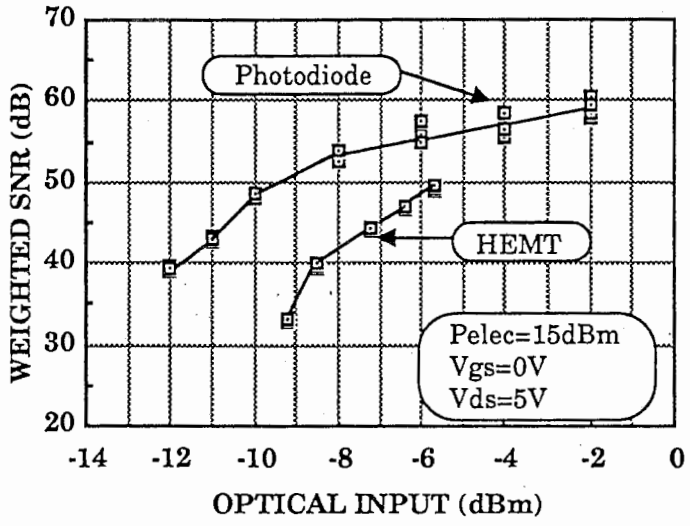

(b)

Fig.3.7. (a) BER vs. CNR performance of 0.83 υm RF (26 GHz subcarrier) link with both HEMT and PIN receivers. The Tx-Rcvr. link has no optical devices. (b) Weighted SNR versus optical input piower.

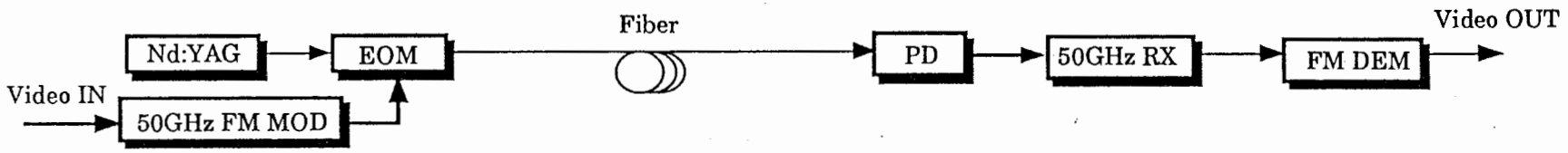

(a) Millimeter-Wave Direct Modulation Link

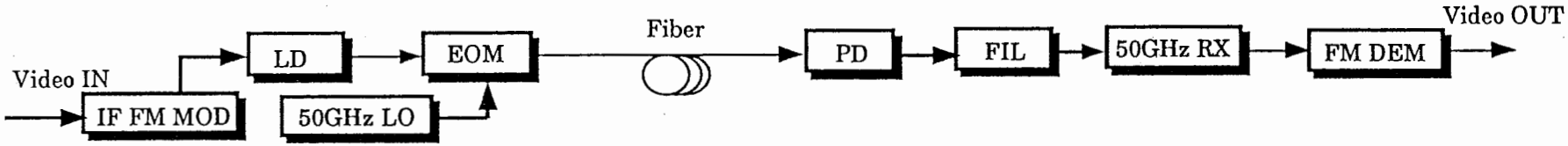

(b) Millimeter-Wave Upconversion Link

図 3.8　外部変調器を用いたミリ波信号伝送用光ファイバリンクの構成（ダウンリンク）

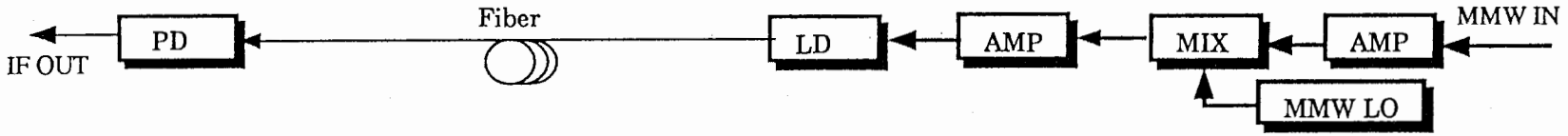

図 3.9　LD直接変調を用いたアップリンクの構成

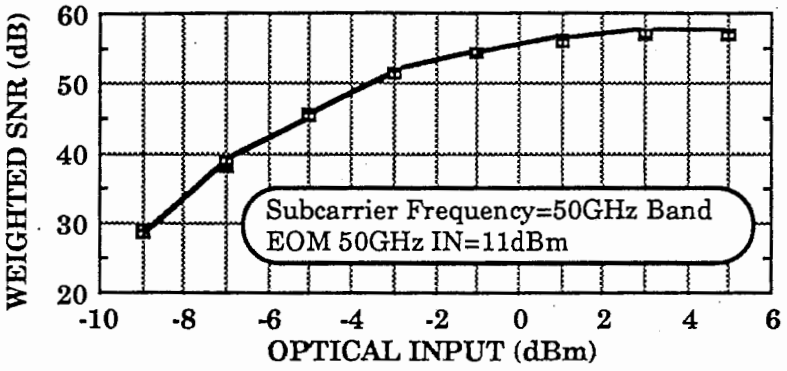

(a)

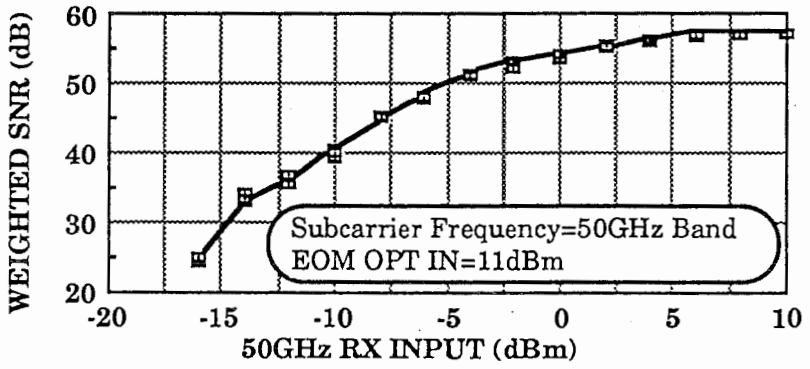

(b)

図 3.10　(a) フォトダイオード光入力パワーvs評価SNR
(b) 50GHz帯RX入力パワーvs評価SNR

4. 光デバイスの非線型特性を利用した光ファイバリンク

本章では、光デバイスの非線型特性をマイクロ波～ミリ波周波数変換特性および高調波発生特性に応用した新機能を有する光ファイバリンクについて述べる。レーザダイオードのI-V特性は半波整流を有しているため周波数変換に応用することができる。さらに、レーザダイオードは受光器としても動作させることができため、１つのレーザダイオードで受光かつ周波数変換も可能である。また、フォトダイオードに関しても光波とマイクロ波との周波数混合を行なわせ、さらにはサブハーモニックミクサとしても使用できる。以下、これらのリンク構成法、実験結果等について述べる。

4.1 Laser Diode Links

A number of fiber optic links have been investigated for microwave and millimeter-wave signal transmissio. The performance of optical devices is being improved and the maximum operating bandwidth has exceeded the Ka-band. Another technique which can extend the bandwidth of fiber optic links is the utilization of the inherent nonlinearities of the optical devices, i.e. laser diodes and photodiodes. A laser diode modulated by a high RF signal power near the relaxation oscillation frequency generates harmonics. The generated harmonics can then be used as the carrier reference signal. A photodiode nonlinearity can also produce harmonics and these can be used to convert the detected modulation signal frequency. Harmonics not only extend the fiber optic link bandwidth, but often generate undesired spurious signals. To suppress undesired spurious signals, microwave filters must be used.

In this section, three fiber optic link configurations are proposed, that utilize the combination of microwave functional components (e.g. in-/out-of-phase combiners/dividers) and optical devices (e.g. laser diodes and photodiodes). These links can suppress undesired spurious frequencies generated by the laser diode nonlinearity. The phase of the RF signals supplied to the laser diode is determined by the microwave circuits. In addition to the fundamental laser diode RF frequency, harmonics or converted frequencies are received in the photodiodes. The RF signals detected by the photodiodes are then recombined using microwave circuits. This recombination process suppresses the undesired signals. The three fiber optic links proposed in this paper utilize these technologies of signal suppression and are summarized as follows:

Balanced Laser Harmonic Generation Link: Even and odd harmonics of RF frequencies generated by the laser diode nonlinearity are added and suppressed, respectively. One configuration consists of two laser diodes, two photodiodes, an out-of-phase divider, an in-phase combiner and two fibers. The other utilizes an optical combiner or an optical divider to reduce the number of fibers and optical devices from two to one, respectively. The primary objective of the link is to extend

the link bandwidth which is beyond the relaxation oscillation limit of the laser diodes. The link can be applied to transmit the carrier reference signal which is used for the injection locking of local oscillator or the local oscillator power of frequency mixer.

Balanced Laser Mixing Link: The laser diode nonlinearity is utilized to up-/down-convert signal frequencies in the links. The link configurations not only suppress local frequencies but also add the converted frequencies from each laser diode. The links are composed of two laser diodes, one or two photodiodes, out-of-phase dividers, in-phase combiners, and one or two fibers. Two fibers and two photodiodes can be reduced to one, respectively, by connecting an optical combiner. The objective of the laser mixing link is to eliminate electrical mixers in the optical receiver. This makes it possible to configure the receiver compact and cost-effective. The balanced laser mixing link can realize more compact and inexpensive optical receiver hardware than conventional laser mixing links.

Image Cancellation Laser Mixing Link: The up-converted frequencies, e.g. upper sideband and lower sideband frequencies are obtained separately from each output port. The link is composed of two laser diodes, two photodiodes, an out-of-phase divider, two in-phase combiners, two 90° hybrid circuits, and two fibers. The objective of the image cancellation laser mixing link is the same as that of the balanced laser mixing link.

The fundamental behavior of these configurations is discussed and their basic performance experimentally investigated at microwave frequency bands using commercially available optical devices.

4.1.1 Link Analysis

To describe the basic idea of the proposed fiber optic links, several equations have been derived in this section. The intensity modulated light output of the laser diode is generally written as

$$P=P0 * [1+m * \cos(\omega t)] \quad (1)$$

where P0 is the average light output, m is the optical intensity modulation index and ω is the modulation RF angular frequency. If the RF signal is split by the out-of-phase divider and supplied to each laser diode, the light output P1 and P2 from each diode is written as

$$P1=P01 * [1+m1 * \cos(\omega 1t)] \quad (2)$$

$$P2=P02 * [1+m2 * \cos(\omega 1t+\pi)] \quad (3)$$

where P01 and P02 are the average light outputs, m1 and m2 are the optical intensity modulation indices. The output of large-signal modulated laser diodes is expressed as

$$P1=P01*[1+m1*\cos(\omega 1t)+A2*\{m1*\cos(\omega 1t)\}2+A3*\{m1*\cos(\omega 1t)\}3+ - - - -]$$

$$=P01*[1+m1*\cos(\omega 1t)+A2*\{m12*\cos(2\omega 1t)\}+A3*\{m13*\cos(3\omega 1t)\}+----] \quad (4)$$

$$P2=P02*[1+m2*\cos(\omega 1t+\pi)+B2*\{m2*\cos(\omega 1t+\pi)\}2+B3*\{m2*\cos(\omega 1t+\pi)\}3+---]$$

$$=P02*[1+m2*\cos(w1t+\pi)+B2*\{m22*\cos(2\omega 1t)\}+B3*\{m23*\cos(3\omega 1t+\pi)\}+---]. \quad (5)$$

If two optical signals are detected by photodiodes and combined by an in-phase combiner, and the amplitude coefficients are equal, the fundamental and odd harmonics are suppressed and even harmonics added, due to the out-of-phase and in-phase relationship, respectively. Thus, both high frequency transmission above a relaxation oscillation frequency of laser diodes and suppression of undesired spurious frequencies is feasible using the laser diode nonlinearity and an RF-signal phase shift. A link with a function determined from Eqs. (4) and (5) will be proposed using a combination of optical devices and microwave passive components.

If two modulation signals are superimposed onto the bias current of the laser diodes, the laser diodes can operate as an optical source and a frequency converter simultaneously. The intensity modulated light output of the laser diode is expressed as

$$P=P0*[1+m1*\cos(\omega 1t)+m2*\cos(\omega 2t)] \quad (6)$$

where ω1 and ω2 are the modulation angular frequencies. If the laser diode nonlinearity is used, Eq.(6) is expanded to:

$$P=P0*[1+m1*\cos(\omega 1t)+m2*\cos(\omega 2t)+A2*\{m1*\cos(\omega 1t)+m2*\cos(\omega 2t)\}^2$$
$$+A3*\{m1*\cos(\omega 1t)+m2*\cos(\omega 2t)\}^3+----]$$
$$=P0*[1+m1*\cos(\omega 1t)+m2*\cos(\omega 2t)+A2/2*m12*\cos(2\omega 1t)+A2/2*m22*\cos(2\omega 2t)$$
$$+A2*m1m2*\cos(\omega 1\pm\omega 2)t+3/4*A3*m12m2*\cos(2\omega 1\pm\omega 2)t$$
$$+3/4*A3*m1m22*\cos(\omega 1\pm 2\omega 2)t+----]. \quad (7)$$

If both signal frequencies of ω1 and ω2 are divided out-of-phase and supplied to two laser diodes, the modulated light output of one diode is given by Eq.(7), while that of the other diode is expressed as

$$P'=P0'*[1+m'1*\cos(\omega 1t+p)+m'2*\cos(\omega 2t+p)+A2'*m'12*\cos(2\omega 1t)$$
$$+A2'/2*m'22*\cos(2\omega 2t)+A2'/2*m'1m'2*\cos(\omega 1\pm\omega 2)t$$
$$+3/4*A'3*m'12m'2*\cos(2\omega 1\pm\omega 2+\pi)t$$
$$+3/4*A'3*m'1m'22*\cos(\omega 1\pm 2\omega 2+\pi)t+----]. \quad (8)$$

If two optical signals, P and P', are combined in-phase, the fundamental frequencies of ω1 and ω2 are cancelled, and the sum and difference frequencies of w1±w2 added. This balanced behavior is achieved using laser diode nonlinearities and microwave out-of-phase dividing functions. If one signal is divided by a 90° hybrid circuit, Eq.(8) is rewritten as

$$P''=P0''*[1+m'1*\cos(\omega 1t+\pi)+m'2*\cos(\omega 2t+\pi/2)+A2'/2*m'12*\cos(2\omega 1t)$$
$$+A2'/2*m'22*\cos(2\omega 2t+p)+A2'*m'1m'2*\cos(\omega 1+\omega 2+3\pi/2)t$$
$$+A2'*m'1m'2*\cos(\omega 1-\omega 2+\pi/2)t+3/4*A'3*m'12m'2*\cos(2\omega 1+\omega 2+\pi/2)t$$

+3/4*A'3*m'12m'2*cos(2ω1-ω2+3π/2)t

+3/4*A'3*m'1m'22*cos(ω1±2ω2)t+ - - - -]. (9)

If two optical signals, P and P", are combined by a 90° hybrid circuit, the upper and lower sideband signals are obtained separately from the output port of the 90° hybrid circuit. This operation is the same as that of the image cancel microwave mixer[17]. These functions are accomplished utilizing a combination of the laser diode nonlinearity and the phase shift of modulation frequencies.

4.1.2 Link Configuration

A. Balanced Laser Harmonic Generation Link

The configurations of the balanced laser harmonic generation link are shown in Fig.4.1. The single-fiber links consist of an out-of-phase divider, one or two laser diodes, an optical combiner or divider, one or two photodiodes, and a fiber cable. The 180° RF signal phase shift is achieved using the out-of-phase divider which is connected to laser diodes in link A, while in link B the detected RF signals are combined by the out-of-phase combiner. Links C and D consist of two laser diodes, two photodiodes, an in-phase combiner, an out-of-phase divider and two fiber cables. The disadvantage of link B which uses only one laser diode is a 3-dB increase in link loss. The others could have the same link loss, if the laser diode and photodiode characteristics are equal.

As the basic behavior of the single-fiber link is the same as that of the twin-fiber link, the mechanism to cancel undesired signals is discussed below using the single-fiber link as an example for both. The input microwave signal is divided out-of-phase and then it modulates the laser diodes. Two intensity modulated optical signals which contain input RF frequency harmonics are combined by an optical combiner and detected by a photodiode. These two optical signals are expressed by Eqs.(4) and (5), respectively. The fundamental and odd harmonics are cancelled due to a 180° phase difference. The even harmonics are added due to the in-phase relationship. The basic behavior of Figs.4.1(b) and (d) is different from that of Figs.4.1(a) and (c). The out-of-phase combiner is designed to give np phase shift to the fundamental (n=1) and odd harmonics (n=odd number), and mp phase shift to the even harmonics (m=even number). This circuit is configured simply using a quarter wavelength distributed transmission line whose length is designed at the fundamental frequency. Thus, in principle the detected microwave frequencies include only the even harmonics of the input RF frequency. Although the same idea was demonstrated using an optical interferometer, the link configuration proposed here utilizes microwave functional circuits such as out-of-phase dividers and combiners, and a couple of optical devices.

B. Balanced Laser Mixing Link

Since the laser diode can operate as an optical source as well as a microwave frequency mixer, the laser diode mixer generates up-/down-converted signals and a local frequency, if two frequencies (local and IF/RF signals) are supplied. The output power level at the local frequency is larger than that of the upper and lower sideband signals if the IF signal level is low. To suppress the local frequency, a microwave filter must be connected to the photodiode output. The balanced laser mixing link shown in Fig.4.2 can eliminate local frequency without using filters. Two out-of-phase dividers and two in-phase combiners are required to supply the out-of-phase local frequencies ($\omega 1$) and out-of-phase IF signals ($\omega 2$) to the laser diodes. The light output of the laser diodes is expressed by Eqs.(7) and (8). Since two detected local frequencies have a phase difference of 180°, they are cancelled at detector output. Thus in principle, the detected output does not include the local frequency, only the up-/down-converted signals.

C. Image Cancellation Laser Mixing Link

If the out-of-phase divider for the IF signal is replaced by a 90° hybrid circuit, the link can transmit the upper and lower sideband signals separately. The configuration of the image cancellation laser mixing link is shown in Fig.4.3. The image cancellation configuration is based on the image cancel microwave mixer. The local frequency ($\omega 1$) is divided out-of-phase, while the IF signal ($\omega 2$) is divided at a 90° phase difference. These divided frequencies are supplied to the laser diodes and then the frequency is mixed using the laser diode nonlinearity. The optical output power of the laser diodes is written in Eqs.(7) and (9). Two photodiodes detect the modulated optical power, and the detected microwave frequencies are combined using the 90° hybrid circuit. The upper and lower sideband signals are obtained separately from each output port.

4.1.3 Experimental Results

To verify the fundamental behavior of fiber optic links, the balanced laser harmonic generation link, the balanced laser mixing link and the image cancellation mixing link are experimentally investigated. Two InGaAsP laser diodes (Ortel 1515A) are used as harmonic generators and laser mixers. The first and second laser diodes have a threshold current of 19mA and 15mA and a cw output power of 1mW at a forward bias current of 36mA and 38mA, respectively. The InGaAs pin photodiode (Ortel 2515A) has a 3dB bandwidth of 10GHz and a responsivity of 0.6mA/mW. A conventional microwave 180° hybrid circuit is used as the out-of-phase divider. The optical coupler is used as the optical power combiner with a 3dB optical power loss.

The detected harmonic levels of the balanced laser harmonic generation

links (Figs.4.1(a) and (c)) are shown in Figs.4.4 and 4.5. The fundamental frequencies of the single- and twin-fiber links are 3GHz and 2.5GHz, respectively. The detected second, third and fourth harmonic levels of the single-fiber link at an RF input power level of 12dBm are -35.8dBm, -52dBm and -47.8dBm, respectively. As the detected fundamental frequency level is less than -80dBm, the suppression ratio of the fundamental and second harmonic is greater than 44dB. Frequency response of the single-fiber link is shown in Fig.4.4(b). Although this link is balanced at the fundamental frequency of 3GHz, the third-order suppression is worse than that of the fundamental because of the imbalance of components at the third-order frequency. Detected harmonic output of the twin-fiber link is shown in Fig.4.5(a). The second harmonic level is improved due to the absence of an optical combiner. Its value is -30.6dBm at an input power level of 12dBm. Since the detected power level of the fundamental is -76dBm, the suppression ratio of the fundamental and second harmonic is 45.4dB. Frequency responses of each harmonic are shown in Fig.4.5(b). The odd harmonics are suppressed in the vicinity of the fundamental frequency of 2.5GHz, as the even harmonic level increases.

Balanced laser mixing link performance is shown in Fig.4.6. The frequency responses of the upper and lower sideband frequencies as well as local frequency are shown in Fig.4.6(a). The balanced mixing link is optimized at an IF frequency of 1.3GHz. The detected power of the local frequency is -80.5dBm, while that of the upper and lower sideband frequencies is -38.6dBm and -39 dBm, respectively. A suppression ratio greater than 41.5dB is obtained. Detected output power versus local input power of laser diodes is shown in Fig.4.6(b). Since the two laser diodes used in the experiment have a different light output, the detected local power at photodiodes is strongly dependent on the local input power level of the laser diodes.

The frequency response of the image cancellation laser mixing link is shown in Figs.4.7(a) and (b). In Fig.4.7(a), the upper sideband frequency corresponds to an RF frequency and the lower sideband frequency to an image frequency. On the other hand, in Fig.4.7(b), the lower sideband frequency corresponds to an RF frequency and the upper sideband frequency to an image frequency. The bias condition of the two laser diodes is optimized at a local frequency of 8GHz, a local input power level of 14dBm, and an IF frequency of 1.25GHz. An image rejection of 39.3dB and 23.4dB is achieved in Figs.4.7(a) and (b), respectively. The detected up-converted (9GHz) and down-converted (7GHz) output power versus the IF (1GHz) input power is shown in Fig.4.7(c). The detected power is proportional to the input local and IF power level of the laser diodes.

4.1.4 Discussion

Signal suppression is feasible at microwave frequency bands using a combination of microwave functional circuits and optical devices. The proposed configurations use the phase relationship between the input signals of laser diodes and the output signals generated from laser diode nonlinearities to eliminate microwave filters. Experimental results of the three fiber optic links are summarized in Table 4.1. The suppression ratio of the fundamental and second harmonic is greater than 40dB at the balanced laser harmonic generation link. The balanced laser mixing link achieves a high suppression ratio (>40dB) at the 6-GHz band. Therefore, these balanced configurations can operate as undesired signal suppression filters.

The frequency response deviation of laser diodes, and the amplitude and phase deviation of each microwave circuit causes an imbalance in the suppression ratio in the image cancellation link. However, despite the large number of circuit components in the optical links, a suppression ratio greater than 20dB is obtained at the 8-GHz band. The disadvantage of these proposed links is the narrow transmission bandwidth. The frequency responses of each fiber optic link are shown in Figs.4.4(b), 4.5(b), 4.6(b), 4.7(a) and (b). The bandwidth obtained is between 200MHz and 400MHz. Because of the limited bandwidth, these links are suitable for use as carrier transmission links which transmit an RF frequency or a local frequency. The imbalance of components will be significantly improved using monolithic integrated circuit technologies which make optical devices uniform and also incorporate optical devices and microwave passive circuits.

4.2 Laser Diode Receiving Link

Optical device nonlinearities of laser diodes and photodiodes have received much attention since these nonlinearities can not only extend the fiber optic transmission bandwidth but also make transmitter/receiver hardware simple and cost-effective. The laser diodes can operate as an optical source and a microwave mixer simultaneously if the electrical local power is supplied to the laser diode. The frequency conversion characteristics of laser diodes have been utilized to make the configuration of fiber optic links simple. As for photodiodes, they can operate as a optical detector as well as a microwave frequency mixer. The sufficient electrical local power must be supplied to the photodiodes to convert the detected frequency to the RF-band. Since the photodiode mixing receiver can eliminate an electrical mixer, the receiver hardware can be simplified. Additionally, the photodiode mixing architecture can extend the equivalent bandwidth of fiber optic links because the detected frequencies are up-converted by the local oscillator power whose frequency is in the RF-band.

Despite their advantages such as simplification and bandwidth extension, the fiber optic links which have been investigated for bidirectional communication networks require several optical devices, as shown in Fig.4.8(a) and (b). Although the space division multiplexing link is simple, two fiber cables are needed for bidirectional communications. In the wavelength division multiplexing system, two laser diodes whose wavelength is different and two wavelength multiplexers are used to configure the bidirectional transmission systems. To avoid above complexity, the time compression multiplex transmission system was proposed, as shown in Fig.4.8(c). It is named as the LD-LD link in this paper. The optical devices required for this system are only two laser diodes which operate as not only an optical source but also a photodetector. The transmitted frequency is strongly dependent on the laser photodetection capability. It is difficult to transmit high subcarrier frequencies because of relatively large junction capacitance of laser diodes.

In this section, new fiber optic bidirectional links (LD-LD MIX link) which utilize laser diode photodetection and frequency mixing capabilities are proposed to extend the transmission bandwidth of the LD-LD links. The frequency mixing performance is achieved by the nonlinearity of the laser diode. The laser diode that has two functions, i.e. an optical detection and a frequency mixing is called an LD receiving mixer in this paper. Additionally, two fiber optic links which utilize the combination of LD receiving mixers and microwave components are proposed. The one is the LO suppression link which suppresses the undesired electrical LO power at mixer output ports, and the other is the image cancellation link where the upper and lower sideband signals are obtained at the different output port.

4.2.1 Link Configuration

A. LD-LD MIX Link

The LD-LD MIX link configuration is shown in Fig.4.8(d). The link consists of two laser diodes, two electrical local oscillators, two broadband microwave switches, and one fiber cable. Although data signals are transmitted in burst mode (ping-pong transmission) in the LD-LD link, the proposed LD-LD MIX link carries analog subcarrier frequencies in burst mode. The control signals are supplied to the local oscillators and switches. When the LD1 is in the emitting mode, i.e. the LD1 operates as a direct intensity optical modulator and the LO1 power is in off-state, the LD2 is in the receiving mixer mode which up-converts the detected subcarrier. The LO2 is in on-state and the up-converted frequency is obtained from the SW2 output. On the other hand, when the LD2 is in the emitting mode, the LD1 is in the receiving mixer mode, and the LO1 and LO2 are in on- and

off-state, respectively.

The disadvantage of the LD-LD link is the limited frequency response. The reduction of the active layer length of the laser diodes is proposed to decrease the large capacitance of the laser diodes. But this might modify or damage the performance of the laser diodes. The LD-LD MIX link is proposed to extend the fiber optic link bandwidth as well as to simplify the fiber optic link configuration. The laser diode has the inherent nonlinearities which are utilized to transmit high frequencies. Additionally, the laser diode has a rectifying performance, as shown in Fig.4.9(a). The experiment was done using a commercially available laser diode which will be explained in the next section. This electrical nonlinearity can be exploited to realize frequency mixing functions which have been achieved by PIN photodiode devices. The rectified current of the local oscillator is used to up-/down-convert the detected subcarrier frequency, as shown in Fig.4.9(b). Fig.4.9(b) shows the schematic I-V characteristics of the laser diode. The frequency mixing process is the same as that of the photodiode mixing. The transmission bandwidth extension of an LD receiving mixer is dependent on the frequency conversion efficiency as an electrical mixer as well as the responsivity as a photodetector.

B. Balanced LD-LD MIX Link

The output frequencies of an LD receiving mixer are upper and lower sideband frequencies as well as a local frequency. Microwave filters must be connected to the laser diode to suppress the undesired spurious frequencies. Since the LD-LD MIX link is the bidirectional transmission link and the input and output ports are commonly used, it is difficult to suppress the undesired frequencies by filters which are connected to the input/output port. In order to solve the problem, two novel fiber optic link configurations that utilize the combination of microwave functional circuits and optical devices are proposed. This technique was successfully applied to configure the laser mixing links. Fig.4.10 shows two bidirectional link configurations, i.e. the local suppression link and the image cancellation link. The difference between two links is the splitter / combiner circuits which divide the input signal to the laser diodes and combine the output signals from the laser diodes. The local suppression link consists of a 180° hybrid circuit, while the image cancellation link a 90° hybrid circuit.

The basic behavior of the image cancellation link is described as follows: The IF signal is first divided by a 90° hybrid circuit and then two divided signals are respectively supplied to LD11 and LD21. The local oscillator LO1 is in off-state. Two laser diodes are intensity modulated by the IF signal. Two transmitted optical carriers P1 and P2 are expressed as

$$P1=P01 * [1+m1 * \cos(\omega t)] \quad (10)$$

$$P2=P02 * [1+m2 * \cos(\omega t+\pi/2)] \quad (11)$$

where P01 and P02 are the averaged light output, m1 and m2 are the optical intensity modulation index and ω is the modulation IF angular frequency. Two optical carriers are detected by LD21 and LD22, respectively. The local oscillator power from LO2 whose angular frequency is ω0 is first divided and then supplied to LD21 and LD22. The output frequencies S1 and S2 are expressed as

$$S1=A1 * \cos(\omega 0 \pm \omega)t + A2 * \cos(\omega 0 \pm 2\omega)t + - - - - - \quad (12)$$

$$S2=A'1 * \cos(\omega 0+\omega+\pi/2)t + A'1 * \cos(\omega 0-\omega-\pi/2)t + - - - - - . \quad (13)$$

If S1 and S2 are combined by a 90° hybrid circuit, the upper and lower sideband signals are separately obtained from each output port. If the 90° hybrid circuit is replaced by a 180° hybrid circuit, the local frequency component is suppressed at the output port. Thus in principle, the desired and undesired frequencies can be selected without microwave filters.

4.2.2 Experimental Results

To verify the basic behavior of proposed fiber optic links, the LD-LD MIX link and the image suppression LD-LD MIX link are experimentally investigated using commercially available devices. The 1.3-μm laser diodes (FU-42SLD) were used for the experiment. The light is output through a pigtailed fiber. The electrical matching is employed by a series 47-ohm resistor. Averaged threshold current is 10mA and the 3-dB electrical bandwidth is approximately 4GHz. Conventional microwave components were used as the 90° or 180° splitter/ combiner circuits.

The static characteristics of the laser diode is shown in Fig.4.9(a). The light current is proportional to the optical input power. The laser diodes have an averaged responsivity of 0.3mA/mW. The frequency response and the bias dependence of the LD-LD MIX link is shown in Fig.4.11. The performance of the LD-LD link is also shown in Fig.4.11(a) for reference. The IF frequency is fixed at 70MHz. The increase of the detected output power at a frequency of 3.6GHz is due to the relaxation oscillation frequency of the laser diode. The laser diode has a strong nonlinear behavior in the vicinity of relaxation oscillation frequencies. The upper and lower sideband signal levels are higher than that of the LD-LD link at 3.6GHz. The frequency mixing efficiency is strongly dependent on the bias condition of the laser diode. Fig.4.11(b) shows the upper sideband signal level and the detected current of the laser diode versus the applied bias voltage at a local frequency of 3.6GHz and a local input power of 15dBm. The frequency mixing efficiency becomes maximum at a forward bias voltage of 0.6V. This voltage is determined from a turn-on voltage of the laser diode. The turn-on voltage is estimated to be 0.8V from Fig.4.9(a). The detected current of the laser diode

consists of the light current of the optical power and the rectified current of the local oscillator power. Thus the important design parameters for an LD receiving mixer are the relaxation oscillation frequency and turn-on voltage of the laser diode.

The LD-LD MIX image cancellation link is configured using four laser diodes, two local oscillators, two in-phase dividers and two 90° hybrid circuits, as shown in Fig.4.10(b). The frequency response of the lower and upper sidebands is shown in Fig.4.12. The upper sideband frequency corresponds to an RF signal and the lower sideband frequency to an image, in Fig.4.12(a). On the other hand, the lower sideband frequency corresponds to an RF signal in Fig.4.12(b). The local frequency is fixed at 3.6GHz. An image cancellation ratio of 26dB and 23dB is achieved at an IF frequency of 90MHz in Fig.4.12(a) and 100MHz in Fig.4.12(b), respectively. Fig.4.13 shows the image cancellation characteristics of the link. The IF frequency is fixed at 90MHz. The suppression ratio is not sensitive to the local frequency change, because the direct detection performance of the laser diode in the frequency range of 2-4GHz has the small amplitude deviation characteristics less than 5dB. However, since the frequency amplitude response of the LD detector in the frequency range less than 1GHz varies large as the frequency increases, the IF frequency response of image cancellation has the limited bandwidth.

4.2.3 Link Performance

The LD-LD MIX link is characterized using the QPSK modulated subcarrier frequency. Fig.4.14 shows the experimental setup for QPSK transmission. The output and clock frequencies are 70MHz and 6.312MHz, respectively. The local oscillator frequency and power are 3.8GHz and 10dBm, respectively. The applied bias voltage of the laser diode is 0.6V. The BER was measured by the noise and interference measurement test set (HP3708A). The MIX-MIX link (Fig.4.14(b)) which consists of microwave mixers and an electrical local oscillator is first characterized for reference. Then the LD-LD+MIX link which is composed of the LD-LD link and MIX-MIX link is measured using the same experimental setup to evaluate the influence of the laser diode intensity noise. Fig.4.15 shows the BER performance of these links. The same performance is achieved by the MIX-MIX and LD-LD+MIX links. Since the local oscillation frequency of 3.8GHz is determined from the large nonlinearity of the laser diode, the signal transmission characteristics of the LD-LD MIX link is influenced by the laser diode nonlinearity. This is the reason why the local oscillation frequency of 3.8GHz is selected. A CNR degradation from the theoretical value of the LD-LD MIX link is 1.7dB larger than that of LD-LD+MIX or MIX-MIX links. Although

the QPSK transmission characteristics are deteriorated by the nonlinearity of the laser receiving mixer, a CNR degradation from the theoretical value is within 3.2dB.

4.3 Harmonic Mixing Links

The basic configurations of the fiber optic links proposed in this section are shown in Figs.4.16, 4.17 and 4.18. The functions of the central terminal are modulation /demodulation, and E/O - O/E conversion. The data signal is obtained by the electrical modulator, and then converted to the optical signal by the optical modulator (laser diode). The intensity modulated optical signal from the laser diode is transmitted to the sub-central terminal through the fiber optic link and detected by the photodetector. The data signal is converted to the rf frequency in accordance with the following link architectures.

A. Harmonic Laser Diode Mixing Link -Link E-

Although the laser diode can operate as an optical source and a microwave mixer simultaneously, the transmitted microwave frequency is limited by the bandwidth of the laser diodes. The use of harmonics permits the modulation capability of the laser diode to be extended beyond the relaxation oscillation frequency limit. This allows better utilization of the fiber optic link bandwidth capability. The fiber optic link shown in Fig.4.16 exploits both laser diode harmonics and laser diode mixing, i.e. laser diode nonlinearities. The baseband signal is converted to the data signal and supplied to the laser diode mixer. The laser diode is biased to produce high harmonic levels. The harmonics are used as the laser local oscillator power for the laser mixer. The data signal and microwave harmonics are mixed in the laser diode. The intensity modulated optical signal from the laser diode contains the upconverted and down-converted signals as well as microwave harmonics. These signals are transmitted to the sub-central terminal and detected by the photodiode. The desired frequency is selected by the microwave filter. The frequency multiplication factor is determined from the laser diode harmonic order. The relationship between the output frequency fs of the sub-central terminal and the laser local oscillation frequency fl is expressed as

$$fs = Ml \quad fl \pm fd \tag{14}$$

where Ml is the frequency multiplication factor of the laser diode and fd is the data signal frequency. To increase the output frequency of the sub-central terminal, a laser diode with a high relaxation oscillation frequency must be used. The received rf signals at the sub-central terminal are amplified, then are converted to the intermediate frequency which can drive the optical modulators. The optically modulated signal is transmitted to the central terminal and then

detected by the photodiode.

B. Photodiode Mixing Link -Link F-

The fiber optic link using harmonic generation and optoelectronic mixing is shown in Fig.4.17. The mixer local oscillator power for the optoelectronic mixer is obtained from the harmonic generator in the central terminal. The amplitude of the harmonics is optimized using the bias condition of the laser diode, the input laser local oscillator power level and laser local oscillator frequencies. The received harmonics are detected by the photodiode and the desired frequency is selected by the microwave filter. The data signal is transmitted by another fiber cable and supplied into the optoelectronic mixer, then mixed with the mixer local oscillator power. The up- or down-converted signals are obtained from photodiode nonlinearities. Since the photodiode mixing efficiency strongly depends on the bias condition of the photodiodes, the photodiode bias voltage must be approximately zero. The output frequency is determined from the mixer local oscillator frequency and the data signal frequency. More explicitly, the relationship between the output frequency fs of the sub-central terminal and the mixer local oscillator frequency fl is expressed as

$$fs = Ml \quad Mm \quad fl \pm fd \tag{15}$$

where Mm is the frequency multiplication factor of the optoelectronic mixer. Mm =1 corresponds to fundamental optoelectronic mixing and Mm >1 corresponds to subharmonic optoelectronic mixing.

C. Photodiode Mixing Link -Link G-

In Fig.4.18, it is the optically pumped mixer rather than the optoelectronic mixer that is used for generation of microwave signals. Harmonics generated from the laser diode are detected by the mixer and used as mixer local oscillator input power. The data signal is detected by the photodetector and supplied into the optically pumped mixer, then mixed with mixer local oscillator power. The up- or down-converted signals are obtained by photodiode nonlinearities. The relationship between the output frequency fs of the sub-central terminal and the mixer local oscillator frequency fl is expressed as

$$fs = Ml \quad fl \pm fsub. \tag{16}$$

Eq.(16) is the same as Eq.(14). However, the inherent nonlinearities of the photodiode are exploited in Link G.

4.3.1 Experimental Results

Three fiber optic links are experimentally investigated. The harmonic laser mixing and harmonic modulation are accomplished with an InGaAsP laser diode (Ortel 1510A). The laser diode has a threshold current of 20mA and an cw output power of 0.6mW at a forward bias current of 50mA. The laser diode's 3dB

electrical bandwidth is approximately 7GHz at a bias current of 35mA. The InGaAs pin photodiode (Lasertron QDEUHS-035) used as the mixer has a 3-dB bandwidth of 10GHz and a responsivity of 0.58A/W. In the laser diode mixing experiment, a microwave power divider was used to combine the laser local oscillator power and data signal frequency. The microwave 3-dB hybrid was used to separate the mixer local oscillator/data signal input power and the upconverted/down-converted output signals of the optoelectronic mixer and the optically pumped mixer. To compare the characteristics of three fiber optic links, the local oscillator frequency of the laser diode is fixed at 4GHz, and the data signal frequency at 0.9GHz.

The nonlinear frequency response of the laser diode is shown in Fig.4.19. The modulated optical power is detected by the photodiode. The harmonic level is optimized by adjusting the modulation frequencies and the bias current of the laser diode. The link loss of the 2nd harmonic at 8GHz is 40.4dB, while that of the 3rd harmonic at 12GHz is 45.2dB, both measured with laser local oscillator input power equal to 10dBm, and at a laser diode bias current of 35mA. The significant link loss reduction of the harmonics is achieved under the large-signal modulation close to the relaxation oscillation frequency. The performance of the harmonic laser diode mixer is shown in Fig.4.20. Fig.4.20(a) shows the output power of the 2nd harmonic (8GHz) and the upconverted signal (8.9GHz). The maximum signal output power is -36.1dBm at a signal input power of 0dBm, and the minimum signal link loss of 31.4dB is achieved at a signal input power less than -10dBm. Since the link loss of the 0.9-GHz signal is 42.5dB, a conversion gain of 11.1dB from the 0.9-GHz signal to the 8.9-GHz upconverted signal is obtained. Fig.5(b) shows the output power of the 3rd harmonic (12GHz) and the upconverted signal (12.9GHz). Due to the reduction of the 3rd harmonic level as shown in Fig.4.19, the output power of the upconverted signal decreases. However, a conversion gain of 7.9dB from the 0.9-GHz signal to the 12.9-GHz upconverted signal is obtained. The maximum output power is -41.3dBm at a signal input power of -4dBm, and the minimum link loss of 34.6dB is achieved.

An other important parameter of the harmonic laser diode mixer is the third-order intermodulation product (IM3). The IM3 of the harmonic laser diode mixer is experimentally evaluated. Fig.4.21 shows the output power of the upconverted signal and IM3. Two equal-amplitude signals at 0.9GHz and 0.91GHz are used to examine IM3 at 9.89GHz and 9.92GHz for the 2nd harmonic, and at 12.89GHz and 12.92GHz for the 3rd harmonic. The power ratio of the upconverted signal and IM3 using the 2nd and 3rd harmonics is 30dB and 24.8dB, respectively, at a signal input power of -12dBm. Although the ratio can be improved by reduction of the signal input power, IM3 deteriorates at higher order

harmonics.

The output power of the optoelectronic mixer and subharmonic optoelectronic mixer is shown in Fig.4.22. The data signal input power and the bias current of the laser diode are 13dBm and 45mA, respectively. The mixer local oscillator frequency is fixed at 8GHz. Minimum conversion loss is achieved at the reverse bias voltage of 0.5V, as shown in Fig.4.22(b). The mixing efficiency is optimized when the bias voltage is approximately zero, because the mixer local oscillator power generates photodiode nonlinearities. An output power of -37.6dBm is obtained at a mixer local input power of 7dBm. This corresponds to a link loss of 50.6dB. The intrinsic conversion loss of the mixer is estimated to be 8.1dB because the link loss of the data signal at 0.9GHz is 42.5dB. Since the second order local harmonic is generated in the photodiode, the mixer can function as a subharmonic mixer. Fig.4.22(a) also shows the characteristics of the subharmonic optoelectronic mixer. The second harmonic frequency of the mixer becomes 16GHz. The link loss of the upconverted signal (16.9GHz) is 60dB, and the obtained output power is -47dBm. The conversion loss of the subharmonic mixer is 17.5dB. Fig.4.23 shows the other experimental results of the subharmonic mixer. The link loss of the upconverted signal (12.9GHz) is 51.7dB at a mixer local oscillator input power of 13dBm, and a mixer local oscillator frequency of 6GHz. An output power of -37.7dBm is obtained. The upconverted signal (17.1GHz) generated by the 3rd order mixer local oscillator power (18GHz) is observed in the experiment. The link loss is 63.7dB and the output power is -49.7dBm at a data signal input power of 14dBm.

The signal output power and the bias voltage dependences of the optically pumped mixer are shown in Fig.4.24. The 2nd harmonic at 8GHz and the 3rd harmonic at 12GHz are directly detected by the mixer and used as mixer local oscillator frequencies. The 0.9-GHz data signal is directly supplied to the mixer diode. The signal conversion loss of 47.7dB and 57dB is achieved at a local frequency of 8GHz and 12GHz, respectively. The output power of the mixer is -40.1dBm at 8.9GHz, and -45.9dBm at 12.9GHz. Since the mixer local oscillator input power is dependent on the harmonic level generated in the laser diode, the signal conversion loss of the optically pumped mixer is larger than that of the optoelectronic mixer. In order to decrease the conversion loss, higher laser diode output power is required. The mixing efficiency is optimized at a bias voltage of approximately zero.

4.3.2 Discussion

The feasibility of frequency multiplication by harmonic laser mixing, optoelectronic mixing or optically pumped mixing is demonstrated in the X band.

Table 4.2 summarizes and compares the experimental results of three fiber optic link configurations. Link E has features high conversion gain, low link loss and simplification of the fiber optic link architecture. Conversion gain and output power decrease as the harmonic order increases. To extend the effective bandwidth of Link E, laser diodes capable of generating high harmonic levels must be used. Although the laser diode mixing link has the advantage of reducing the number of microwave components at the central terminal and the number of fiber cables between the central terminal and the sub-central terminal, the dynamic range of the link is limited by low intermodulation product distortion.

The output power of the optoelectronic mixer is larger than that of the optically pumped mixer, because the local level for the optoelectronic mixer is much larger than that for the optically pumped mixer. The local input power of the optoelectronic mixer can be amplified by microwave amplifiers, while that of the optically pumped mixer is directly detected by the mixer itself. To increase the output power of the optically pumped mixer, high harmonic levels must be transmitted from the harmonic generator (laser diode) in the sub-central terminal. Since the photodiode in Link F is driven by the electrical local oscillator power, the harmonics of the mixer local oscillator frequency can be generated from photodiode nonlinearities. These harmonics are exploited to extend the fiber optic link effective bandwidth. The photodiode mixing link configuration can eliminate microwave frequency converters in the sub-central terminal. This makes it possible to realize a small and cost-effective sub-central terminal. The photodiode mixing link can extend the link bandwidth up to millimeter-wave frequencies under the frequency limitation of opto-devices as well as of achieve simple and inexpensive equipment. Although Link F is composed of three fiber cables, each link can be optimized to have a wide dynamic rang. The photodiode mixing links realize signal conversions at the sub-central terminal, while the laser diode mixing link does so at the central terminal. The photodiode frequency conversion can eliminate the influence of the laser diode relative intensity noise. This helps to decrease the noise floor of the converted signals. The system noise figure is based on the operating condition of the laser diode. The relative intensity noise contributes to noise figure when the laser diode is operated near the relaxation oscillation frequency. The photodiode mixing link is usually the least sensitive to laser noise because of the low frequency signal transmission.

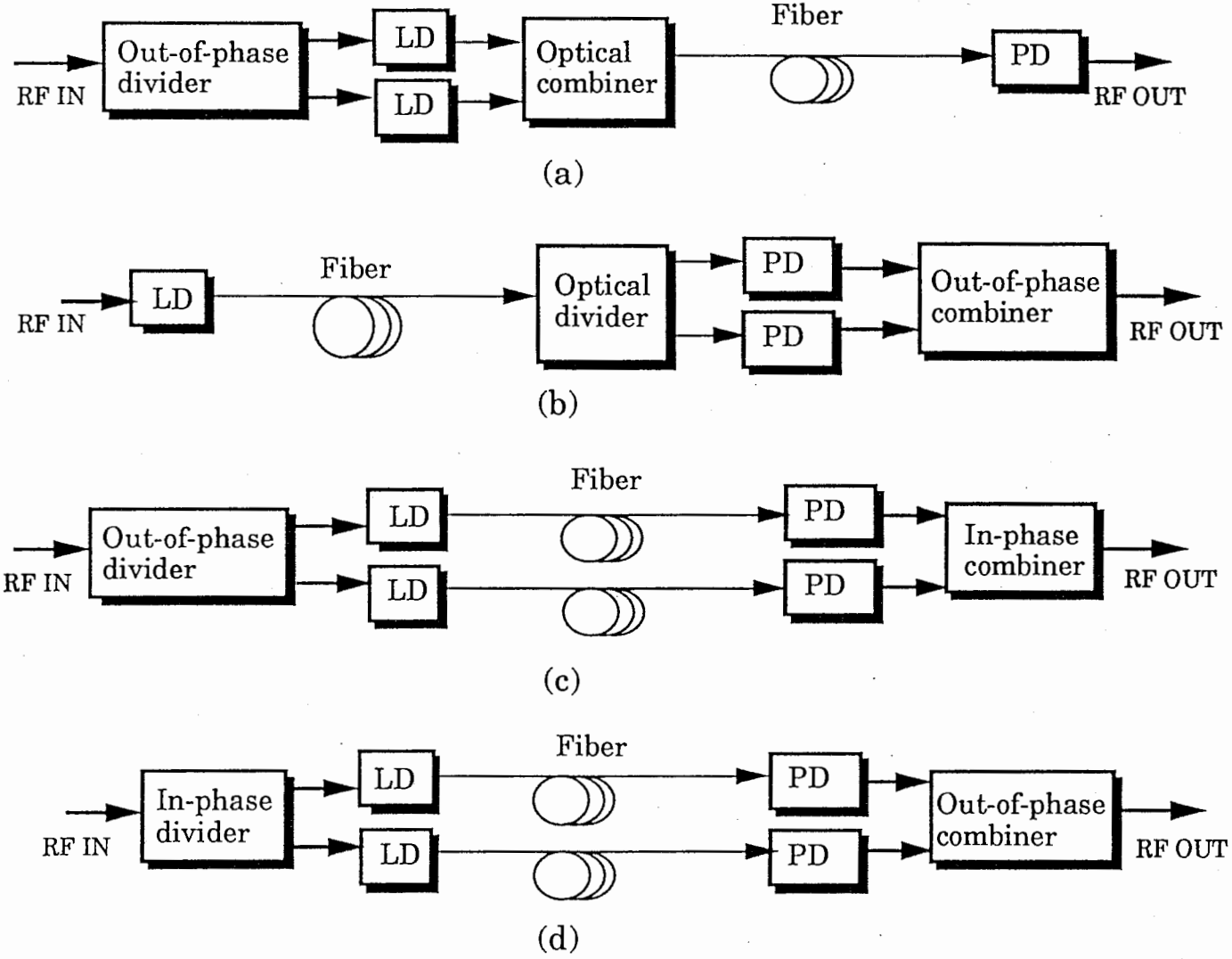

Fig.4.1. Link configurations of balanced laser harmonic generation. (a) Single-fiber link configuration A using two laser diodes. (b) Single-fiber link configuration B using one laser diode. (c) Twin-fiber link configuration C. (d) Twin-fiber link configuration D.

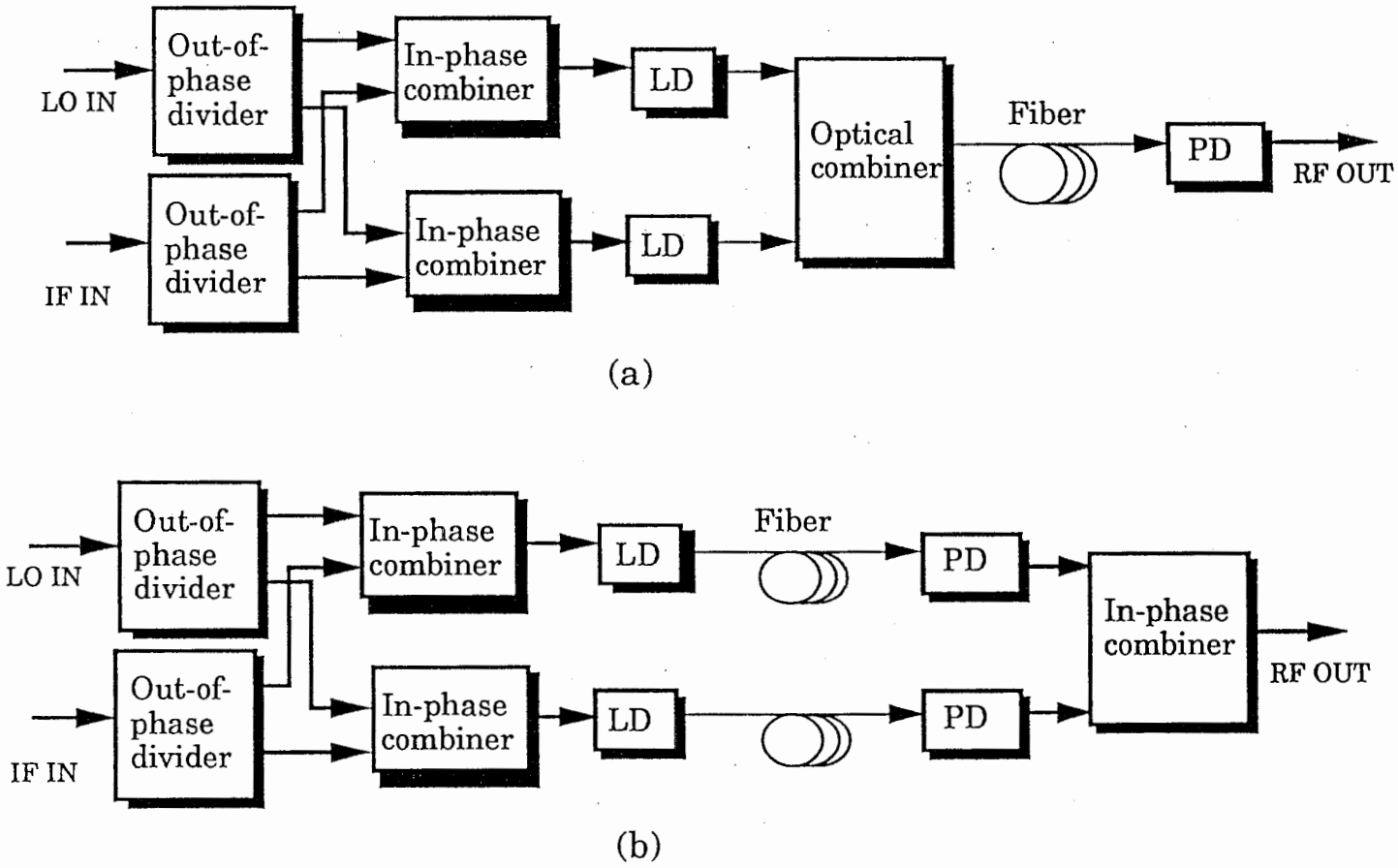

Fig.4.2. Link configuration of balanced laser mixing. (a) Single-fiber link configuration. (b) Twin-fiber link configuration.

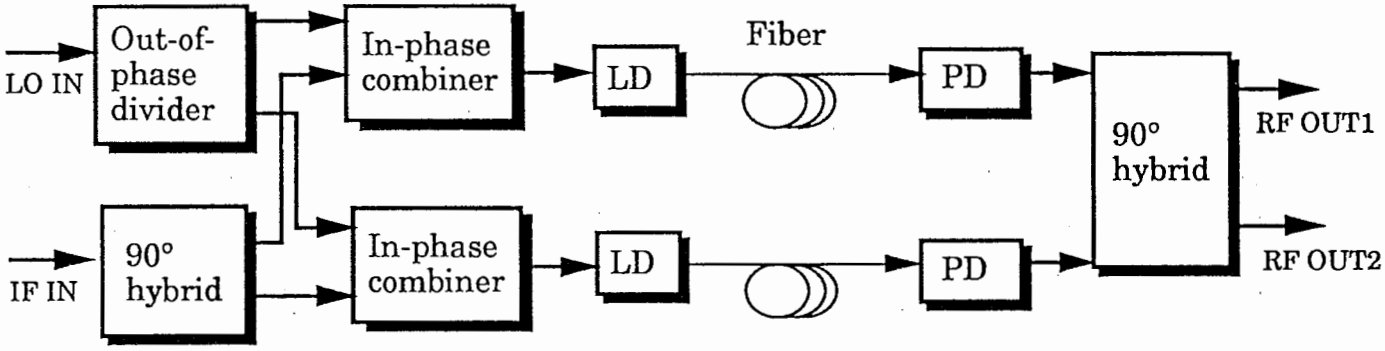

Fig.4.3. Link configuration of image cancellation laser mixing.

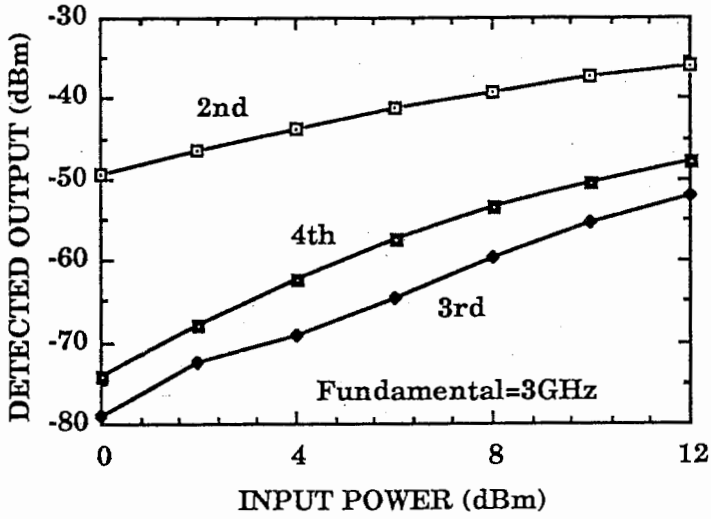

(a)

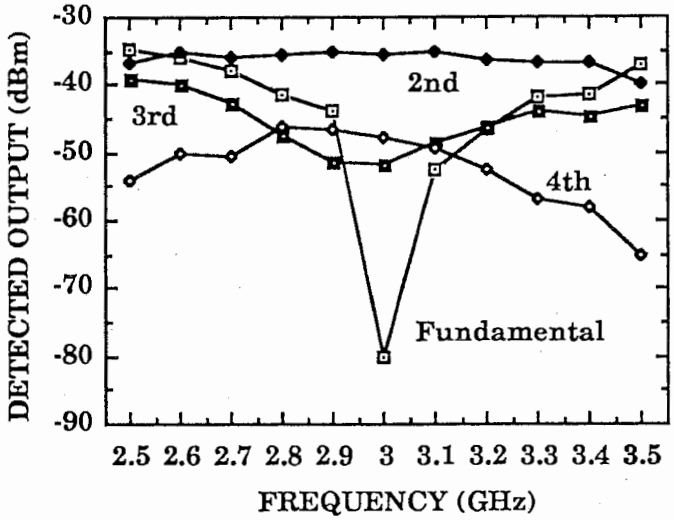

(b)

Fig.4.4. Performance of single-fiber balanced laser harmonic generation link. The fundamental, 2nd harmonic, 3rd harmonic, and 4th harmonic frequencies are 3GHz, 6GHz, 9GHz, and 12GHz, respectively. (a) RF input power dependence. (b) Frequency response.

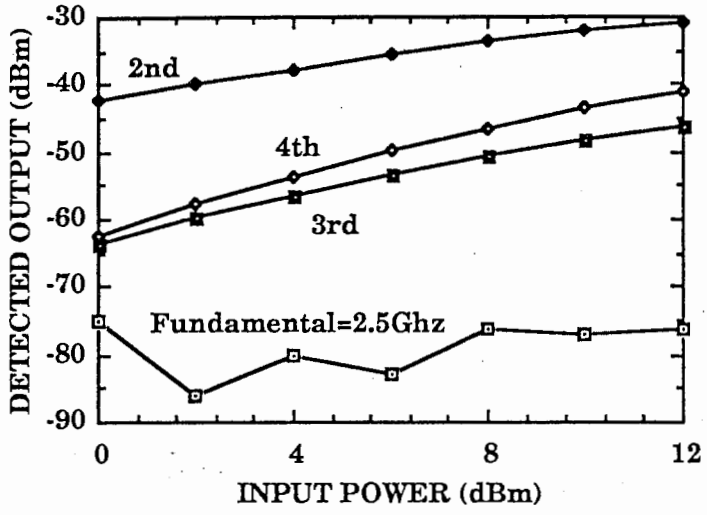

(a)

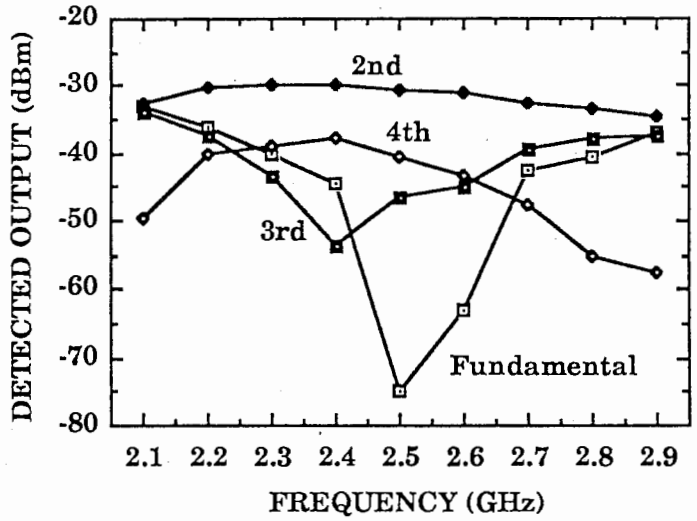

(b)

Fig.4.5. Performance of twin-fiber balanced laser harmonic generation link. The fundamental, 2nd harmonic, 3rd harmonic, and 4th harmonic frequencies are 2.5Ghz, 5GHz, 7.5GHz, and 10GHz, respectively. (a) RF input power dependence. (b) Frequency response.

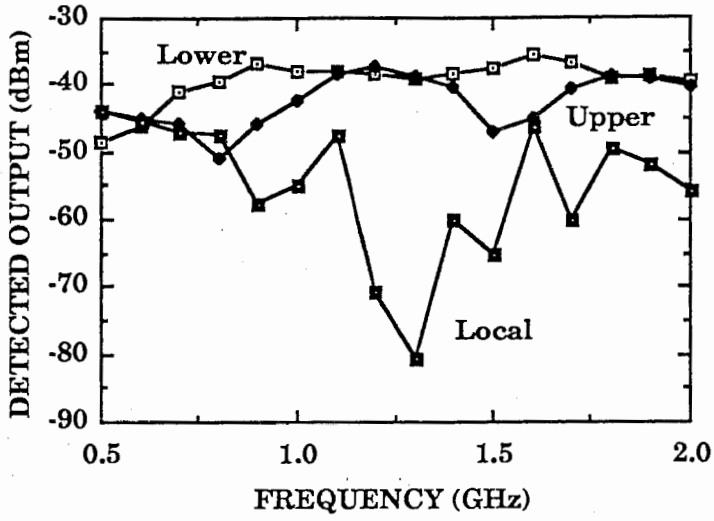

(a)

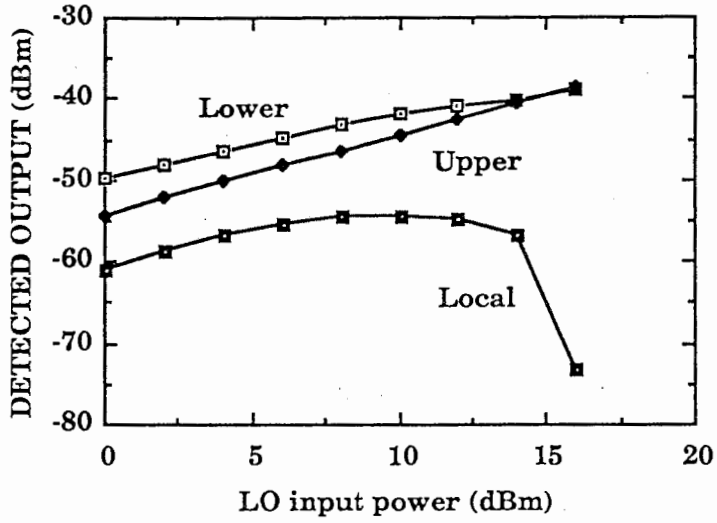

(b)

Fig.4.6. Performance of balanced laser mixing link. (a) The local frequency is 6GHz, and the local input power is 16dBm. (b) The IF frequency is 1.3GHz.

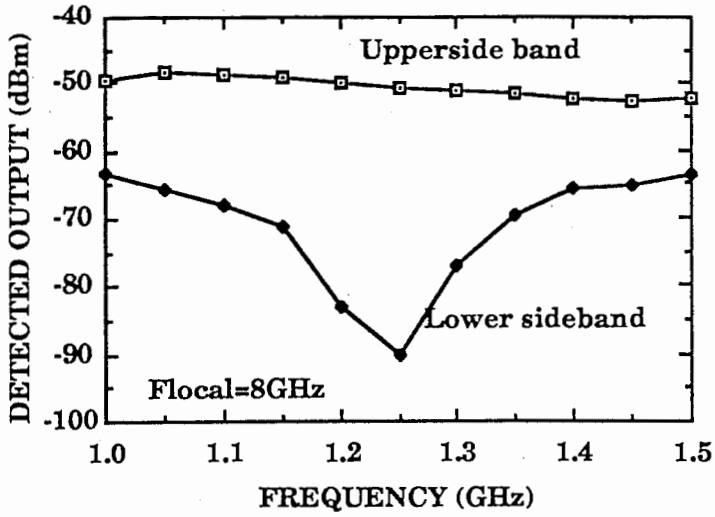

(a)

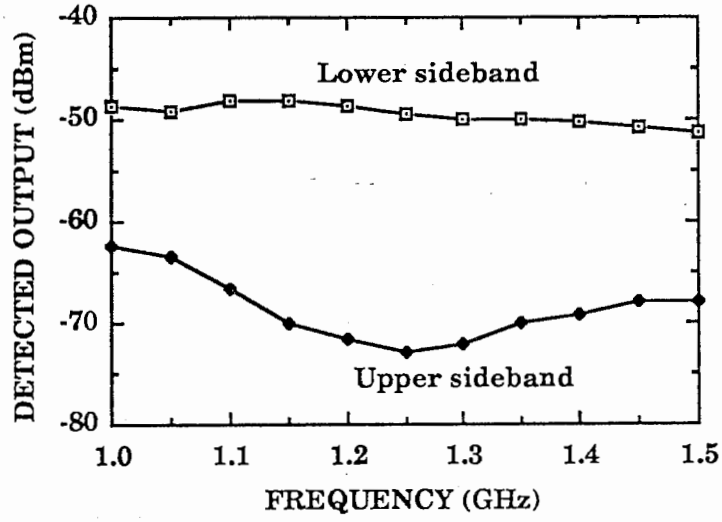

(b)

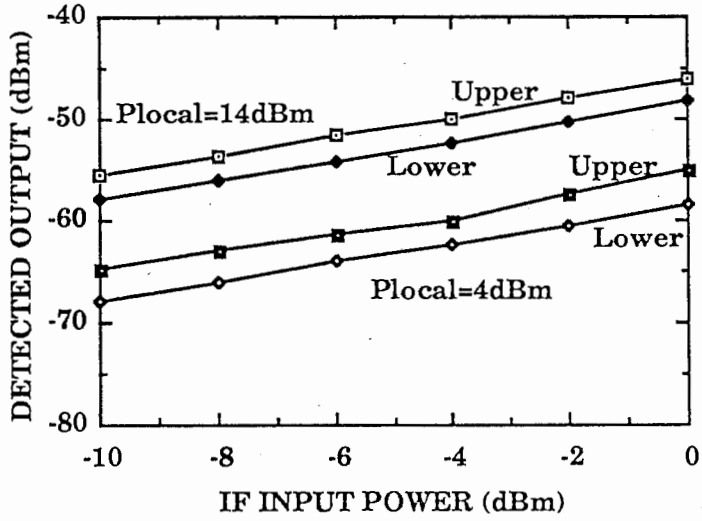

(c)

Fig.4.7. Performance of image cancellation link. The local frequency is 8GHz. (a) Frequency response of upper sideband. The local input power is 14dBm. (b) Frequency response of lower sideband. (c) IF input power dependence. The local and IF frequencies are 8GHz and 1GHz, respectively.

Table 4.1 Expeimental Results of Three Fiber Optic Links

	Balanced laser harmonic generation link		Balanced laser mixing	Image cancellation
	Single-fiber link	Twin-fiber link	twin-fiber link	mixing link
Fundamental frequency (RF)	3GHz	2.5GHz		
Local frequency (LO)			6GHz	8GHz
Intermediate frequency (IF)			1.3GHz	1.25GHz
Upper sideband frequency (Upper)			7.3GHz	9.25GH
Lower sideband frequency (Lower)			4.7GHz	6.75GHz
Suppression Ratio				
2nd harmonic/RF	>44dB	45.4dB		
3rd harmonic/RF	>28dB	29.7dB		
4th harmonic/RF	>33dB	35dB		
Upper/LO			41.9dB	
Lower/LO			41.5dB	
Upper/Lower				39.3dB
Lower/Upper				23.4dB

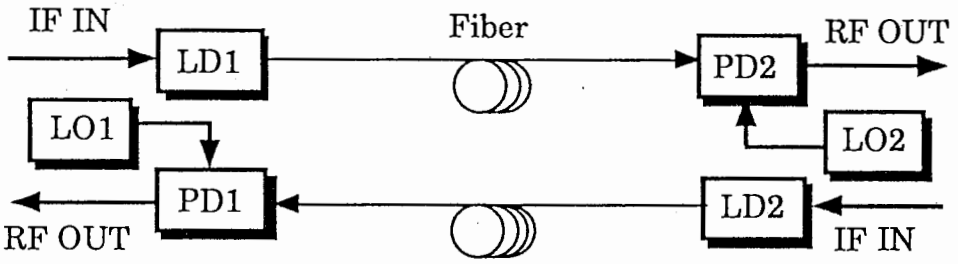

(a)

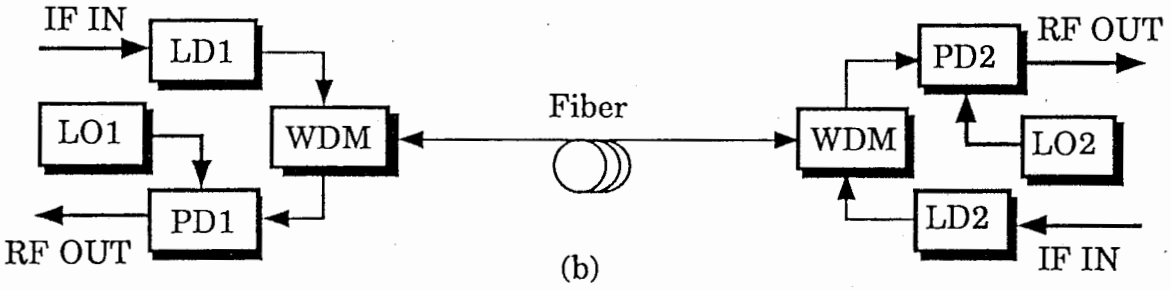

(b)

Fig.4.8. Link configurations of bidirectional fiber optic transmission systems using laser diode direct modulation and photodiode mixing. (a) Space division multiplexing. (b) Wavelength division multiplexing. (c) Time compression multiplexing using LD detector (LD-LD link). (d) Time compression multiplexing using LD receiving mixer (LD-LD MIX link).

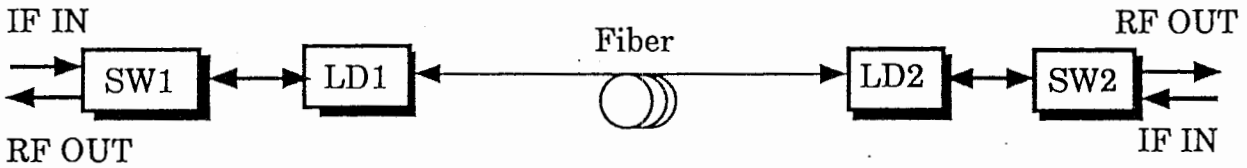

(c)

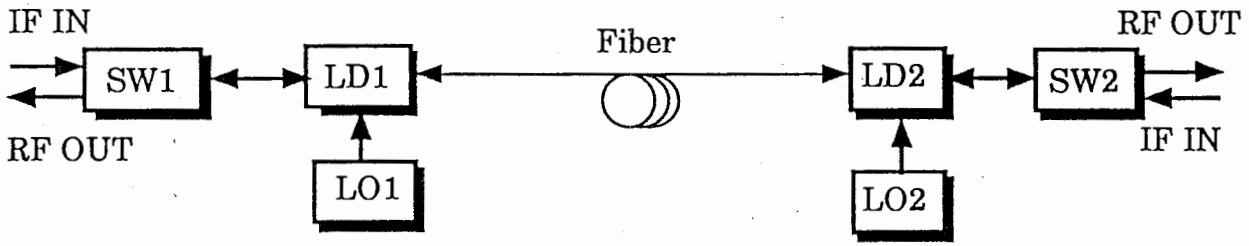

(d)

Fig.4.8. Link configurations of bidirectional fiber optic transmission systems using laser diode direct modulation and photodiode mixing. (a) Space division multiplexing. (b) Wavelength division multiplexing. (c) Time compression multiplexing using LD detector (LD-LD link). (d) Time compression multiplexing using LD receiving mixer (LD-LD MIX link).

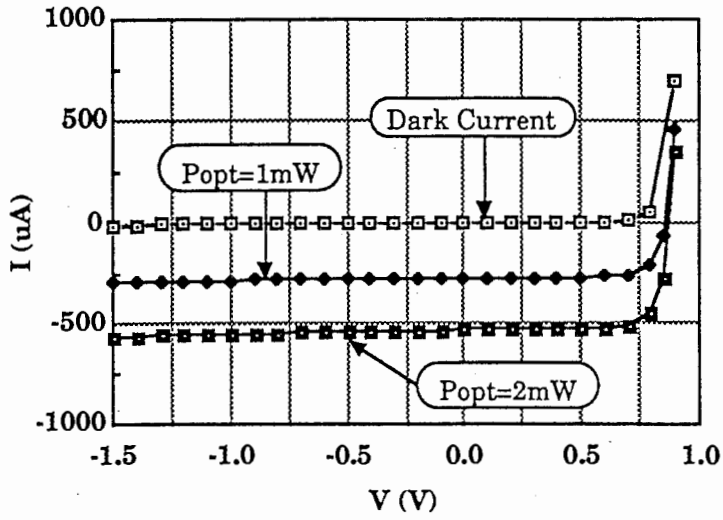

(a)

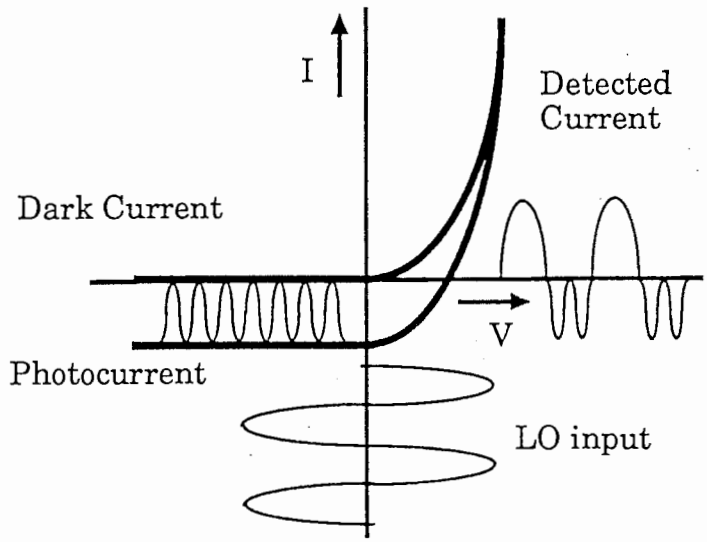

(b)

Fig.4.9. Static performance of laser diode. (a) I-V characteristics. (b) Schematic frequency mixing process.

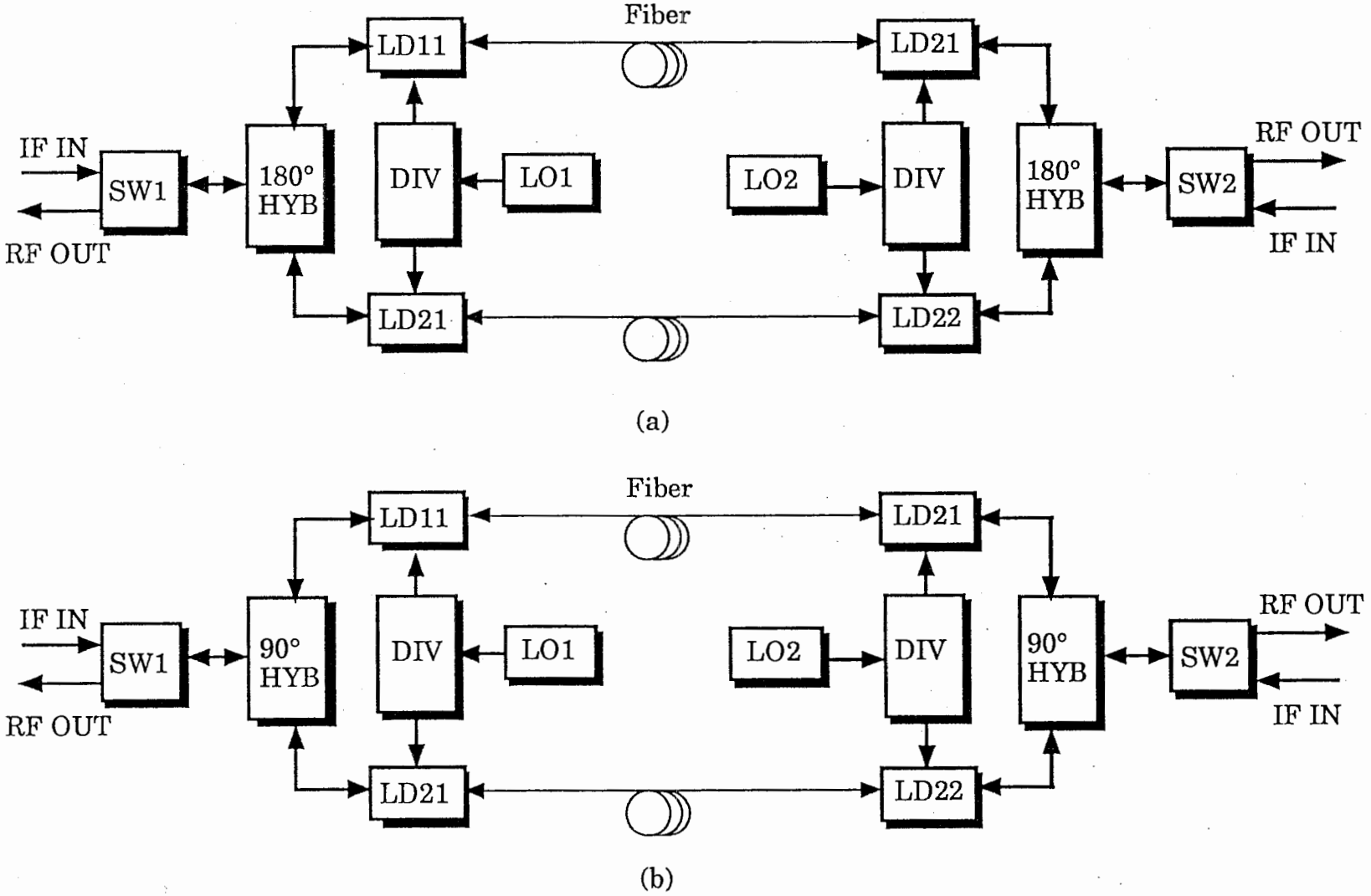

Fig.4.10. Link configuration of bidirectional fiber optic transmission systems using LD receiving mixers. (a) LO suppresion link. (b) Image cancellation link.

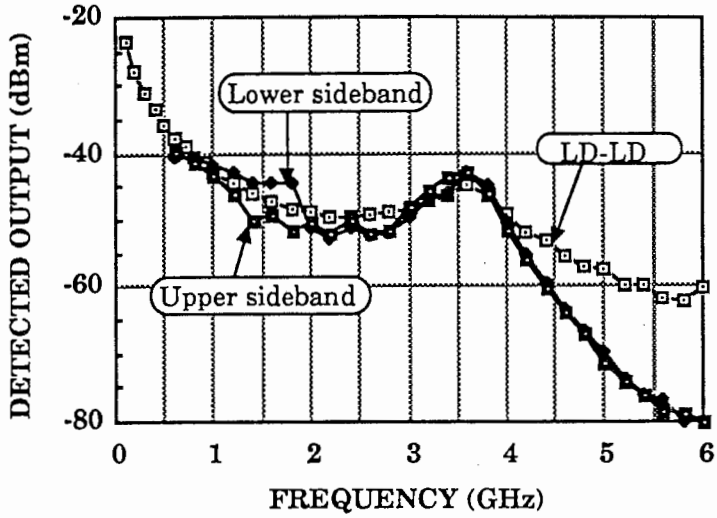

(a)

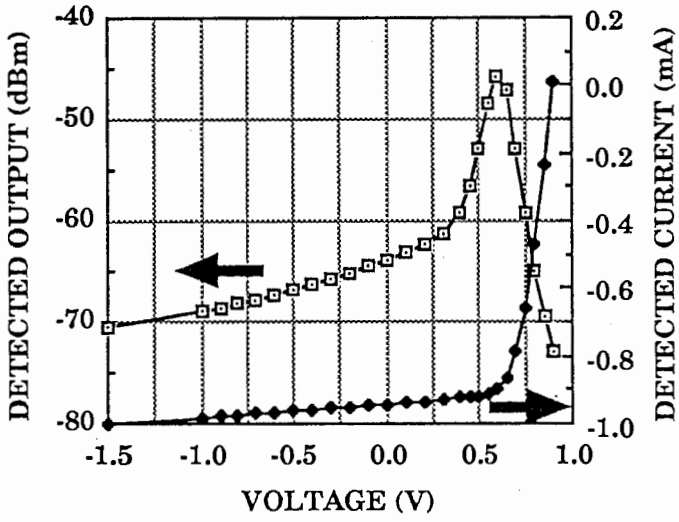

(b)

Fig.4.11. Basic performance of LD-LD MIX link. (a) Frequency response. (b) Bias dependence.

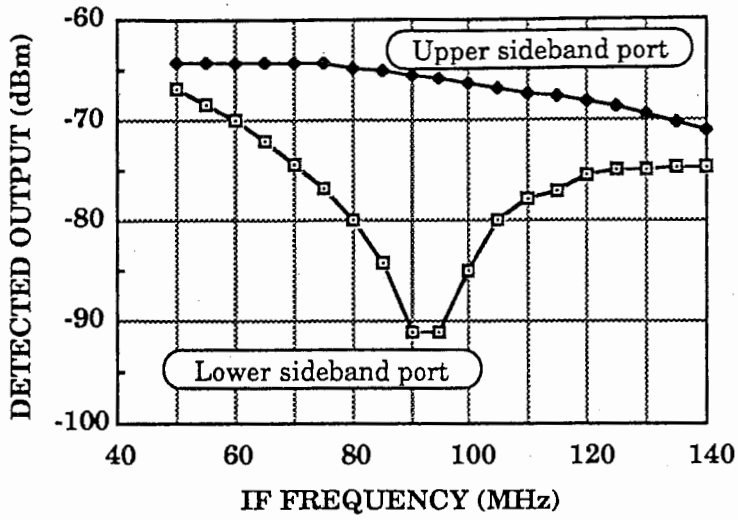

(a)

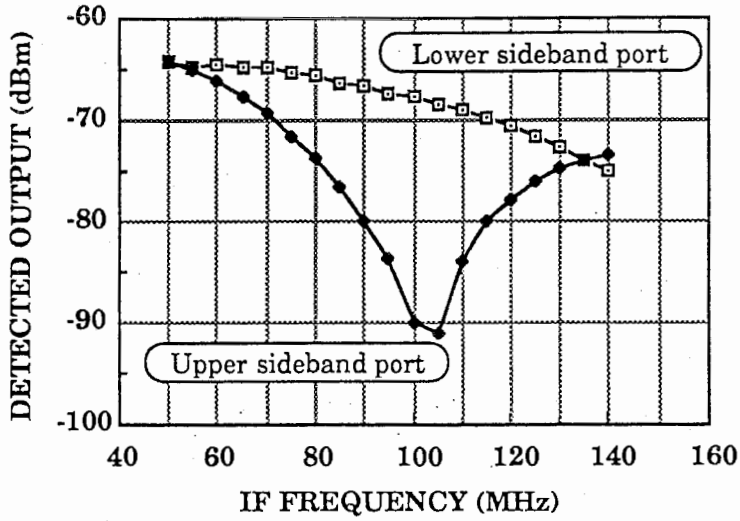

(b)

Fig.4.12. IF frequency characteristics of image cancellation link. (a) Upper sideband frequency corresponds to RF frequency. (b) Lower sideband corresponds to RF frequency.

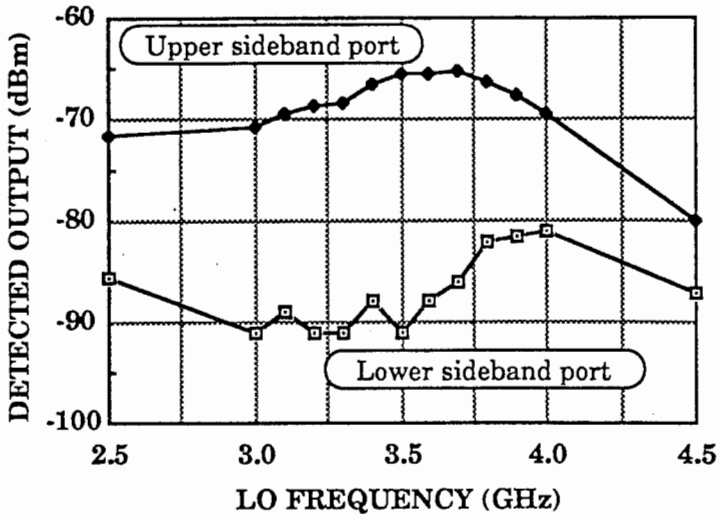

(a)

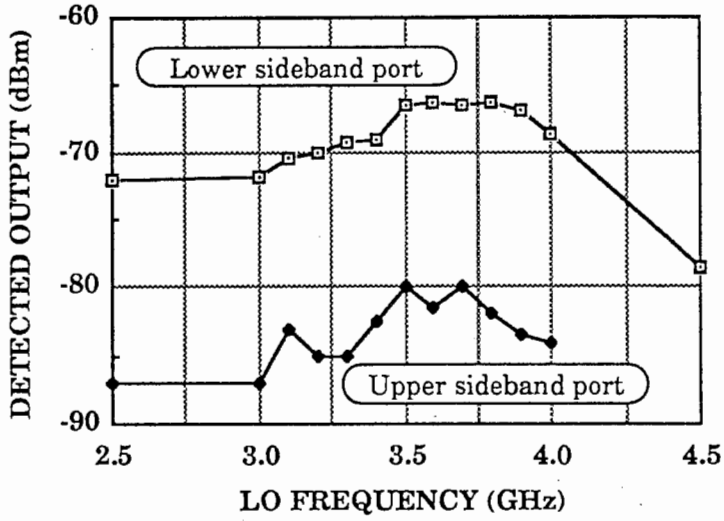

(b)

Fig.4.13. RF frequency characteristics of image cancellation link. (a) Upper sideband frequency corresponds to RF frequency. (b) Lower sideband frequency corresponds to RF frequency.

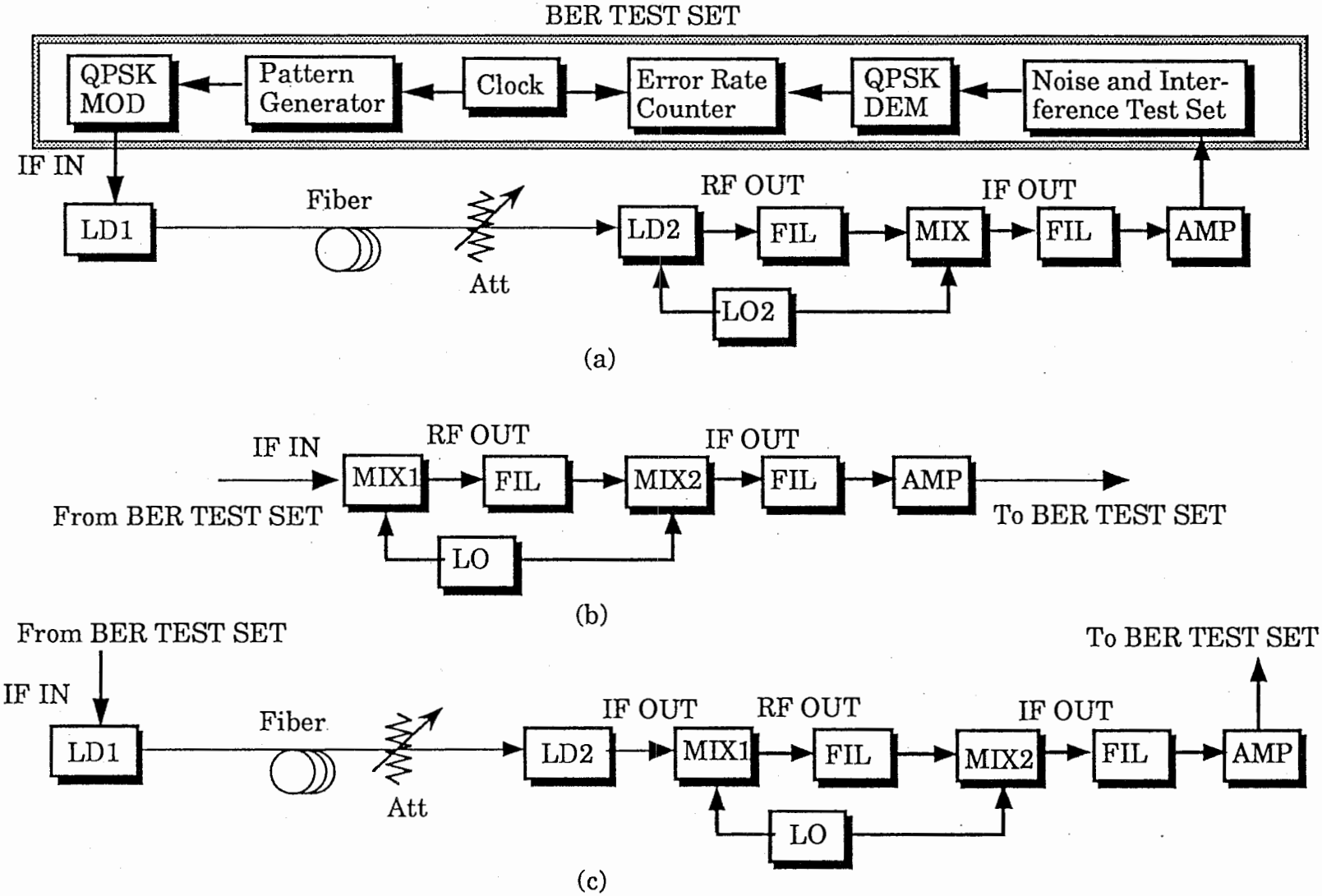

Fig.4.14. Experimental setup for measurement of the bit error rate. IF frequency is 70MHz and LO2 frequency is 3.8GHz. (a) Setup for LD-LD MIX link. (b) Setup for MIX-MIX link which has no optical components. (c) Setup for LD-LD+MIX link which consists of LD-LD link and MIX-MIX link.

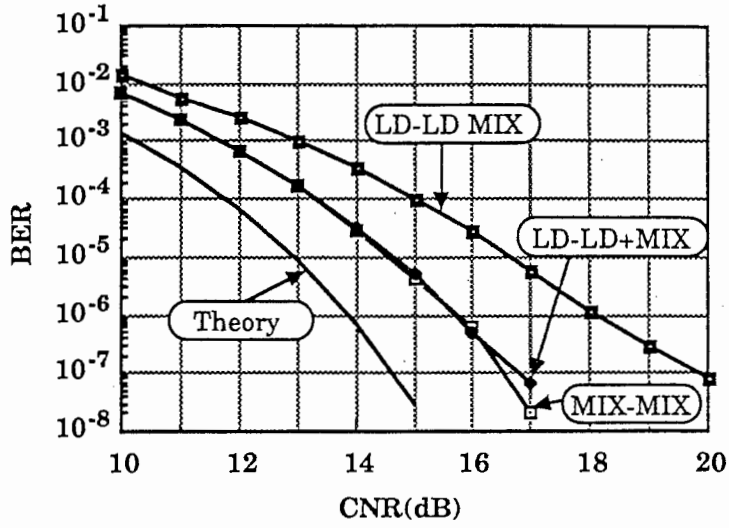

Fig.4.15. QPSK transmission characteristics of LD-LD MIX link.

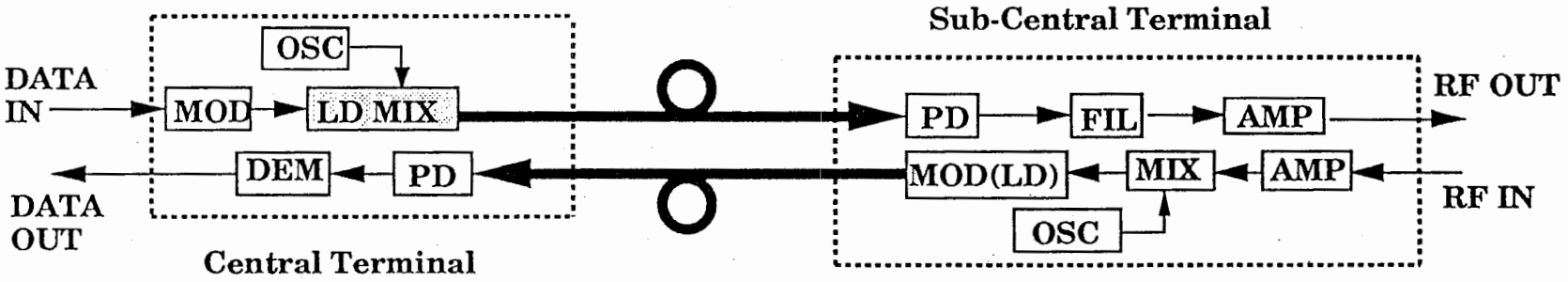

Fig.4.16. Fiber optic link configuration for microwave and millimeter-wave transmissions using harmonic laser diode mixing (Laser diode mixing link - Link E) .

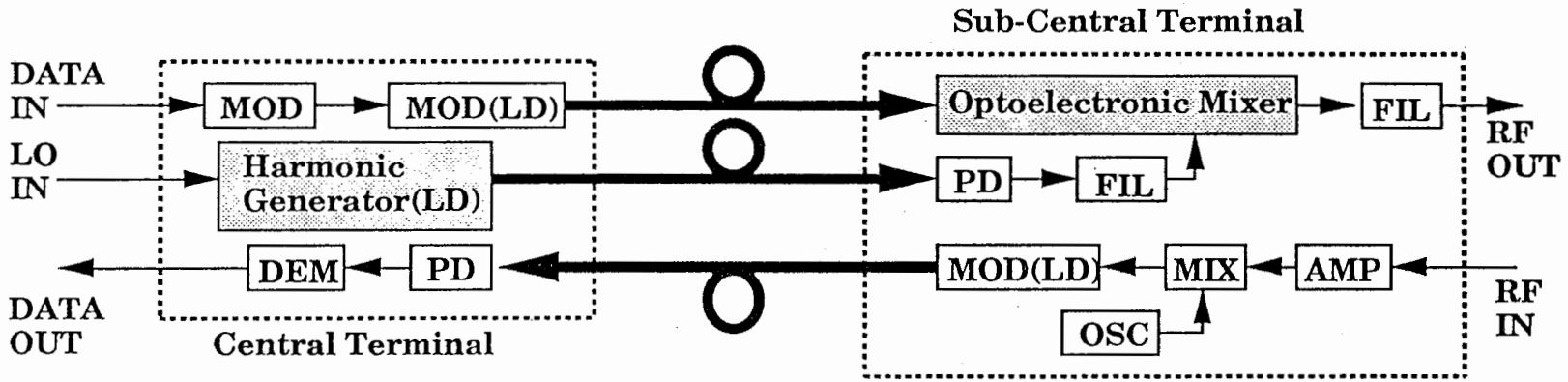

Fig.4.17. Fiber optic link configuration for microwave and millimeter-wave transmissions using harmonic generation and optoelectronic mixing/subharmonic optoelectronic mixing (Photodiode mixing link - Link F).

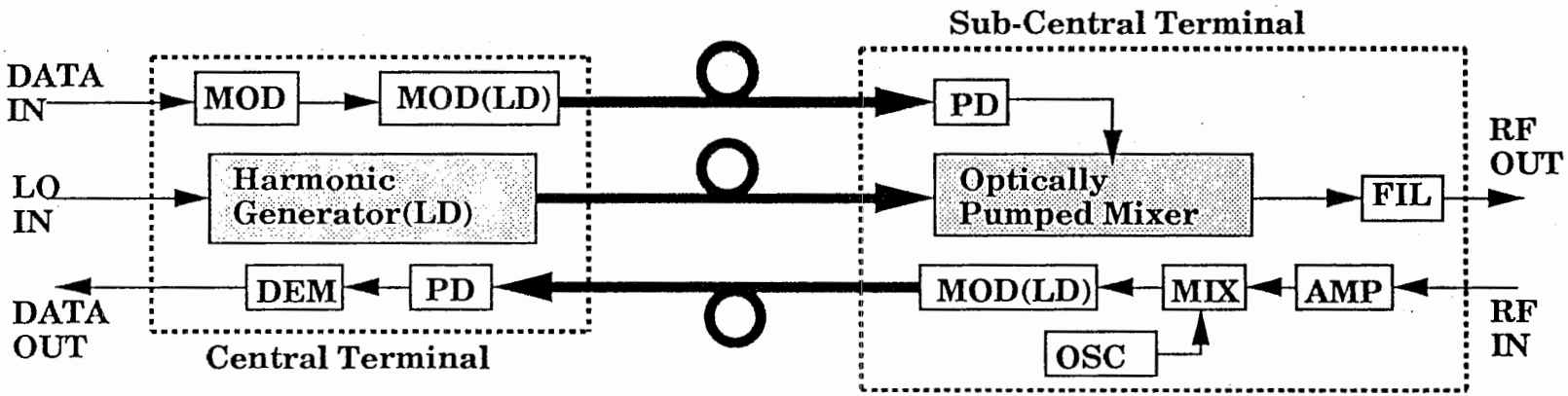

Fig.4.18. Fiber optic link configuration for microwave and millimeter-wave transmissions using harmonic generation and optically pumped mixing (Photodiode mixing link - Link G).

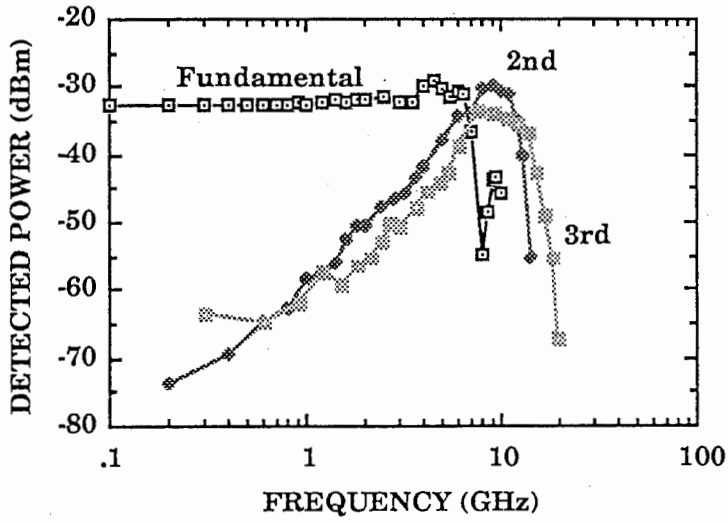

Fig.4.19. Frequency response of laser diode (Laser local oscillator input power=10dBm, Laser diode bias current=35mA).

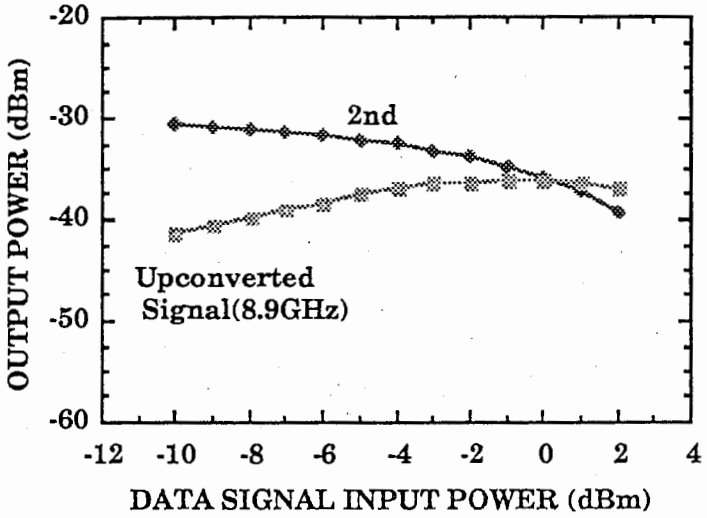

(a)

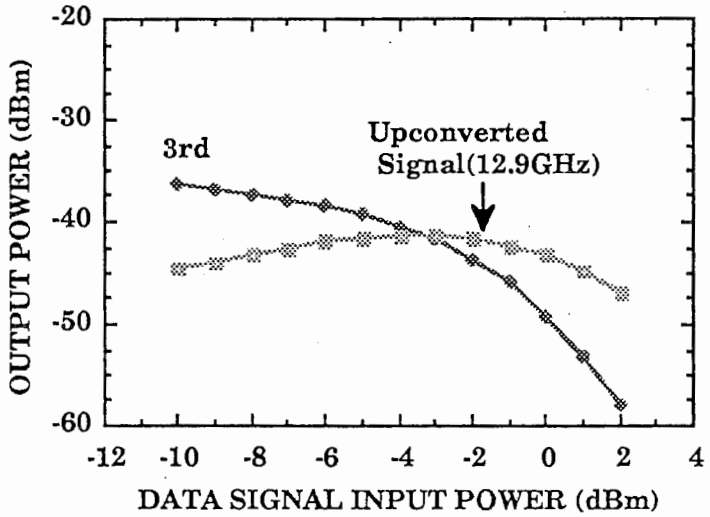

(b)

Fig.4.20. Output power of harmonic laser mixer (Laser local oscillator frequency=4GHz, Laser local oscillator input power=10dBm, Laser diode bias current=35mA, Data signal frequency=0.9GHz). (a) Second harmonic response. (b) Third harmonic response.

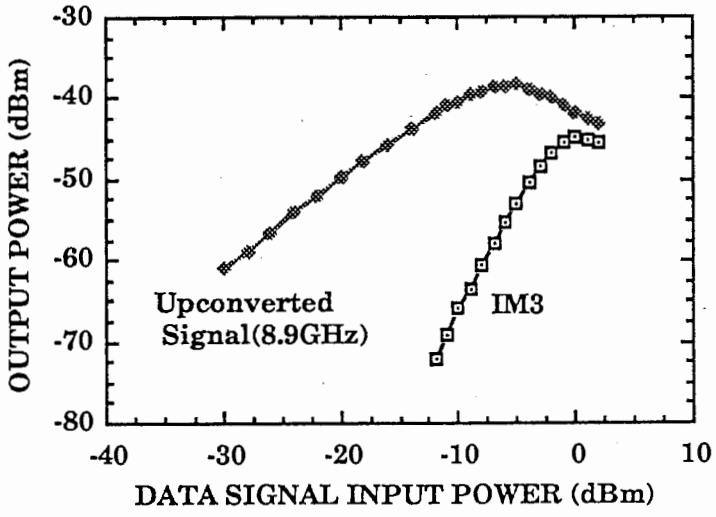

(a)

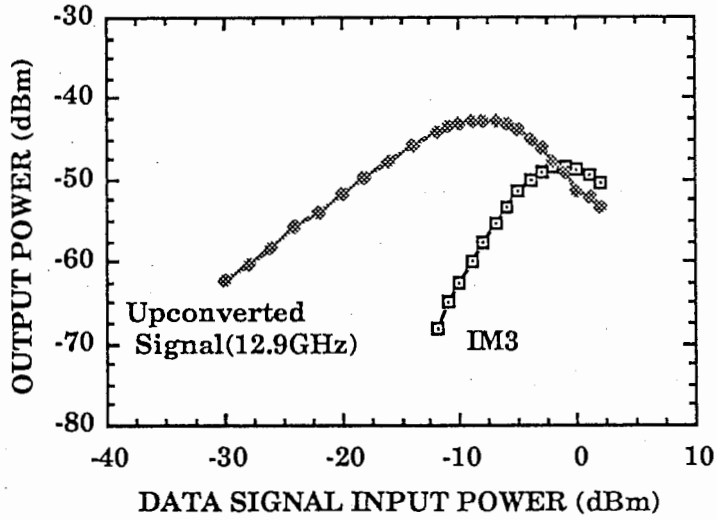

(b)

Fig.4.21. Intermodulation product of harmonic laser mixer (Laser local oscillator frequency=4GHz, Laser local oscillator input power=12dBm. Laser diode bias current=35mA, Data signal frequency=0.9GHz and 0.91GHz). (a) Second harmonic response. (b) Third harmonic response.

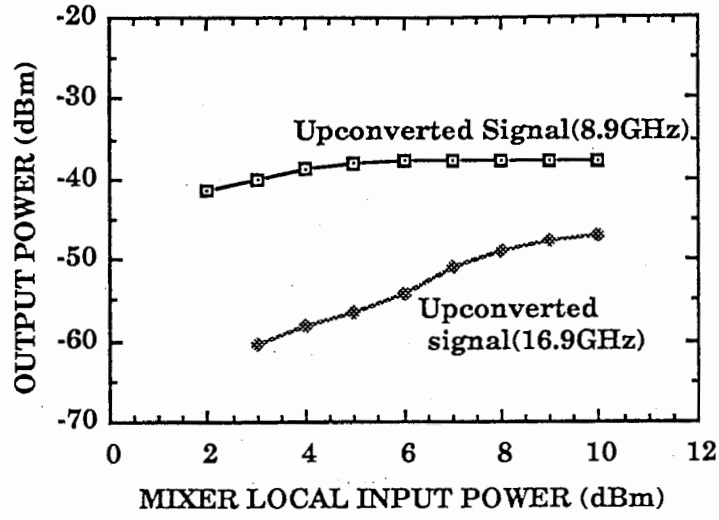

(a)

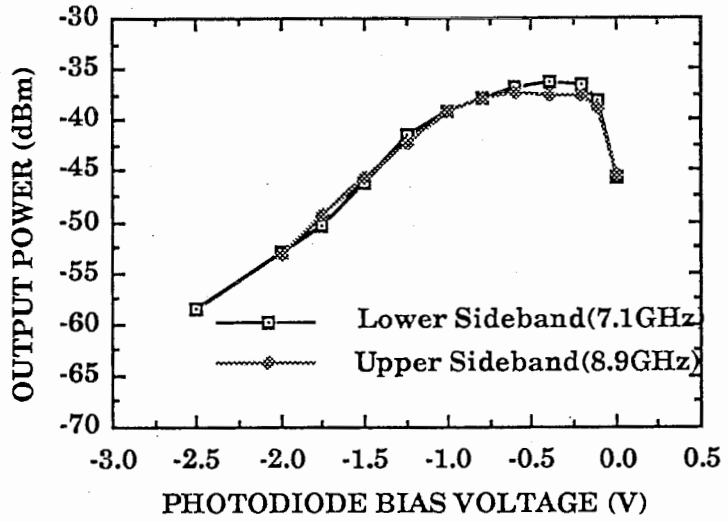

(b)

Fig.4.22. Performance of optoelectronic mixer (Mixer local oscillator frequency=8GHz, Data signal frequency=0.9GHz, Data signal input power=13dBm, Laser diode bias current=45mA). (a) Photodiode bias voltage=-0.5V. (b) Mixer local oscillator input power=8dBm.

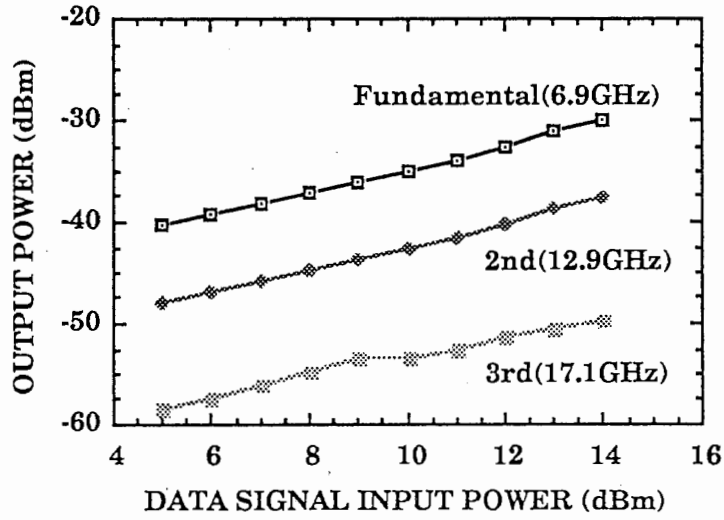

Fig.4.23. Performance of subharmonic optoelectronic mixer (Mixer local oscillator frequency=6GHz, Mixer local oscillator input power=13dBm, Data signal frequency=0.9GHz, Laser diode bias current=45mA, Photodiode bias voltage=-0.5V).

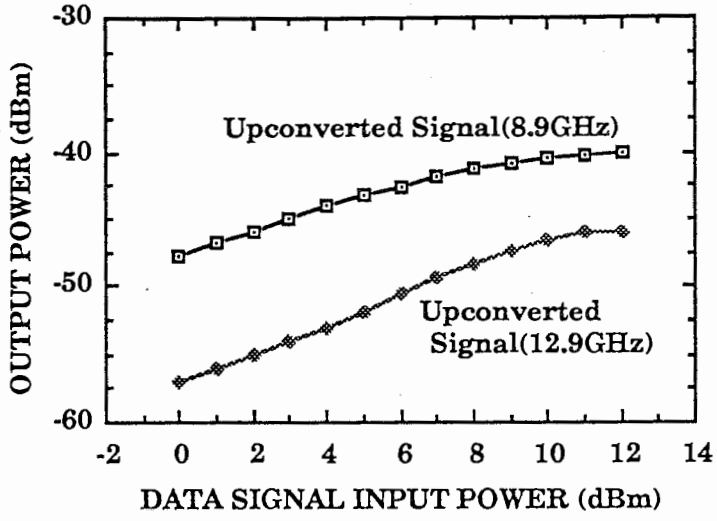

(a)

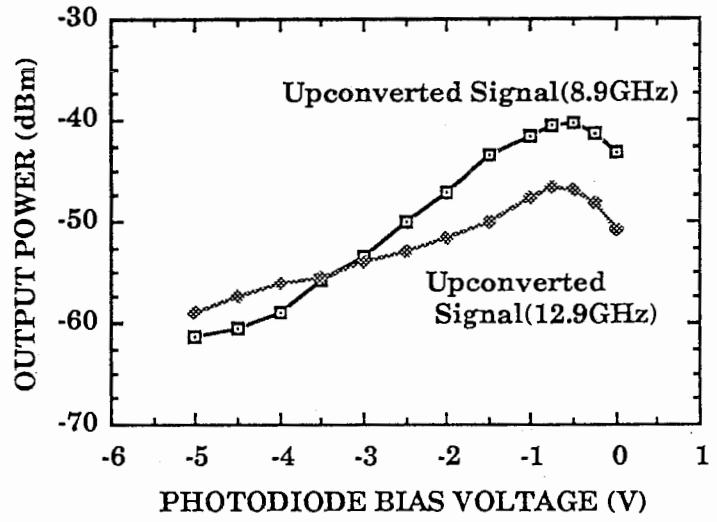

(b)

Fig.4.24. Performance of optically pumped mixer (Laser local oscillator frequency=4GHz, Laser local oscillator input power=15dBm, Laser diode bias current=35mA, Data signal frequency=0.9GHz). (a) Photodiode bias voltage=-0.7V. (b) Data signal input power=15dBm.

Table 4.2 Comparison of three fiber optic links.
(Data signal frequency=0.9GHz, Laser local oscillator frequency=4GHz, Mixer local oscillator frequency=6GHz and 8GHz)

Link	Upconverted Signal Frequency	Local Frequency	Output Power	Conversion Loss	Link Loss
Link E	8.9GHz	4GHz	-36.1dBm	-11.1dB	31.4dB
	12.9GHz	4GHz	-41.3dBm	-7.9dB	34.6dB
Link F	8.9GHz	8GHz	-37.6dBm	8.1dB	50.6dB
	12.9GHz*	6GHz	-37.7dBm	9.2dB	51.7dB
	16.9GHz*	8GHz	-47dBm	17.5dB	60dB
Link G	8.9GHz	4GHz	-40.1dBm	47.7dB	——
	12.9GHz	4GHz	-45.9dBm	57dB	——

* Subharmonic optoelectronic mixing

5. 今後の展望

光ファイバを用いたミリ波サブキャリア信号伝送のための各種技術に関して述べてきたが、本章では回路技術に焦点を絞って今後の技術動向さらには研究の方向等についての議論を行なう。

5.1 Quasi-Optical Techniques（準光学的回路技術）

弟１章の図1.3で示した無線基地局の特に光受信回路に関して、弟２章で議論した光／マイクロ波モノリシック集積回路技術が有効であることを明らかにした。無線基地局の機能はミリ波信号の検出のみでなく、マイクロセルゾーンへのミリ波放射も重要である。ミリ波帯のアンテナを送受分波器に接続して使用するのが最も一般的であるが、無線機がMMICで構成されることを考慮すると、アンテナに対してもMMICとの整合性を図る必要がある。最近、MIC化あるいはMMIC化平面アンテナが盛んに検討されるようになってきたが、放射パターンと他の回路機能とが完全に分離されている。一方、アンテナパターンとデバイスが一体となった放射回路の検討も行なわれており、種々の機能型放射回路あるいは受信回路が提案されている。これらの回路技術は準光学的テクニック（英語ではQuasi-Optical Techniques）と言われており、空中での電力合成や指向制御等に活用されている。無線基地局の光受信器（無線機としてはミリ波送信機）にこの技術を適用すると、図5.1に示すように放射機能を有する１チップ化光受信器が可能と思われる。すなわち、チップ内には光検出器、RF増幅器、放射器が集積化されている。

一方、光送信器（無線機としてはミリ波受信機）は受信したミリ波周波数を光周波数に変換すために、光変調機能が要求される。そこで、図5.2に示すようにアンテナと光変調器を一体化した受信アンテナ一体化集積回路を光送信器に適用することを提案する。この回路はセンサー等で検討が行なわれているが、本格的に無線受信機として使用する例はない。このように構成できれば、光送信機に必要とされる素子は発光源と変調器のみになり大幅な簡易化が達成可能である。

これらの機能を集積化した無線基地局構成例を図5.3に示す。無線へのインタフェースは全て集積回路で行なわれており、機能素子としては発光源（これも最終的には集積化可能）、変調器、受信器の３つである。このように、準光学的考え方を導入することにより無線（マイクロ～ミリ波）と光とのハードウエア上でのインタフェースを極端に簡単化できる。

5.2 ウエーハスケールインテグレイション化へ

光コンピュータ等に用いる大規模システムを１枚のウエーハ上に構築するウエーハスケールインテグレション(Wafer Scale Integration: WSI)は超高集積、高機能型集積回路の典型例である。この考え方は準光学的回路へも容易に拡張できる。すなわち、図5.4に示すように全ての機能素子、回路が１枚の半導体基板上に集積化する。放射器の数を増加させることができので、無線領域での機能拡大にも最適である。図では無線基地局と書いてあるが、もちろん端末側にも用いることができる。

これまではMMIC化という形容詞が回路に使われていたが今後はWSI化何々というマ

イクロ波～ミリ波回路等が実現されていくであろうという期待を込めて本報告のエンディグにしたい。

謝辞

本研究を進めるにあたって、日頃御指導、御援助して頂いた葉原会長、古濱社長、赤池前室長、小川英一室長に感謝します。また、いっしょに研究を行ってきた本グループの各研究員（概要のリスト参照）に感謝します。

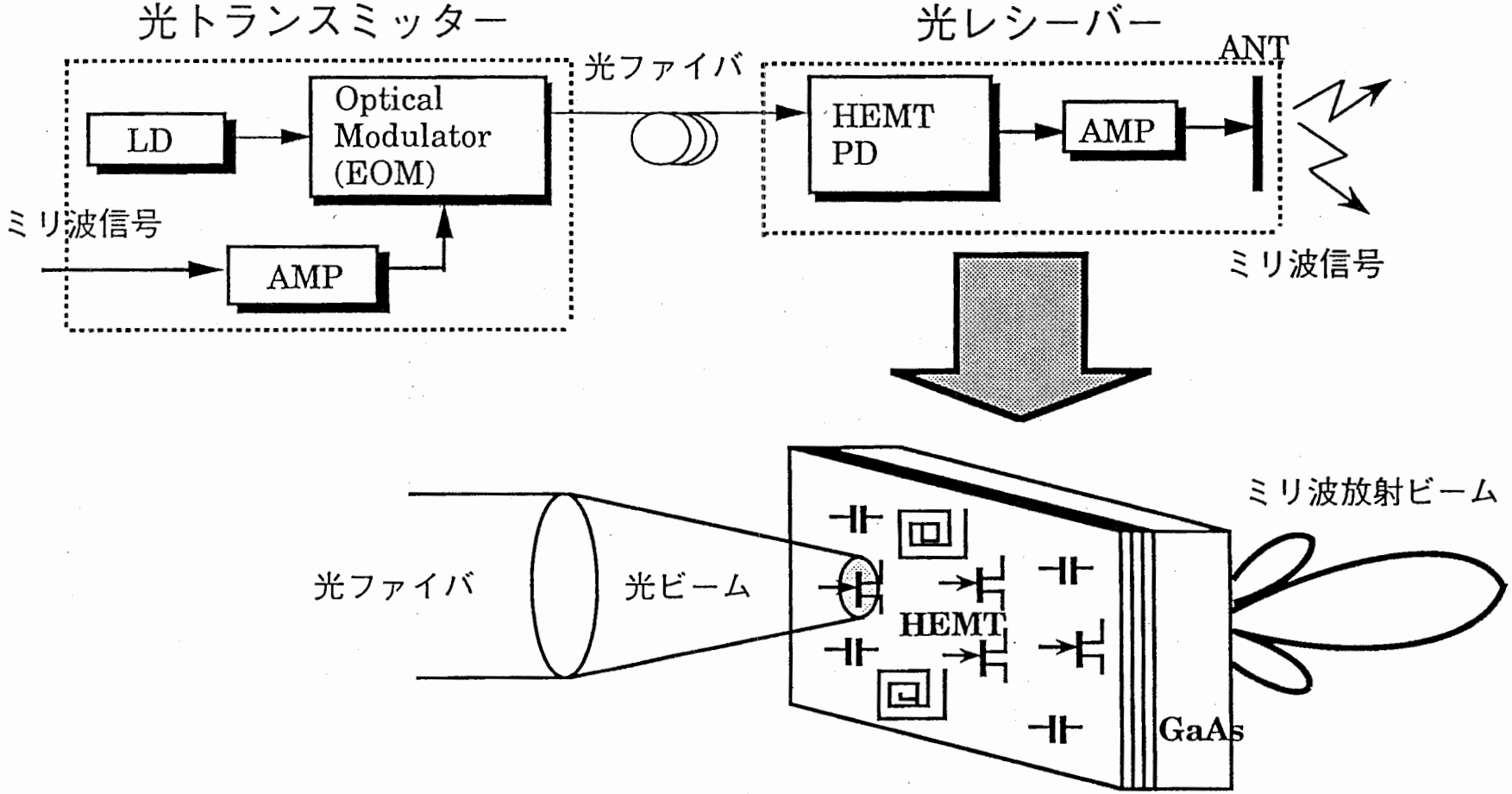

図5.1　1チップ化放射器一体型光受信器

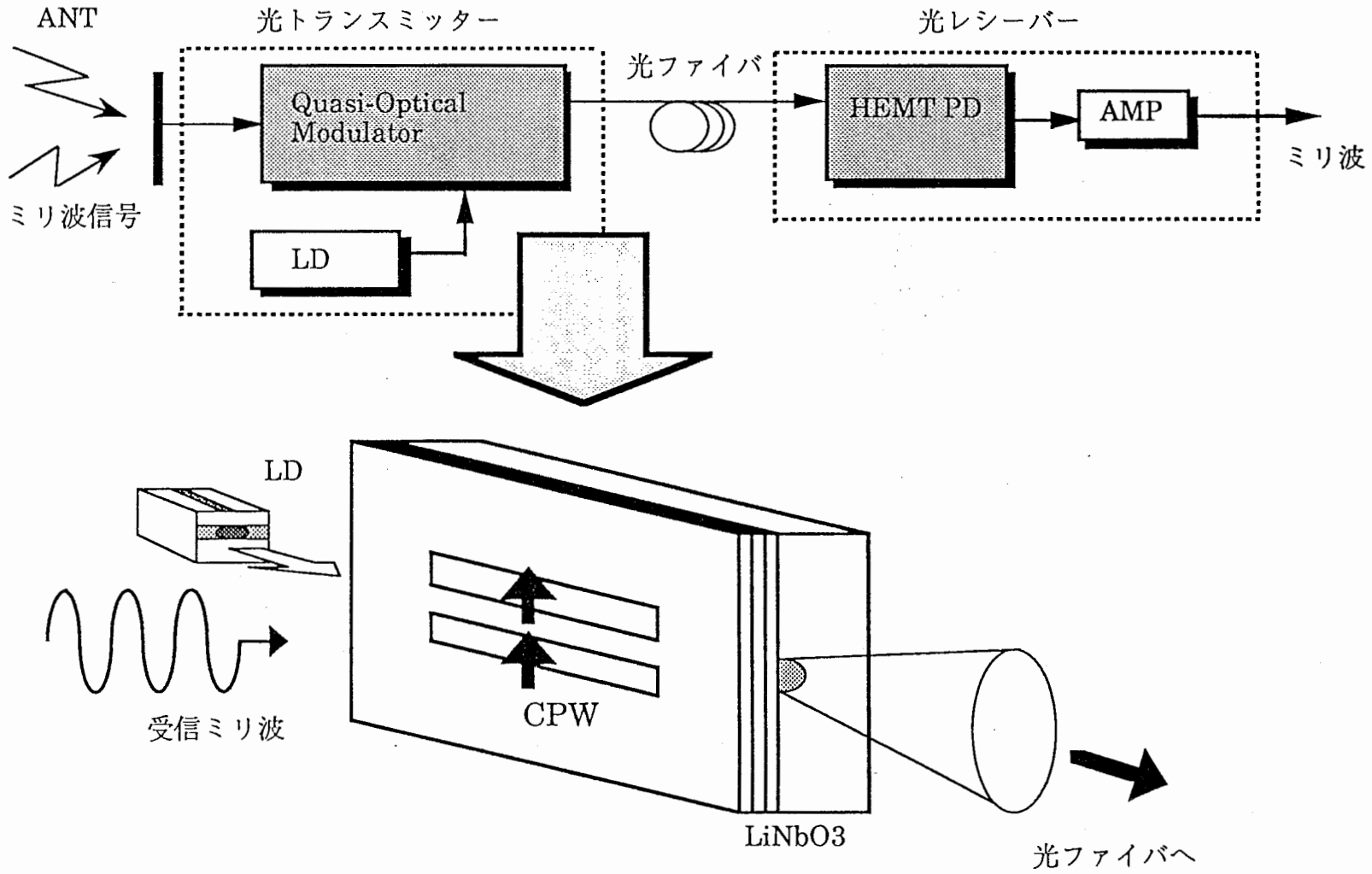

図5.2　受信アンテナ一体型光送信器

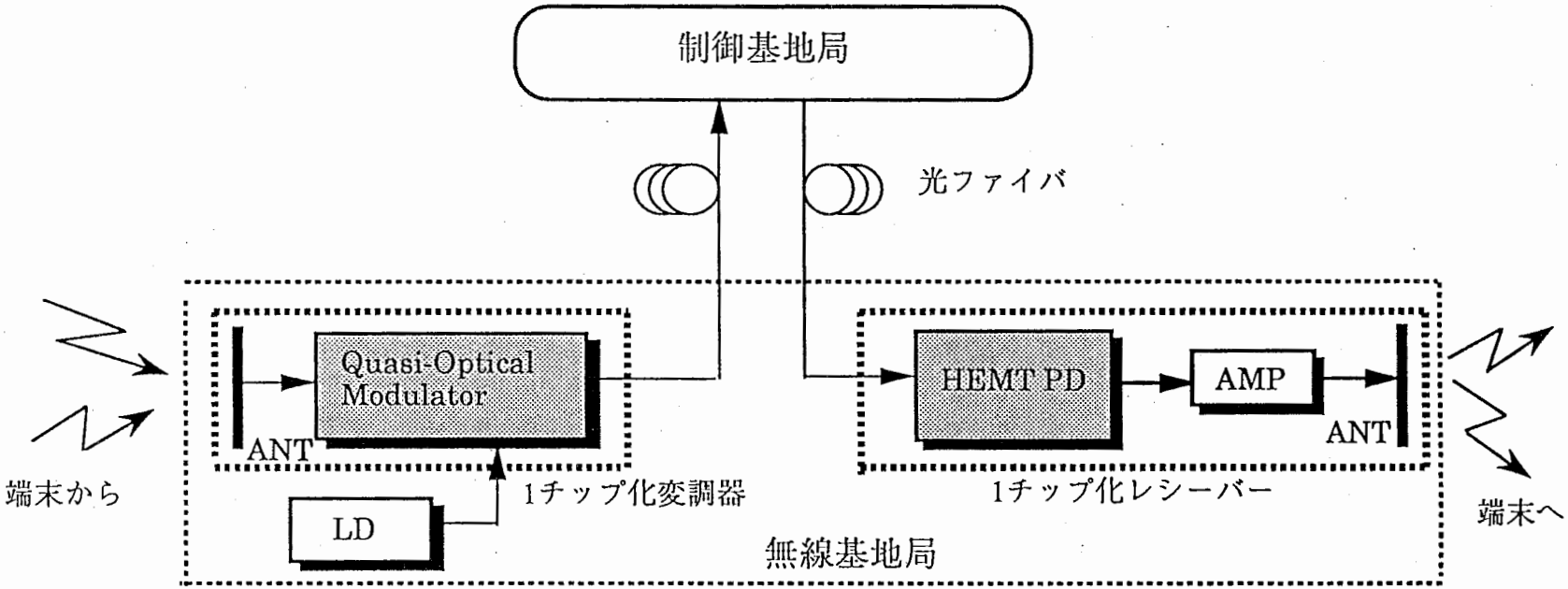

図5.3　機能集積化無線基地局の構成

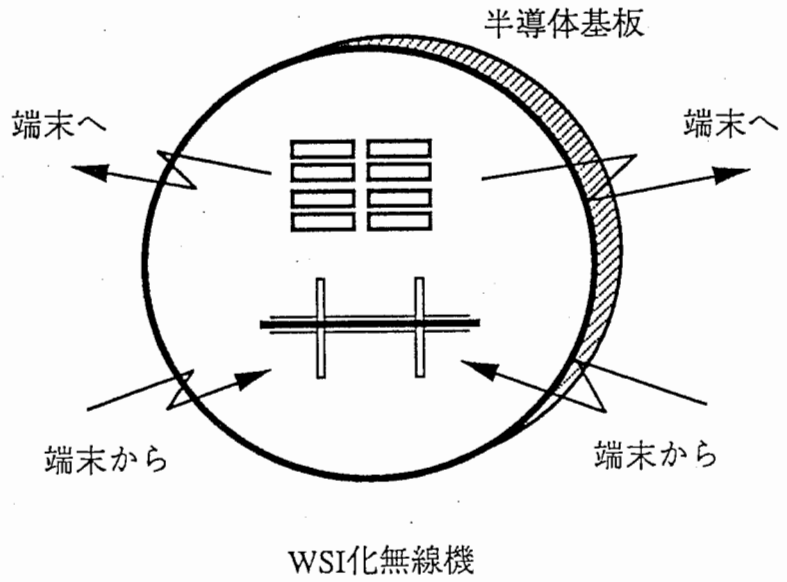

図5.4　ウエーハスケールインテグレション化無線基地局